

Aus dem Zentrum für Orthopädie, Unfallchirurgie und Paraplegiologie der Universität Heidelberg

Zentrumssprecher: Prof. Dr. med. Norbert Weidner

Klinik für Paraplegiologie-Querschnittzentrum

Ärztlicher Direktor: Prof. Dr. med. Norbert Weidner

**Mechanisms and Therapeutic Potential of Treadmill Activity-
Based Intervention in Alleviating Neuropathic Pain Following
Spinal Cord Injury: Considering Sex Differences and Sensory
Input Modulation**

Inauguraldissertation

zur Erlangung des Doctor scientiarum humanarum (Dr. sc. hum.)

an der

Medizinischen Fakultät Heidelberg

der

Ruprecht-Karls-Universität

vorgelegt von

Jing Chen

aus

Fujian, Volksrepublik China

2024

Dekan: Herr Prof. Dr. Michael Boutros

Doktorvater: Herr Prof. Dr. med. Norbert Weidner

*In memory of my grandparents, who always believed in me and taught me life's most important values - I
hope I have made you proud*

Contents

Contents	I
Abbreviations	IV
Figures and Tables.....	VI
1. Introduction.....	1
1.1. Spinal Cord Injury-Induced Neuropathic Pain.....	1
1.2. Maladaptive Alterations Within the Somatosensory Processing Pathways Related to SCI-NP Development	3
1.2.1. <i>Aberrant Changes in the Spinal Cord and Connected Peripheral Nervous System.....</i>	<i>5</i>
1.2.1.1. Neuroimmune processes: reactive gliosis and neuroinflammation	5
1.2.1.2. Neuronal hyperexcitability: central and peripheral sensitization	6
1.2.1.3. Loss of inhibitory control and aberrant neuronal reactivity	8
1.3. Sex May Serve as A Biological Variable in SCI-NP Development.....	10
1.4. Understanding the Mechanisms of SCI-NP and Its Alleviation Through Activity-Based Interventions	11
2. Materials and Methods.....	15
2.1. Animal Subjects and Experimental Groups	15
2.2. Experimental Model of SCI	16
2.2.1. <i>SCI modeling.....</i>	<i>16</i>
2.2.2. <i>Animal-care medications.....</i>	<i>17</i>
2.3. Activity-Based Intervention Paradigms	18
2.3.1. <i>Early increasing-velocity ABI</i>	<i>18</i>
2.3.2. <i>ABI modification via treadmill belt replacement: unpatterned vs. patterned belt</i>	<i>19</i>
2.4. Behavioral Testing.....	19
2.4.1. <i>Mechanical sensitivity test: von Frey monofilaments.....</i>	<i>20</i>
2.4.2. <i>Operant testing of cognitive perception of mechanical hypersensitivity: Place Escape/Avoidance Paradigm (PEAP).....</i>	<i>20</i>

2.4.3.	<i>Thermal sensitivity test: Hargreaves method</i>	21
2.4.4.	<i>Gross motor function test: Basso Mouse Scale</i>	22
2.5.	c-Fos Induction.....	22
2.6.	Tissue Processing.....	23
2.7.	Immunohistochemistry.....	23
2.8.	Antibodies.....	24
2.9.	Buffer and Solutions.....	25
2.10.	Confocal Microscopy Image Segmentation and Measurement.....	26
2.10.1.	<i>CGRP-labeling density profile</i>	27
2.10.2.	<i>PKCγ immunodensity, number of PKCγ-positive cells</i>	27
2.10.3.	<i>Laminar distribution analysis of c-Fos-expressing cells</i>	28
2.10.4.	<i>Analysis of inflammation in the lumbar spinal cord</i>	29
2.11.	Statistical Analysis.....	29
2.12.	Schematic Illustrations.....	30
3.	Results	31
3.1.	Female and Male Mice Exhibit Analogous Sensorimotor Deficits and Progression of NP Following SCI.....	31
3.1.1.	<i>Moderate contusion SCI elicits sustained hindlimb sensorimotor deficits in mice of both sexes</i>	31
3.1.2.	<i>Female and male mice demonstrate similar progression patterns of NP-associated behaviors following SCI</i>	37
3.2.	ABI Mitigates SCI-NP-Associated Symptoms in Both Sexes of Mice.....	39
3.2.1.	<i>High-frequency ABI manifests instability in efficacy for alleviating SCI-NP: readout from comparative analysis with lower-frequency ABI</i>	40
3.2.2.	<i>Female and male SCI mice demonstrate comparable responses to ABI and present amelioration of mechanical allodynia</i>	43
3.3.	ABI on a Patterned Treadmill Belt Promotes Faster SCI-NP Reduction Compared to an Unpatterned Treadmill Belt.....	48

3.4.	ABI Inhibits Maladaptive Plasticity of CGRP-Expressing Nociceptors into the Deeper Dorsal Horn	53
3.5.	ABI Depresses Heightened Neuronal Activity in the Spinal Cord Dorsal Horn after SCI	56
3.6.	ABI Subsides SCI-Induced Enhancement of Activation in Dorsal Horn PKC γ -Expressing Interneurons	60
3.7.	Neuroglial Reaction Does Not Differ in the Dorsal Horn of Below-Lesion Spinal Cord	63
4.	Discussion	67
4.1.	Sex Does Not Act as a Significant Variable in the Development of SCI-NP and Its Amelioration by ABI	67
4.2.	Increasing Mechanoreceptive and Proprioceptive Input Enhances ABI Efficiency in Mitigating SCI-NP	69
4.3.	Reversing SCI-Increased Neuronal Activation in Spinal Cord Dorsal Horn through the ABI Paradigm	71
4.4.	Regulating Enhanced Activation of PKC γ -Positive Neurons in Spinal Cord Dorsal Horn Following SCI by ABI	76
4.5.	Conclusion and Future Perspectives	79
5.	Summary	80
6.	Zusammenfassung	82
7.	Reference List	84
8.	Personal Contribution to Data Acquisition / Assessment and Personal Publications	99
	Appendix / Appendices	100
	Curriculum Vitae / Résumé	105
	Acknowledgements	108
	Eidesstattliche Versicherung	110

Abbreviations

ABI(s)	Activity-based intervention(s)
ATP	Adenosine 5'-triphosphate
BDNF	Brain-derived neurotrophic factor (BDNF)
BMS	Basso Mouse Scale
CD11b	Cluster of differentiation molecule 11b, also known as integrin alpha M (ITGAM)
CGRP	Calcitonin gene-related peptide
CNS	Central nervous system
DH	Dorsal horn
dpi	Days post-injury
DRG	Dorsal root ganglion/ganglia
GABA	Gamma-aminobutyric acid
GAD 65/67	Glutamic acid decarboxylase 65/67
GFAP	Glial fibrillary acidic protein
i.p.	Intraperitoneal
IB4	Isolectin B4
Iba1	Ionized calcium-binding adaptor molecule 1
KCC2	Potassium-chloride cotransporter 2
NLI	Neurological level of injury
NMDA	N-methyl-d-aspartate
NP	Neuropathic pain
NT-3	Neurotrophin-3
PB	Patterned belt

PB (only in “ <i>Materials and Methods</i> ”)	Phosphate buffer
PBS	Sodium phosphate buffer
PEAP	Place Escape/Avoidance Paradigm
PFA	Paraformaldehyde
PKCγ	Gamma isotype of protein kinase C
PNI	Peripheral nerve injury/injuries
PSDC	Postsynaptic dorsal column
s.c.	Subcutaneous
SCI	Spinal cord injury
SCI-NP	Spinal cord injury-induced neuropathic pain
SD	Standard deviation
STT	Spinothalamic tract
TrkB	Tropomyosin receptor kinase B
UPB	Unpatterned belt
WDR	Wide dynamic range

Figures and Tables

Table 1: Positive and negative symptoms of SCI-NP	2
Figure 1: Spinal and supraspinal processing of noxious stimuli and crude touch perception within the spinothalamic tract under physiological conditions.	4
Figure 2: Working hypothesis of the “gate control” circuit involving PKC γ -expressing excitatory interneurons in the spinal cord dorsal horn.	9
Table 2: Animal medications	17
Table 3: Antibody list.....	24
Table 4: List of buffer and solutions	25
Figure 3, Study 1: Investigating potential sex differences in the development of SCI-NP and its alleviation through ABI	32
Figure 4: Moderate contusion SCI leads to evident hindlimb gross motor deficits in both sexes of mice. ...	33
Figure 5: Persistent SCI-induced below-level mechanical allodynia in female and male mice.	35
Figure 6: SCI-induced below-level mechanical hypoalgesia in female and male mice.....	36
Figure 7: Sustained and robust SCI-induced below-level thermal hyperalgesia in female and male mice. .	37
Figure 8: The progression of mechanical and thermal hypersensitivity in female and male mice following the induction of SCI.....	38
Figure 9: High-frequency ABI exhibits instability in alleviating below-level mechanical hypersensitivity compared to lower-frequency ABI.....	41
Figure 10: Daily ABI velocity recordings for female and male mice.	43
Figure 11: ABI mitigates SCI-induced below-level mechanical allodynia in both female and male mice...	44
Figure 12: Lack of improvement in SCI-induced mechanical hypoalgesia and thermal hyperalgesia in mice of both sexes following ABI.	46
Figure 13: No promotion of hindlimb gross motor recovery induced by ABI observed in mice of both sexes.....	47
Figure 14, Study 2: Examining the role of increased sensory input during ABI in improving its efficacy in mitigating SCI-NP.....	49
Figure 15: Representative images of an unpatterned belt and a patterned belt.....	50

Figure 16: Daily ABI velocity recordings for female mice trained on an unpatterned belt or a patterned belt.	50
Figure 17: Patterned ABI exhibits higher efficiency in mitigating SCI-induced mechanical allodynia compared to unpatterned ABI.	51
Figure 18: The projection patterns of nociceptors and mechanoreceptors into the dorsal horn of the spinal cord.	53
Figure 19: ABI inhibits the aberrant sprouting of CGRP-expressing nociceptive fibers into laminae III-IV induced by SCI.	55
Figure 20: ABI diminishes touch-evoked SCI c-Fos neuronal activation in the dorsal horn.	57
Figure 21: Touch-induced c-Fos neuronal activation in the dorsal horn exhibit a strong connection with the development of below-level mechanical allodynia.	59
Figure 22: ABI reduces SCI-induced heightened reactivity of PKC γ -expressing interneurons in the below-lesion spinal cord dorsal horn.	61
Figure 23: ABI paradigms do not promote axonal regeneration of the dorsal corticospinal tract below the level of injury.	63
Figure 24: Astrocytes do not exhibit alterations in the dorsal horn of the below-level spinal cord in response to SCI or ABI paradigms.	64
Figure 25: Microglia do not demonstrate changes in the dorsal horn of the spinal cord below the lesion in response to SCI or ABI paradigms.	65
Figure S1: Both high-frequency and lower-frequency ABI paradigms fail to improve partial hindlimb sensorimotor deficits in SCI mice.	100
Figure S2: Both unpatterned and patterned ABI paradigms fail to improve partial hindlimb sensorimotor deficits in SCI mice.	101
Figure S3: Both unpatterned and patterned ABI paradigms successfully inhibit SCI-induced sprouting of CGRP-expressing nociceptors into the deeper dorsal horn within the below-level spinal cord.	102
Figure S4: Both unpatterned and patterned ABI paradigms significantly depress the SCI-induced enhancement in touch-evoked c-Fos activation within the below-level spinal cord.	103
Figure S5: Both unpatterned and patterned ABI paradigms effectively reduce SCI-induced heightened reactivity of PKC γ -positive interneurons in the below-lesion spinal cord dorsal horn.	104

1. Introduction

In 2022, under the guidance of Dr. Radhika Puttagunta and Prof. Dr. med. Norbert Weidner, I wrote and published a review article titled “*The Impact of Activity-Based Interventions on Neuropathic Pain in Experimental Spinal Cord Injury*” (Chen et al. 2022). This review focused on the cellular and molecular mechanisms underlying neuropathic pain (NP)-associated behaviors in rodent models of spinal cord injury (SCI) and explored how activity-based interventions (ABIs) can mitigate NP following SCI. The objectives and experimental designs of the current study draw heavily from the insights offered in this review. Consequently, the introduction section of my doctoral dissertation, which synthesizes the topics of my work throughout my doctoral studies, may exhibit similarities to the review, reflecting continuity in research focus and an extension of the scholarly discourse initiated therein.

1.1. Spinal Cord Injury-Induced Neuropathic Pain

A lesion or damage to the spinal cord can lead to a partial or complete disconnection of the neural communication pathways from the brain to body regions below the level of injury. This disruption significantly affects the descending modulatory pathways, resulting in pronounced symptoms of motor dysfunction (Franz et al. 2023). Furthermore, neuropathic pain (NP), arising from a complex cascade of pathological processes within the somatosensory nervous system following spinal cord injury (SCI), is recognized as a highly debilitating and refractory sensory impairment in patients (Burke et al. 2017; Finnerup et al. 2014). NP affects more than 50% of individuals with SCI (Burke et al. 2017; Cragg et al. 2015; Finnerup et al. 2014), and its prevalence notably increases beyond the six-month mark following SCI (Burke et al. 2017). The International Association for the Study of Pain (IASP) has developed a classification for SCI pain, wherein SCI-induced NP (SCI-NP) is categorized based on its occurrence at or below the neurological level of injury (NLI) (Bryce et al. 2012; Widerstrom-Noga 2017). At-level SCI-NP is attributed to damage to the spinal cord or nerve roots at the neurological level of injury and/or within three dermatomes below it, without affecting lower dermatomes; below-level SCI-NP is characterized by pain perceived more than three dermatomes below the

neurological level of injury, considered to be closely linked to SCI-induced maladaptive changes across the somatosensory pathways affecting regions distant from the lesion.

Upon examination, patients often exhibit a combination of positive (increased sensitivity and abnormal unpleasant sensations) and negative (sensory deficits) symptoms of SCI-NP (Table 1) (Bryce et al. 2012; Vranken 2013; Widerstrom-Noga 2023). Individuals with SCI-NP frequently report pain hypersensitivity in response to stimuli, manifesting as allodynia and hyperalgesia (Vranken 2013). Allodynia, defined as pain sensation in response to a stimulus that does not usually provoke pain (non-noxious), indicating altered sensory processing. Hyperalgesia, characterized by an intensified response to noxious stimuli, reflects an amplified sensory pathway response to pain (Cavalli et al. 2019; Widerstrom-Noga 2017). SCI-NP frequently co-occurs with motor dysfunctions, such as muscle weakness or spasticity, which can exacerbate the conscious perception of pain (Widerstrom-Noga 2017). Consequently, SCI-NP poses a significant challenge to patients, markedly impacting their quality of life and impeding the rehabilitation process (Bokel et al. 2020; Burke et al. 2018).

Table 1: Positive and negative symptoms of SCI-NP

Positive symptoms (painful and/or abnormal sensations)	Negative symptoms (sensory deficits and/or weakness)
Spontaneous ongoing pain	Hypoalgesia: reduced response to a noxious stimulus
Allodynia: pain sensation to a non-noxious stimulus	Hypoesthesia: decreased sensitivity to sensory stimuli
Hyperalgesia: increased response to a noxious stimulus	
Hyperesthesia: heightened sensitivity to sensory stimuli, encompassing both allodynia and hyperalgesia	
Abnormal sensations (spontaneous or evoked): include paresthesia and dysesthesia, such as tingling, pins and needles, or numbness	

1.2. Maladaptive Alterations Within the Somatosensory Processing

Pathways Related to SCI-NP Development

Under normal circumstances, both noxious and non-noxious stimuli are transduced and conducted from peripheral receptors to the central somatosensory nervous system for further processing. This process involves organized transmission and modulation within the spinal and supraspinal neural circuitry. The ascending spinothalamic tract (STT), which plays a critical role in somatosensory processing, is primarily responsible for the transmission of pain, crude touch, and temperature sensations from peripheral receptors to the brain (Figure 1). Under physiological conditions, this complex neural pathway begins with the activation of primary afferent neurons (first-order neurons such as nociceptors, mechanoreceptors for crude touch, and thermoreceptors) located in the dorsal root ganglia (DRG), which detect noxious stimuli, non-discriminative touch, and temperature changes through their peripheral terminals. These first-order neurons convey sensory information via their central terminals to the dorsal horn of the spinal cord, where they synapse with second-order neurons (sensory-processing neurons) (Todd 2010). In the dorsal horn, two main types of second-order neurons are involved in processing sensory information: nociceptive-specific neurons and wide dynamic range (WDR) neurons. These neurons comprise the STT as spinothalamic projection neurons, which cross to the contralateral side of the spinal cord and ascend signals to the thalamus, and subsequently to various cortical areas for conscious perception (Basbaum 2000; Sandkuhler 2009).

Following SCI, this finely tuned system can become significantly disrupted, resulting in maladaptive structural and functional alternations within the somatosensory processing pathways, leading to the development of NP. Structurally, SCI can result in axonal damage and demyelination of the STT, impairing sensory transmission through ascending pathways, further leading to altered connectivity and plasticity at various supraspinal sites (Wrigley et al. 2009). Functionally, this disruption can lead to aberrant signal processing, including increased excitability of neurons in the dorsal horn and altered synaptic plasticity, which may manifest

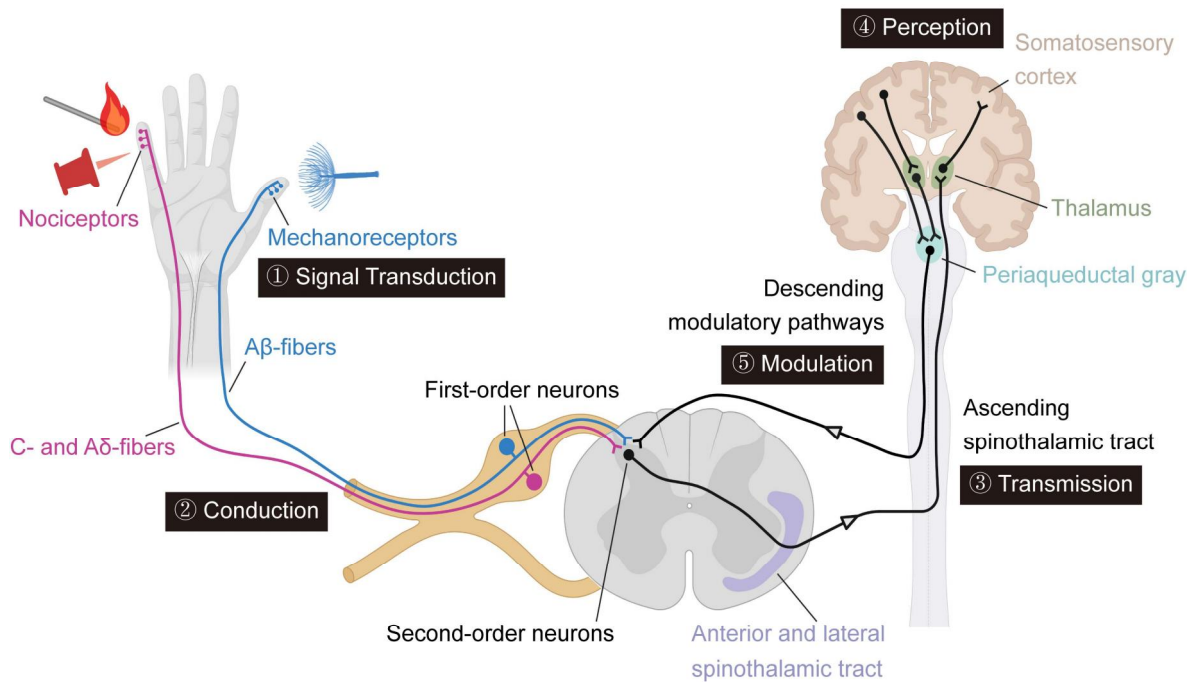


Figure 1: Spinal and supraspinal processing of noxious stimuli and crude touch perception within the spinothalamic tract under physiological conditions.

This schematic illustrates the sensory pathways from peripheral detection to central processing. Noxious stimuli are detected by nociceptors and relayed through C- and A δ -afferent fibers, while non-noxious crude touch is sensed by mechanoreceptors and conveyed through A β -fibers. These signals travel from the dorsal root ganglion to the spinal cord. In the dorsal horn, noxious and crude touch signals are transmitted to spinothalamic projection neurons, which cross the spinal cord midline and ascend to the brain. Upon reaching the thalamus, the signals are distributed to various cortical areas for advanced processing and conscious perception. The illustration also shows the descending modulatory pathway, demonstrating top-down control of sensory signaling. This figure was adapted from (Crucianelli and Morrison 2023).

as hyperalgesia or allodynia (Finnerup et al. 2016; Finnerup et al. 2014; Gwak et al. 2017; Hains et al. 2003; Kuner and Flor 2016; Siddall and Loeser 2001; Siddall et al. 2003). At the cellular and molecular levels, SCI triggers an inflammatory response characterized by the activation of microglia and astrocytes, leading to the release of pro-inflammatory cytokines and chemokines. This neuroinflammatory milieu can exacerbate neuronal excitability within

STT associated with SCI-NP (Gwak et al. 2017; Knerlich-Lukoschus and Held-Feindt 2015). Moreover, SCI induces changes in the expression and function of ion channels and neurotransmitter receptors on neurons interacting with or making up the STT pathway, further distorting sensory signal processing and enhancing pain transmission (Crown et al. 2008; Hulsebosch et al. 2009). However, due to our limited understanding of the intricate mechanisms involved in SCI-NP pathogenesis, complications in treatment arise.

1.2.1. Aberrant Changes in the Spinal Cord and Connected Peripheral Nervous System

1.2.1.1. Neuroimmune processes: reactive gliosis and neuroinflammation

Immediately following SCI, the physical trauma causes neuronal and axonal damage, triggering the release of neurotransmitters, ions, and damage-associated molecular patterns. These molecules and signals activate local neuroglial cells (reactive gliosis), including microglia and astrocytes. Simultaneously, peripheral immune cells (e.g., macrophages) infiltrate the spinal cord lesion through the compromised blood-spinal cord barrier, intensifying the local immune response (Chhaya et al. 2019; Grace et al. 2014). Microglia, the resident immune cells of the central nervous system (CNS), undergo activation and proliferation in response to SCI, exhibiting morphological changes and the upregulation of surface markers such as ionized calcium-binding adaptor molecule 1 (Iba1) and integrin α -M (CD11b). Upon activation, microglia release a variety of pro-inflammatory mediators, including cytokines (tumor necrosis factor- α , interleukin-1 β , interleukin-6) and chemokines (C-C motif chemokine ligand 2, C-X-C motif chemokine ligand 8). These substances increase neuronal sensitivity in the spinal cord and DRG, driving maladaptive changes in the peripheral and central somatosensory nervous systems, contributing to SCI-NP (Chen et al. 2022; Fleming et al. 2006; Gwak et al. 2012; Hulsebosch 2008; Sun et al. 2023). Elevated expression of pro-inflammatory cytokines has been detected at the injury site and beyond. Cytokine levels increase within four months post-SCI in below-lesion spinal cord segments and remain elevated for up to 24 months, correlating with below-level SCI-NP (Detloff et al. 2008; Dugan et al. 2020; Dugan et al. 2021).

Research has also shown that remote microglial activation in the lumbar spinal cord dorsal horn is strongly associated with below-level NP following SCI (Carlton et al. 2009; Chhaya et al. 2019; Detloff et al. 2008; Gwak and Hulsebosch 2009; Gwak et al. 2012; Hains and Waxman 2006; Kim et al. 2013). Pro-inflammatory mediators from microglia can exacerbate the activation of astrocytes (Gwak et al. 2017; Liddelow et al. 2020). Astrocytes, which undergo hypertrophy and increase the expression of glial fibrillary acidic protein (GFAP), amplify inflammation by releasing cytokines, chemokines, and other substances such as nitric oxide and prostaglandins, thereby facilitating crosstalk between immune cells and neurons at the spinal and supraspinal levels. They influence synaptic transmission and neuronal excitability by modulating neurotransmitter uptake/release and altering extracellular ion concentrations, enhancing nociceptive signaling beyond the injury site (Gwak et al. 2017; Ji et al. 2016; Sofroniew 2015). SCI-induced activation of astrocytes occurs both acutely/subacutely (a few days post-SCI) and persistently (beyond three months) in the spinal cord dorsal horn, including at the lesion epicenter as well as in intact rostral and caudal areas (Gwak et al. 2012; Lepore et al. 2011). Inhibiting astrocytic activation after SCI has been shown to mitigate the abnormal hyperexcitability of dorsal horn neurons in response to both non-noxious and noxious stimuli (Gwak and Hulsebosch 2009; Gwak et al. 2009).

1.2.1.2. Neuronal hyperexcitability: central and peripheral sensitization

Precise neuronal response properties in the spinal cord gray matter are critical for the central somatosensory transmission of sensory signals, enabling accurate identification of external stimuli from peripheral initiation. Sensory-processing neurons can be divided into three types based on their physiological response properties to stimuli of varying intensities: low-threshold neurons (non-nociceptive) exhibit the strongest activity in response to non-noxious stimuli; high-threshold neurons (also known as nociceptive-specific neurons) display the strongest activity in response to moderate and noxious stimuli, with few or no responses to non-noxious stimuli; and WDR neurons exhibit graded activity patterns in response to increasing stimulation intensity (greater stimulation intensity yields greater response activity) (Leem et al. 2010). In

terms of spinal cord neuroanatomical architecture, low-threshold/non-nociceptive neurons are predominantly located in the dorsal horn laminae III, IV, and deeper laminae V, VI. These neurons primarily receive non-nociceptive, mechanoreceptive information via myelinated A β -primary afferent fibers, processing sensations like touch and pressure, and projecting through the dorsal column-medial lemniscal pathway (fine touch) and the spinothalamic tract (crude touch). High-threshold/nociceptive-specific neurons are mainly found in the superficial dorsal horn (laminae I and II), receiving nociceptive information from C- and A δ -fibers. WDR neurons are distributed across both the superficial and deep laminae, predominantly in lamina V, but also extending to laminae I, II, and VI. (Eisenach 2001; Netter 2023). Following SCI, spinal cord neuronal hyperexcitability below the level of injury has been identified through electrophysiological studies in rodent SCI models. This hyperexcitability is characterized by the enhanced responsiveness of sensory-processing neurons to both non-noxious and noxious peripheral stimuli, evidenced by increased spontaneous activity and post-discharge activity, indicative of central sensitization (Gwak et al. 2008; Gwak and Hulsebosch 2011b; Hao et al. 2004). This observed spinal hyperexcitability closely correlates with the behavioral manifestations of below-level SCI-NP.

Neuronal hyperexcitability in the spinal cord gray matter is facilitated not only by spinal mechanisms but may also be influenced by alterations in peripheral conduction. This includes altered response properties of DRG sensory neurons and subsequent changes in peripheral somatosensory transmission. The hyperexcitability of nociceptors can lead to an increase in the release level of neurotransmitters such as glutamate, substance P, calcitonin gene-related peptide (CGRP), and adenosine 5'-triphosphate (ATP), to second-order neurons in the spinal cord (Boadas-Vaello et al. 2016). Research has demonstrated that peripheral nociceptors exhibit spontaneous activity in the absence of stimuli and an enhanced response to evoked stimuli following SCI (a phenomenon of peripheral sensitization). This is accompanied by hyperexcitability of DRG sensory neurons and postsynaptic spinal sensory-processing neurons, as well as SCI-NP-associated behaviors within the innervated body regions (Carlton et al.

2009). Studies have shown that post-SCI neuronal hyperexcitability in both the spinal cord and DRG may be attributed to the increased activation of neuroglial cells. Specifically, upon the activation of immune cells, the release of substances such as pro-inflammatory cytokines induces alterations in membrane integrity. These alterations affect receptor and ion channel function, altering signal transmission in sensory-processing neurons and initiating enhanced calcium influx. This cascade increases activation of intracellular downstream pathway, resulting in sustained neuronal hyperexcitability in the spinal cord (Crown et al. 2008; Detloff et al. 2008; Gwak et al. 2008; Hains and Waxman 2006).

1.2.1.3. Loss of inhibitory control and aberrant neuronal reactivity

In the aftermath of SCI, there is a notable downregulation of neurotransmitters and their receptors that are crucial for local endogenous inhibitory signaling within the spinal cord. This involves key neurotransmitters such as gamma-aminobutyric acid (GABA) and glycine. The downregulation of GABA and glycine receptors, including GABA_A receptors and glycine receptors, further compromises inhibitory neurotransmission, failing to adequately counterbalance the increased synaptic transmission in the spinal cord due to glutamate-mediated neuronal excitation following SCI (Drew et al. 2004; Gwak and Hulsebosch 2011a; Li et al. 2020; Malcangio 2018). Central terminals from functionally distinct classes of primary afferent fibers are segregated into different laminae within the dorsal horn of the spinal cord: thinly unmyelinated C-fibers and myelinated A δ -fibers, which constitute most nociceptors, terminate in the superficial laminae I and II (Lu and Perl 2005; Sugiura et al. 1986), while the cutaneous-sensing, heavily myelinated A β -fibers of mechanoreceptors innervate the inner segment of lamina II (IIi) and the deeper dorsal horn, laminae III-IV (Hughes et al. 2003; Todd 2010). Furthermore, research has demonstrated that excitatory interneurons and sensory-processing or projection neurons located in lamina I and the outer layer of lamina II (lamina IIo) are primarily inhibited via GABAergic mechanisms, while those in lamina IIi and lamina III are predominantly subjected to glycinergic inhibition (Cioffi 2021; Takazawa et al. 2017).

Under physiological conditions, it is proposed that the separation of nociceptive and non-nociceptive pathways in the dorsal horn is maintained by the action of 'gate control' units, consisting of glycinergic and GABAergic inhibitory interneurons located in lamina II (Kwon et al. 2014; Takazawa and MacDermott 2010; Torsney and MacDermott 2006; Zeilhofer et al. 2012). This mechanism involves a local circuit including neurons in lamina Iii expressing the gamma isoform of protein kinase C ($PKC\gamma$) (Figure 2). The functional inhibition from glycinergic interneurons onto $PKC\gamma$ -expressing ($PKC\gamma+$) excitatory interneurons prevents them being activated from $A\beta$ -mediated inputs. Studies have demonstrated that peripheral nerve injuries (PNI) lead to a reduction in glycinergic postsynaptic inhibition onto lamina Iii $PKC\gamma+$ excitatory interneurons. This is accompanied by an increase in intracellular chloride concentration ($[Cl^-]_i$) in spinal cord neurons, resulting in decreased efficacy of both glycinergic

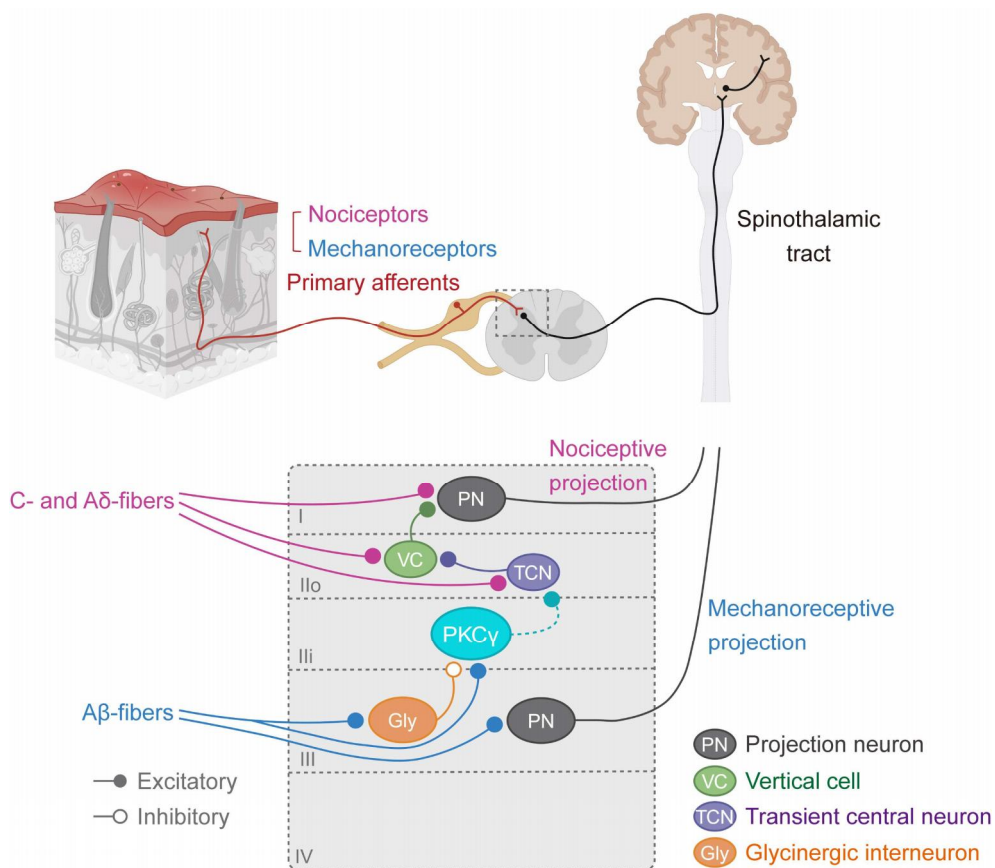


Figure 2: Working hypothesis of the “gate control” circuit involving $PKC\gamma$ -expressing excitatory interneurons in the spinal cord dorsal horn.

PKC γ -expressing excitatory interneurons are typically inhibited by glycinergic interneurons, thus gating non-nociceptive mechanical information under normal conditions. However, inflammation and neuropathic conditions can impair this endogenous inhibition mechanism, leading to increased activation of PKC γ + interneurons. As a result, stimuli that are normally innocuous can activate nociceptive pathways, leading to mechanical allodynia.

and GABAergic inhibition. Consequently, the disinhibition of PKC γ + neurons fails to prevent their activation upon receiving A β -mediated inputs, further transmitting excitatory signals to dorsally-located neurons, ultimately exposing nociceptive-specific projection neurons to activation and generating pain sensations, leading to mechanical allodynia (Bardoni et al. 2013; Braz et al. 2014; Lu et al. 2013; Zheng et al. 2010). This suggests that injury-induced mechanical allodynia can be mediated through a circuit involving PKC γ + interneurons, as increased spinal cord PKC γ + expression has been associated with the development of mechanical allodynia in both inflammatory and neuropathic conditions (Brown et al. 2022; Lu et al. 2013; Neumann et al. 2008; Zhao et al. 2018).

1.3. Sex May Serve as A Biological Variable in SCI-NP Development

Clinical evidence focusing on outcomes related to SCI-NP has revealed a slightly higher prevalence of pain among females than males, with reported prevalence rates of 75% in females compared to 67% in males (Kim et al. 2020), and 46% in females versus 38% in males (Werhagen et al. 2004). However, it is inconclusive given the lower number of females than males experiencing SCI, thus the numbers were not enough to make any statistical conclusions. Clinical studies that employed the Mean Numeric Rating Scale (MNRS) to assess pain intensity have shown that females report experiencing more severe symptoms of SCI-NP more frequently than males (Kim et al. 2020). This highlights the imperative for targeted preclinical studies that aim to comprehensively compare SCI-NP profiles, incorporating an examination of sex differences in the underlying mechanisms. Previous research into the mechanisms behind NP resulting from PNI suggests a hypothesis that sex differences may also exist in the

mechanisms underlying SCI-NP. These differences could potentially influence behavioral responses and treatment outcomes (Chen et al. 2018; Ghazisaeidi et al. 2023; Linher-Melville et al. 2020; Mapplebeck et al. 2018; Rosen et al. 2017; Sorge et al. 2015).

A report on sex inclusion in preclinical SCI rodent studies reveals a substantial gap in research diversity, revealing that only 9% of studies incorporating both female and male subjects (Stewart et al. 2020). This highlights the insufficient consideration given to sex as a biological variable in the investigation of NP development following SCI. Some studies have indicated that female SCI mice and rats demonstrate increased hypersensitivity compared to their male counterparts (Dominguez et al. 2012; Lee et al. 2023), whereas others have reported that males are more susceptible to developing mechanical allodynia (Gaudet et al. 2017; Hubscher et al. 2010). Conversely, several reports have found no significant sex differences in SCI-NP-associated behaviors (Gensel et al. 2019; McFarlane et al. 2020; Walker et al. 2019). Consequently, there is a pressing need for future research to incorporate multi-dimensional assessments of SCI-NP-associated behaviors to foster a more comprehensive understanding not only of potential differences in the perception and interpretation of SCI-NP but also in the response to therapeutic interventions between females and males, as well as the underlying mechanisms.

1.4. Understanding the Mechanisms of SCI-NP and Its Alleviation

Through Activity-Based Interventions

In clinical settings, as first-line rehabilitative treatment for SCI patients, activity-based interventions (ABIs) such as cycling, standing, walking, and treadmill-based stepping are commonly utilized. These interventions are typically customized to each patient's specific needs and progress in motor recovery, often incorporating strategies such as functional electrical stimulation, tonic epidural spinal cord stimulation, or a weight support system. Such tailored approaches aim to maximize physical functioning and prevent secondary complications like joint contracture and muscle atrophy (Behrman and Harkema 2000; Field-

Fote and Roach 2011; Harkema et al. 2011; van Hedel et al. 2009). Extensive preclinical research has demonstrated that ABIs significantly enhance motor recovery and facilitate neuronal regeneration (Griesbach et al. 2004; Ichiyama et al. 2011; Sandrow-Feinberg and Houle 2015). Further investigations conducted by our laboratory and others have shown that a variety of ABIs, such as treadmill training and voluntary wheel running, effectively mitigate NP-associated symptoms at both the early and chronic stages of SCI (Detloff et al. 2014; Dugan et al. 2021; Jergova et al. 2023; Nees et al. 2016; Sliwinski et al. 2018). This effectiveness prompts a deeper exploration into the specific mechanisms through which ABIs exert their ameliorative effects on SCI-NP.

ABIs have been shown to modulate the persistent inflammatory responses triggered by SCI, regulating levels of pro-inflammatory and anti-inflammatory mediators across multiple regions, including the at-level lesion site, below-lesion spinal cords, and DRG, contributing to SCI-NP alleviation (Dugan et al. 2020; Dugan et al. 2021). They also diminish the activation of immune cells such as macrophages and neuroglial cells like microglia at and below the injury level (Cheng et al. 2022; Chhaya et al. 2019). These interventions also promote the restoration of physiological endogenous GABAergic inhibition within the spinal cord dorsal horn. Specifically, ABIs influence the levels of the potassium-chloride cotransporter 2 (KCC2) (Dugan et al. 2020; Dugan et al. 2021) and normalize the synthesis of glutamic acid decarboxylase (GAD-65/67) (Tashiro et al. 2018) towards sham levels in distal spinal regions through BDNF/tropomyosin receptor kinase B (TrkB) signaling. Suppression of this pathway has been shown to decrease the expression of KCC2, GAD-65, and GAD-67, correlating with the emergence of below-level SCI-NP symptoms (Li et al. 2020). Moreover, ABIs have been shown to reduce excitatory mechanisms below the injury site by enhancing the function of the perineuronal net, which, when its expression is diminished following SCI, indicates a hyperexcitatory state of the neural circuitry (Sanchez-Ventura et al. 2021). Furthermore, ABIs modulate maladaptive plasticity of peptidergic C-/A δ - nociceptive fibers in the spinal cord gray matter neural circuitry. This modulation leads to a reduction in SCI-induced increases in

CGRP-expressing nociceptor labeling density in laminae III-IV (Nees et al. 2016; Sliwinski et al. 2018; Tashiro et al. 2018; Tashiro et al. 2015), and decreases CGRP expression in laminae I-II of the L4-L6 lumbar spinal cord segments (Cheng et al. 2022).

In examining the behavioral outcomes and underlying mechanisms of SCI-NP after ABIs, it is observed that ABIs incorporating weight-bearing and rhythmic limb movements—such as free walking, treadmill training, and voluntary wheel running—demonstrate greater efficacy in alleviating SCI-NP. Conversely, interventions that rely on weight support systems (treadmill training with body weight support system, swimming) and/or do not involve alternating limb movements (supported standing) are less effective. Based on these observations, I hypothesize that 'full weight-bearing rhythmic' ABIs may more effectively activate proprioceptive and mechanoreceptive afferents, leading to a reduction in SCI-NP. However, direct evidence supporting this hypothesis is still lacking. As part of this pre-clinical study, I aim to refine and optimize the ABI paradigm to enhance its effectiveness. Therefore, I have modified the treadmill-based activity regimen in the current study by employing two distinct types of treadmill running belts, each with unique textures and patterns. This modification is designed to vary the intensity of sensory stimulation as the animals engage in stepping or running.

Given the evidence from Section 1.3 of the potential sex-dependent differences in the signaling pathways involved in SCI-NP, it becomes crucial to include sex as a biological variable. This inclusion is especially pertinent considering that females and males may respond differently to therapeutic interventions aimed at pain alleviation, due to varying neurobiological mechanisms. Therefore, to address specific gaps in the research field, the present study is structured around the following aims:

Aim 1: To investigate whether there are differences between females and males in the development of NP and its alleviation through a weight-bearing ABI following SCI. This aim is explored through **Study 1**.

Aim 2: To examine whether incorporating increased sensory input during ABI can enhance its efficiency in ameliorating SCI-NP. This aim is addressed in **Study 2**.

Aim 3: To explore the SCI-induced mechanisms that correlate with pain and are altered by ABI. This aim is investigated concurrently with the first two studies.

2. Materials and Methods

2.1. Animal Subjects and Experimental Groups

Animals were maintained in accordance with the protocols approved by the local governing body (Regierungspräsidium Karlsruhe, Germany, Ref. G-100/21), adhering to institutional guidelines and German law on animal welfare and the protection of animals used for scientific purposes (TierSchG, TierSchVersV). Eight-week-old C57BL/6J mice from Janvier Labs (strain: C57BL/6JRj) of both sexes, with females weighing 18-23 grams and males weighing 20-25 grams, were acclimatized to the animal facility for 12 days. After this period, they underwent baseline behavioral testing at 10 weeks of age, followed by spinal cord injury (SCI) surgery and subsequent weekly behavioral assessments as outlined in Figures 3 and 14. Mice were housed in small groups (3-4 per cage), segregated by sex, with food and water available ad libitum, under a natural 12-hour light/12-hour dark cycle. As per ARRIVE guidelines, experimenters were blinded to the identities of the mice in behavioral and immunohistochemical analyses. Initially, the studies included 36 female and 26 male mice; however, three male mice succumbed to bladder infections, and consequently, data from only 23 males were included in the analysis.

In Study 1, which focused on investigating sex differences in the development of SCI-induced neuropathic pain (SCI-NP) and its alleviation through a treadmill activity-based intervention (ABI), mice of both sexes were included and randomly allocated into sham, SCI, and SCI+ABI groups prior to SCI modeling. The sex-specific sham group for each sex comprised 7 animals, while the SCI and SCI+ABI groups each comprised 8 animals. A treadmill equipped with an unpatterned running belt was utilized for both sexes (refer to Figure 3, Sections 3.1 and 3.2). Study 2 was designed to examine the effects of additional sensory stimulation during ABI, focusing exclusively on female mice. The study included four experimental groups: sham, SCI, SCI+ABI-UPB (using an unpatterned belt), and SCI+ABI-PB (using a patterned belt). The sham group comprised 7 female mice, and each of the other three groups included 8 mice.

Notably, a new cohort of 8 female mice was added to the SCI+ABI-PB group for this study (see Figure 14, Section 3.3), while the remaining groups were carried over from Study 1.

2.2. Experimental Model of SCI

2.2.1. SCI modeling

In my studies, all contusion surgeries were performed using the Infinite Horizon Impact Device (IH-0400 Impactor; Precision Systems & Instrumentation, Lexington, KY, USA), equipped with a 1.3 mm diameter steel-tipped impactor specifically designed for mice (Nees et al. 2016; Sliwinski et al. 2024; Sliwinski et al. 2018).

Before the surgical procedures, mice were deeply anesthetized via intraperitoneal (i.p.) injection with a combination of Fentanyl (0.01 mg/kg), Medetomidine (0.3 mg/kg), and Midazolam (4 mg/kg). To ensure anonymity and unbiased handling during surgery, the ear markings of all mice were concealed by covering them with cotton tape by the surgical assistant, Yifeng Zheng, before they were handed to me, the surgeon. Under a surgical microscope (SZ51 zoom stereo microscope, Olympus), I performed a laminectomy at the T9 vertebral level to expose the spinal cord at the T11 level. I used extra fine forceps to stabilize the spinal column by gripping the spinal processes of the adjacent T8 and T10 vertebrae. The impactor tip was positioned 4.4 mm above the exposed spinal cord. For SCI modeling, including both untreated and ABI-treated groups, a moderate contusion at the T11 level was induced using the impactor set to deliver a force of 50 kdyn without dwell time. During the surgery, dehydration was prevented by administering 100 μ l of lactated Ringer's solution subcutaneously (s.c.) mid-procedure. The physiological state of the mice was closely monitored by observing the respiratory movements of the thoracic cavity, measuring body temperature, and assessing reflex responses. After administering the contusion, the muscle layers were sutured using 6/0 terylene, and the skin incision was closed with suture clips designed for mouse use. Anesthesia was reversed through i.p. injections of a wake-up mixture, which included Buprenorphine (0.04

mg/kg), Flumazenil (0.5 mg/kg s.c.), and Atipamezole (2.5 mg/kg s.c.), with no additional analgesic treatment administered.

Post-surgery, the mice were closely monitored, and their bladders were manually expressed at least twice daily to prevent complications. To mitigate the risk of bladder infections, antibiotic treatment with ampicillin (33 mg/kg, 100 µl s.c., twice per day) was administered for 10-14 days post-operation, continuing until reflexive bladder function was restored. Additionally, analgesics consisting of Buprenorphine (0.04 mg/kg, 100 µl s.c.) were administered twice daily to both SCI modeling and sham-operated mice for the first two days post-surgery to manage pain associated with the surgical wound. Approximately one week after the injury, the surgical clips were carefully removed from the conscious mice.

2.2.2. Animal-care medications

Table 2: Animal medications

Medication	Product	Company/Manufacturer
Acepromazine	Tranquinervin®	Dechra Veterinary Products
Ampicillin	Ampicillin-ratiopharm® 5,0 g	Ratiopharm GmbH
Atipamezole	ATIPAZOLE 5 mg/ml	Prodivet pharmaceuticals
Buprenorphine	Buprenovet® Multidose 0,3 mg/ml	VetViva Richter GmbH
Fentanyl	Fentadon® 50 µg/ml	Dechra Veterinary Products
Flumazenil	Flumazenil Kabi 0,1 mg/ml	Fresenius Kabi Deutschland GmbH
Ketamine	Ketamin 10%, 100 mg/ml	Bremer Pharma GmbH
Medetomidine	Dormilan® 1 mg/ml	Alfavet Tierarzneimittel GmbH
Midazolam	Midazolam-hameln 1 mg/ml	Hameln Pharma GmbH
Ringer's solution	Ringer-Infusionslösung Ecoflac plus	B.Braun
Xylazine	XYLARIEM® 20 mg Xylazin	Ecuphar

2.3. Activity-Based Intervention Paradigms

2.3.1. Early increasing-velocity ABI

The ABI paradigm utilized in my studies employs a well-established treadmill training regime developed in our laboratory (Nees et al. 2016; Sliwinski et al. 2018). Mice in the ABI groups underwent moderate training on a custom-built motorized treadmill. This treadmill is equipped with three individual lanes (700 x 100 mm each) and separated by walls made of red acrylic glass to facilitate parallel training for up to three animals. The treadmill belts are driven by a RollerDrive EC310 motor (Interroll Automation GmbH, Sinsheim, Germany) and controlled by proprietary software developed using LabVIEW 2012 (version 12.0; National Instruments Corporation, Austin, TX). This setup ensures a load-independent constant velocity, managed by a proportional–integral–derivative (PID) controller, allowing for adjustable speeds.

Animals assigned to the ABI groups underwent training twice daily for 15 minutes per session, once in the morning and once in the afternoon, with at least a 3-hour break between sessions. For high-frequency ABI, training was conducted 5 days per week, totaling 15 ABI days across a duration of 3 weeks; lower-frequency ABI involved training 3 days per week, totaling 9 ABI days.

Training commenced 8 days post-injury (dpi), determined by the recovery of weight support in the injured mice. The treadmill speed was initially set lower (approximately 0.09 m/s) and gradually increased based on the animals' daily ABI performance. The running velocity was carefully adjusted so that the animals could maintain a position in the middle of the belt, ensuring "moderate ABI intensity" without exhibiting signs of stress, such as falling behind to the end of the belt, increased defecation, or elevated respiration rates. On each day of ABI, control mice (both SCI and sham groups) were placed in the same environment for two 15-minute sessions without treadmill movement, based on findings from previous studies that showed no significant behavioral differences between trained and untrained sham mice.

2.3.2. ABI modification via treadmill belt replacement: unpatterned vs. patterned belt

In Study 2, I incorporated two distinct types of treadmill running belts, each featuring different textures to explore the effects of sensory stimulation. The unpatterned belt was constructed from a foam rubber fabric (3305 Black EVA Foam Rubber Material 2 mm, sourced from Fabrics-City, Germany), providing a smooth and uniform surface. Conversely, the patterned belt was made of Polyvinyl Chloride, specifically the SHEJIO Treadmill Walking Belt (available on Amazon), which included a textured surface designed to enhance sensory stimulation/input during treadmill training.

2.4. Behavioral Testing

Mice aged 10 weeks from both sexes were acclimated to the von Frey and Hargreaves testing apparatus over three consecutive days (-5, -4, and -3 dpi) for a minimum of one hour each day before the baseline testing days (-2 and -1 dpi) and for 30–45 minutes before each testing session on all subsequent testing days. The baseline mechanical and thermal sensitivity was determined by calculating the average value across two consecutive days from -2 and -1 dpi. The animals were not habituated to the open field arena used for the Basso Mouse Scale (BMS) or the Place Escape/Avoidance Paradigm (PEAP) testing arenas. Weekly behavioral tests, including BMS, von Frey, and Hargreaves tests, were conducted every Monday from 7 dpi to 28 dpi, with PEAP administered at 29 dpi (refer to Figures 3 and 14).

All behavioral assessments were performed during the same part of the circadian cycle on awake, unrestrained animals. Gross motor function tests were scheduled early in the morning, followed by sensory testing. The thermal sensitivity test was started at least 30 minutes after finishing the mechanical sensitivity test. To ensure the objectivity of the results, the experimenter was blinded to the group identities of the animals.

2.4.1. Mechanical sensitivity test: von Frey monofilaments

Animals were placed in a plexiglass box (10 cm length x 10 cm width x 14 cm height) on an elevated wire grid (Ugo Basile Inc., Italy) for mechanical sensitivity testing. Calibrated von Frey monofilaments with increasing diameters and target forces (0.16, 0.4, 0.6, and 1.6 g) were applied. Filaments were selected based on results from previous studies conducted by our laboratory using an identical SCI model in mice (Nees et al. 2016; Sliwinski et al. 2024; Sliwinski et al. 2018). The 0.16 and 0.4 g filaments were used to elicit non-noxious mechanical stimuli, while the 0.6 and 1.4 g filaments were deployed for noxious mechanical stimuli. Von Frey hair filaments were applied to the plantar surface of the hindpaw using a brief vertical upward motion for 2-3 seconds. Testing was performed in parallel on up to 12 animals. Each hindpaw was tested with a single stimulus before proceeding to the other hindpaw for all animals; the initial hindpaw was re-tested with the same filament after a minimum interval of 5 minutes between applications on the same animal. Before proceeding to the next filament, an interval of 5-10 minutes was maintained to mitigate the risk of stimulus-induced sensitization in the paw. The withdrawal frequency, which is the proportion of withdrawals to total attempts, was calculated by aggregating the outcomes of 10 applications for each filament, distributed evenly with 5 applications per hindpaw. This methodological approach facilitates a comprehensive quantification of the mechanical sensitivity elicited by each filament.

2.4.2. Operant testing of cognitive perception of mechanical hypersensitivity:

Place Escape/Avoidance Paradigm (PEAP)

The assessment of affective-cognitive perception of mechanical allodynia, induced by non-noxious mechanical stimulation, was conducted on all subjects using the Place Escape/Avoidance Paradigm (PEAP) as delineated in prior studies (Nees et al. 2016; Prabhala et al. 2018; Sliwinski et al. 2018). Each animal was placed in a box (22 cm length x 22 cm width x 14 cm height) situated atop an elevated wire grid. This apparatus was segregated into two chambers: a closed (dark) chamber, with the roof and walls enveloped in black foil, and an open (light) chamber, where the walls were lined with white foil. These chambers were

interconnected via a 3.5 cm passageway in the partitioning wall, allowing free movement between them. The initial 10 minutes of a 25-minute session were designated as an unstimulated reference period for each subject, during which, across two 5-minute exploration phases, the subjects could navigate freely between the dark and light compartments without exposure to stimuli. The duration spent in the dark compartment during each phase was documented and averaged to establish a baseline for each subject. Following this, throughout a 15-minute testing phase, divided into three 5-minute intervals, non-noxious mechanical stimuli were administered to the plantar surface of the hindpaws using a 0.16 g von Frey hair filament, with applications alternating between the left and right paws every 15 seconds whenever subjects ceased movement or remained in the dark chamber. The duration spent in the dark chamber during each interval was again recorded and subsequently compared against the pre-established baseline for each subject to ascertain the proportional change in time spent in the dark. This comparison aimed to elucidate the subjects' aversive responses to the evoked non-noxious mechanical stimuli.

2.4.3. Thermal sensitivity test: Hargreaves method

To evaluate thermal sensitivity, animals were confined within a plexiglass chamber (10 cm length x 10 cm width x 14 cm height) positioned atop a glass floor (Ugo Basile Inc., Italy). Thermal stimuli were administered to the plantar surfaces of the animals' hindpaws using the Hargreaves method (Hargreaves Apparatus, Ugo Basile Inc., Italy), which involved positioning a movable infrared laser beam beneath the glass floor to precisely target the plantar surface of the hindpaws. To minimize the risk of skin damage, the application was limited to a maximum duration of 15 seconds. The protocol allowed for simultaneous testing of up to 12 animals. For each animal, a single stimulus was applied to one hindpaw before testing the opposite hindpaw, ensuring a minimum interval of 5 minutes between successive applications to the same paw. The automatic deactivation of both the laser and the timing mechanism occurred immediately upon the animal's withdrawal of its hindpaw, thereby recording the withdrawal latency as the elapsed time from the onset of stimulation to the withdrawal of the paw. The thermal sensitivity

was quantified based on the average withdrawal latency, derived from eight stimuli per animal (four per hindpaw).

2.4.4. Gross motor function test: Basso Mouse Scale

The Basso Mouse Scale (Basso et al. 2006) was utilized to evaluate the hindlimb gross motor functions of all subjects, providing a measure of their hindlimb motor recovery over time. Mice were individually placed at the center of a circular arena surrounded by white walls (40 cm in height) and allowed to explore the area for 5-10 minutes. Their movements were observed by two experimenters who were unaware of the group identities. The performance of each hindpaw was scored independently by each observer and the average of these assessments was calculated to derive a composite score (left and right) for each subject. Right before the initial hindlimb sensory function testing post-SCI at 7 dpi, the BMS was used to verify sufficient recovery of the animals' plantar placement and weight-bearing capabilities ($BMS \geq 3$). This preliminary assessment was crucial for the subsequent application of the von Frey and Hargreaves tests on their plantar surfaces, which depend on the elicitation of withdrawal reflexes in the hindpaws.

2.5. c-Fos Induction

The expression of the Fos protein, which is the product of the induction of the immediate early gene c-Fos in response to synaptic activity and neuronal activation, was assessed as a neurochemical marker of neuronal activation within a 45-minute to 1-hour window following stimulation. This was done to understand how neural circuits respond to specific neurobiological stimuli (Gan et al. 2021a; Gan et al. 2021b; Renier et al. 2016; Stegemann et al. 2023). To investigate c-Fos activation in the dorsal horn of the spinal cord induced by non-noxious mechanical stimuli, mice underwent a controlled experimental procedure on the day of perfusion (31 dpi). Specifically, mice were confined in a plexiglass chamber (10 cm length x 10 cm width x 14 cm height) placed on an elevated wire grid. The plantar surfaces of the hindpaws were alternately stimulated with a 0.16 g von Frey hair filament at 30-second

intervals for 20 minutes across all experimental groups. Sixty minutes after stimulation cessation, mice were transcardially perfused with a fixative solution of cold 4% paraformaldehyde in phosphate buffer, following a flush with 0.1 M phosphate-buffered saline. Tissues from the L4-L6 lumbar spinal cord segments were then harvested for Fos immunofluorescence analysis. This methodology facilitated the observation of neuronal activation patterns induced by non-noxious stimuli in sham, SCI, and SCI with ABI animals.

2.6. Tissue Processing

All animals in this study were euthanized with i.p. injection using a lethal dose of a mixture containing ketamine (62.5 mg/kg), xylazine (3.175 mg/kg), and acepromazine (0.625 mg/kg), diluted in sterile 0.9% saline. Following euthanasia, the animals underwent transcardial perfusion with 0.9% saline, succeeded by 4% paraformaldehyde (PFA) in 0.1 M phosphate buffer (PB). The spinal cords were then meticulously dissected and post-fixed in 4% PFA/0.1 M PB for three hours at room temperature. Subsequently, the tissues were briefly rinsed with ddH₂O, followed by a 5-minute wash in 0.1 M PB and then cryoprotected in 30% sucrose/0.1 M PB at 4°C until they sank. The spinal cords from T11 thoracic (the lesion site) and L4-L6 lumbar segments, along with dorsal root ganglia (DRG) from L4-L6 levels, were located using anatomical landmarks and embedded in Tissue-Tek O.C.T compound (Sakura Finetek, Staufen, Germany) for serial sectioning. The spinal lesion site was sectioned coronally at 25 µm thickness using a Cryostat (Leica Biosystems), and sections were mounted in series of seven cross-sections per slide on Menzel GmbH glass slides. The lumbar segments (L4-L6) underwent a similar sectioning process but were stored in cryopreservation medium within 96-well plates. The DRGs were sectioned sagittally at 30 µm and similarly mounted on glass slides. All tissue sections were then stored at -20°C until further use.

2.7. Immunohistochemistry

Immunohistochemistry labeling was conducted on serial sections of the lumbar spinal cord (L4-L6). Initially, free-floating sections were transferred to phosphate-buffered saline (PBS)

and rinsed at room temperature with gentle shaking for 20 minutes. To facilitate antigen retrieval, sections were incubated in citrate buffer (pH 6.0) in an 85°C-water bath for 25 minutes, followed by three washes in PBS, each lasting 5 minutes. Sections were then blocked to prevent non-specific antibody binding by incubating in 10% donkey serum mixed with 0.2% Triton X-100 in PBS, allowing tissue permeabilization for 2.5 hours at room temperature. Primary antibodies were diluted in a solution of 5% donkey serum with 0.2% Triton X-100 in PBS and applied to the sections, which were then incubated for overnight (c-Fos antibody was incubated over two nights for 48 hours) at 4°C with gentle shaking. After allowing the sections to equilibrate to room temperature for one hour, they were washed three times with 5% donkey serum and 0.2% Triton X-100 in PBS. Secondary antibodies were then applied, diluted in 5% donkey serum in PBS, and the sections were incubated for 2.5 hours while shaking in the dark. Finally, sections were rinsed, dried, and cover-slipped using Fluoromount G (Southern Biotechnology Associates, Birmingham, AL) to prepare for microscopic examination.

2.8. Antibodies

Table 3: Antibody list

Antibody	Host	Isotype	Dilution	Catalog No.	Company/Manufacturer
CGRP	Rabbit	IgG polyclonal	1:1000	24112	ImmunoStar
c-Fos	Rat	IgG monoclonal	1:500	226017	Synaptic Systems
PKC γ	Guinea pig	IgG polyclonal	1:400	PKCg-GP- AF350	Frontier Institute
NeuN	Mouse	IgG monoclonal	1:1000	MAB377	Sigma-Aldrich
GFAP	Guinea pig	IgG polyclonal	1:1500	GP52	Progen
Iba1	Goat	IgG polyclonal	1:400	011-27991	WAKO

Alexa Fluor™ 405	Donkey (anti-rabbit)	IgG polyclonal (H+L)	1:800	A48258	Invitrogen
Alexa Fluor™ 594	Donkey (anti-rat)	IgG polyclonal (H+L)	1:1500	A-21209	Invitrogen
Alexa Fluor™ 594	Donkey (anti-goat)	IgG polyclonal (H+L)	1:1200	A-11058	Invitrogen
Alexa Fluor™ 488	Donkey (anti-guinea pig)	IgG polyclonal (H+L)	1:800	706-545-148	Jackson ImmunoResearch
Cy5™	Donkey (anti-mouse)	IgG polyclonal (H+L)	1:800	715175151	Jackson ImmunoResearch

2.9. Buffer and Solutions

Table 4: List of buffer and solutions

Buffer/Solutions	Reagent	Amount
<u>Perfusion of Mouse:</u>		
0.2 M Solution phosphate (PO ₄) buffer (1 L)	Part A: sodium phosphate monobasic solution	230 ml Part A
	Part B: sodium phosphate dibasic solution	770 ml Part B
Sodium phosphate monobasic solution (230 ml)	NaH ₂ PO ₄	6.348 g
	ddH ₂ O	Make up to 230 ml
Sodium phosphate dibasic solution (770 ml)	Na ₂ HPO ₄	22.022 g
	ddH ₂ O	Make up to 770 ml
0.1 M Phosphate buffer (1 L)	0.2 M Phosphate buffer	500 ml
	ddH ₂ O	500 ml
4% Paraformaldehyde (1 L)	Paraformaldehyde	40 g
	ddH ₂ O	500 ml
	NaOH (10 N)	4 drops
	0.2 M Phosphate buffer	Make up to 1 L

Phosphate(PO_4) buffer saline (PBS) (1 L)	Sodium chloride (NaCl)	9 g
	0.1 M Phosphate buffer	Make up to 1 L
30% sucrose solution (1 L)	Sucrose	300 g
	0.1 M Phosphate buffer	Make up to 1 L

Tissue cryopreservation fluid:

For free-floating staining sections (1 L)	$\text{NaH}_2\text{PO}_4 \cdot 2\text{H}_2\text{O}$	2.4 g
	Na_2HPO_4	9.06 g
	Sucrose	300 g
	Ethylene glycol (EG)	300 ml
	ddH ₂ O	Make up to 1 L

Antigen Retrieval:

Citrate buffer (1 L)	Citric acid	1.92 g
	ddH ₂ O	800 ml
	NaOH (10 N)	Adjust pH to 6.0
	ddH ₂ O	Make up to 1 L
	Tween 20	500 μl

Free-floating staining:

Blocking solution (10 ml)	Donkey serum	1 ml
	Triton X-100	20 μl
	PBS	8.98 ml
Primary antibody solution (10 ml)	Donkey serum	500 μl
	Triton X-100	20 μl
	PBS	9.48 ml
Primary antibody wash-out solution (10 ml)	Donkey serum	500 μl
	Triton X-100	20 μl
	PBS	9.48 ml
Secondary antibody solution (10 ml)	Donkey serum	500 μl
	PBS	9.5 ml
Secondary antibody wash-out solution (10 ml)	Donkey serum	500
	PBS	9.5 ml

2.10. Confocal Microscopy Image Segmentation and Measurement

Confocal images were acquired using an Olympus FluoView FV1000 confocal laser scanning microscope (CLSM). Labelled sections underwent imaging via sequential line scans at a

resolution of 1024×1024 pixels, with a pixel dwell time of 8-12.5 μ s. To ensure consistency, all acquisitions were performed with identical laser settings (including laser intensity, power, photomultiplier tube (PMT) settings, image size, pixel size, and scanning duration) across an image series for each specific labeling, encompassing all animals studied. A montage of confocal image stacks was generated across a depth of 25 μ m, centered on the region of interest at the mid-level of each section. A 20x oil objective was utilized for low-magnification imaging, while oil-immersion 40x and 60x plan-apochromatic objectives facilitated high-magnification image capture. Image acquisition and subsequent processing for quantification were tailored to various desired parameters. Typically, the maximum z-projection of an image stack was employed for cell counting and analysis in ImageJ software (version 1.54f, National Institutes of Health, USA) using 8-bit images.

2.10.1. CGRP-labeling density profile

The analysis of CGRP-expressing fiber labeling density was performed using methodologies previously established by our laboratory (Nees et al. 2016; Sliwinski et al. 2024; Sliwinski et al. 2018). The region of interest was pinpointed utilizing the mouse spinal cord atlas, with specific reference to PKC γ -labeling within lamina III. The dorsoventral boundary of lamina III, as delineated by PKC γ -labeling, was measured and designated as "x." For analysis, a box was positioned at the center of the dorsal horn just below lamina III, with dimensions set to 2x in the dorsoventral direction and 4x in the mediolateral direction. The quantification of labeling density was carried out blindly using ImageJ software. The labeling threshold was carefully adjusted to minimize background noise while ensuring accurate capture of CGRP+ fiber labeling. The labeling density, representing the percentage of positive labeling within the specified analysis box, was calculated for both dorsal horns of each mouse. Values were averaged from at least three sections per mouse, spanning the L4-L6 lumbar spinal cord.

2.10.2. PKC γ immunodensity, number of PKC γ -positive cells

The immunodensity of PKC γ was quantified by measuring the mean gray value of the staining and subtracting the mean value of the background to account for non-specific staining. To

determine the number of PKC γ -positive cells below lamina Iii, a threshold was manually set to encompass all regions displaying PKC γ signals. The number of PKC γ -positive cells below lamina Iii was then calculated for each image, providing a precise measure of PKC γ expression within the sampled tissues. The mean gray value was averaged from at least three sections per mouse, considering the average value of the left and right dorsal horns. The mean number of PKC γ -positive cells was calculated from three sections per animal, encompassing both the left and right sides of the dorsal horn, to ensure a comprehensive assessment. The sections chosen for analysis spanned the L4-L6 lumbar spinal cord.

2.10.3. Laminar distribution analysis of c-Fos-expressing cells

The analysis of the laminar distribution of c-Fos-expressing/activated (c-Fos+) cells within the dorsal horn of lumbar spinal cord sections (L4-L6 segments) was conducted using a maximum z-projection technique on image stacks captured at 20x magnification with a 2.5 μm step size over 8 slices. This approach ensured comprehensive coverage of all slices exhibiting c-Fos+ signals. Following established protocols (Liu et al. 2022), the distribution of c-Fos+ cells was quantified for each analyzed section. Identification and quantification of c-Fos+ cells were performed using the "analyze particles" function in ImageJ, with a size filter set to 10 to 400 μm^2 and circularity parameters ranging from 0.23 to 1.00. These settings, along with threshold adjustments, were employed to accurately enumerate activated cells. Manual verification was conducted on all automated counts to exclude false positives, such as autofluorescent artifacts, ensuring the reliability of the quantification process. For anatomical reference, the dorsal horn laminae (I-V) were delineated on each image based on the mouse spinal cord atlas (Liu et al. 2022) and confirmed through the visualization of CGRP within lamina I and PKC γ within lamina Iii. The mean number of activated c-Fos cells, either overall or within each delineated lamina, was calculated from three sections per animal, spanning the L4-L6 lumbar spinal cord and encompassing both the left and right sides of the dorsal horn, to ensure a comprehensive assessment.

2.10.4. Analysis of inflammation in the lumbar spinal cord

To assess the inflammatory response of reactive neuroglial cells in the lumbar spinal cord, I quantified the immunolabeling density of astrocyte-specific marker GFAP and microglia/macrophage-specific marker Iba1. Immunolabeling for GFAP and Iba1 was conducted using fluorescent illumination with an Olympus FluoView FV1000 confocal laser scanning microscope (CLSM). Each animal contributed one set of serial tissue sections, with at least three sections spanning the L4-L6 spinal cord segments. Images of the dorsal horns of the spinal cord from each animal were captured at 20x magnification using consistent laser settings. Regions of interest (ROIs) corresponding to the spinal cord laminae I-V were delineated based on the mouse spinal cord atlas as demonstrated in the Allen Spinal Cord Atlas (Allen Institute for Brain Science). Using ImageJ software, the mean gray value of each ROI image was measured following auto-thresholding to quantify the intensity of the labeling. The data, expressed as the intensity of immunolabeling, was averaged from the left and right dorsal horns.

2.11. Statistical Analysis

All data in this study are presented as mean \pm standard deviation (SD). Statistical analyses were conducted using GraphPad Prism version 9 (GraphPad Software, San Diego, CA, USA). For comparisons between two groups, either an unpaired Student's t-test or a Mann-Whitney test was used, depending on whether the data were normally distributed. For analyzing differences among multiple groups with one factor, I employed an ordinary one-way ANOVA with Tukey's post hoc analysis for normally distributed data, and a Kruskal-Wallis test followed by a Dunn's test for non-normally distributed data. In cases involving comparisons of two variables across multiple groups, a two-way repeated measures ANOVA was utilized, followed by either a Tukey's post hoc test or a Bonferroni test based on the data setting to control for multiple comparisons. The threshold for statistical significance was set at $p < 0.05$.

To investigate the relationship between [Independent Variable, e.g., CGRP labeling density in laminae III-IV, PKC γ immunodensity in the dorsal horn (DH)] and [Dependent Variable, e.g., withdrawal frequency to a 0.16 g von Frey hair filament (to represent mechanical sensitivity/hypersensitivity)], I performed both correlation and linear regression analyses. Pearson correlation coefficients were calculated to assess the strength and direction of the linear relationship between the [Independent Variable] and the [Dependent Variable]. Statistical significance was determined with a significance level set at $p < 0.05$. A simple linear regression was conducted with the [Dependent Variable] as the outcome and the [Independent Variable] as the predictor. The regression model provided the equation $Y=a+bX$, where Y is the [Dependent Variable], and X is the [Independent Variable]. The coefficient of determination r or R^2 and p -values were reported to evaluate the model's explanatory power and statistical significance.

2.12. Schematic Illustrations

Schematic illustrations for my doctoral dissertation were created using a combination of BioRender (BioRender Inc., Toronto, Canada), and Adobe Illustrator 2020 (Adobe Inc., San Jose, CA, USA). Each platform was utilized to leverage its specific capabilities for generating clear and informative graphical representations of the research concepts. The final figures were exported from these applications as high-resolution images and integrated into the dissertation document, ensuring that each schematic was clearly rendered and effectively communicated the intended scientific information.

3. Results

3.1. Female and Male Mice Exhibit Analogous Sensorimotor Deficits and Progression of NP Following SCI

To investigate whether sex serves as a biological variable in the development of neuropathic pain (NP) following spinal cord injury (SCI), I included both female and male C57BL/6J mice in this experiment (refer to Study 1, Figure 3). The study commenced by utilizing a moderate thoracic contusion SCI model to induce persistent and robust hindlimb sensorimotor deficits, particularly symptoms associated with NP. Behavioral alterations in response to SCI were assessed longitudinally and compared with those observed in sham-operated subjects to confirm the successful induction of the injury. Accordingly, to assess potential sex differences in the progression of SCI-NP over time, NP-associated behaviors were evaluated at various observational time points to enable cross-sex comparisons.

3.1.1. Moderate contusion SCI elicits sustained hindlimb sensorimotor deficits in mice of both sexes

To establish a robust model for studying SCI-NP, I considered using the low thoracic contusion model (vertebral level T7-T10). This model mimics a clinically relevant, anatomically incomplete lesion and is widely recognized and utilized for this specific emphasis (Chen et al. 2022; Kramer et al. 2017). Therefore, in SCI mice, I induced a moderate contusion (50 kdyn) at the T11 thoracic level of the spinal cord, while sham mice underwent a laminectomy at the T9 vertebra. The actual values of impact force and tissue displacement during contusion modeling were recorded to ensure that the parameters fell within the range necessary for creating consistent injuries and for excluding subjects beyond this range (Figure 4, A and B). The previous study suggested that implementing stringent limits for force (± 5 kdyn) and displacement (within a 200 μm range) could mitigate variability in behavioral and histological outcomes, thereby facilitating the enhanced detection of nuanced alterations (Ghasemlou et al. 2005). The recorded impact force delivered exhibited very little variation from the intended

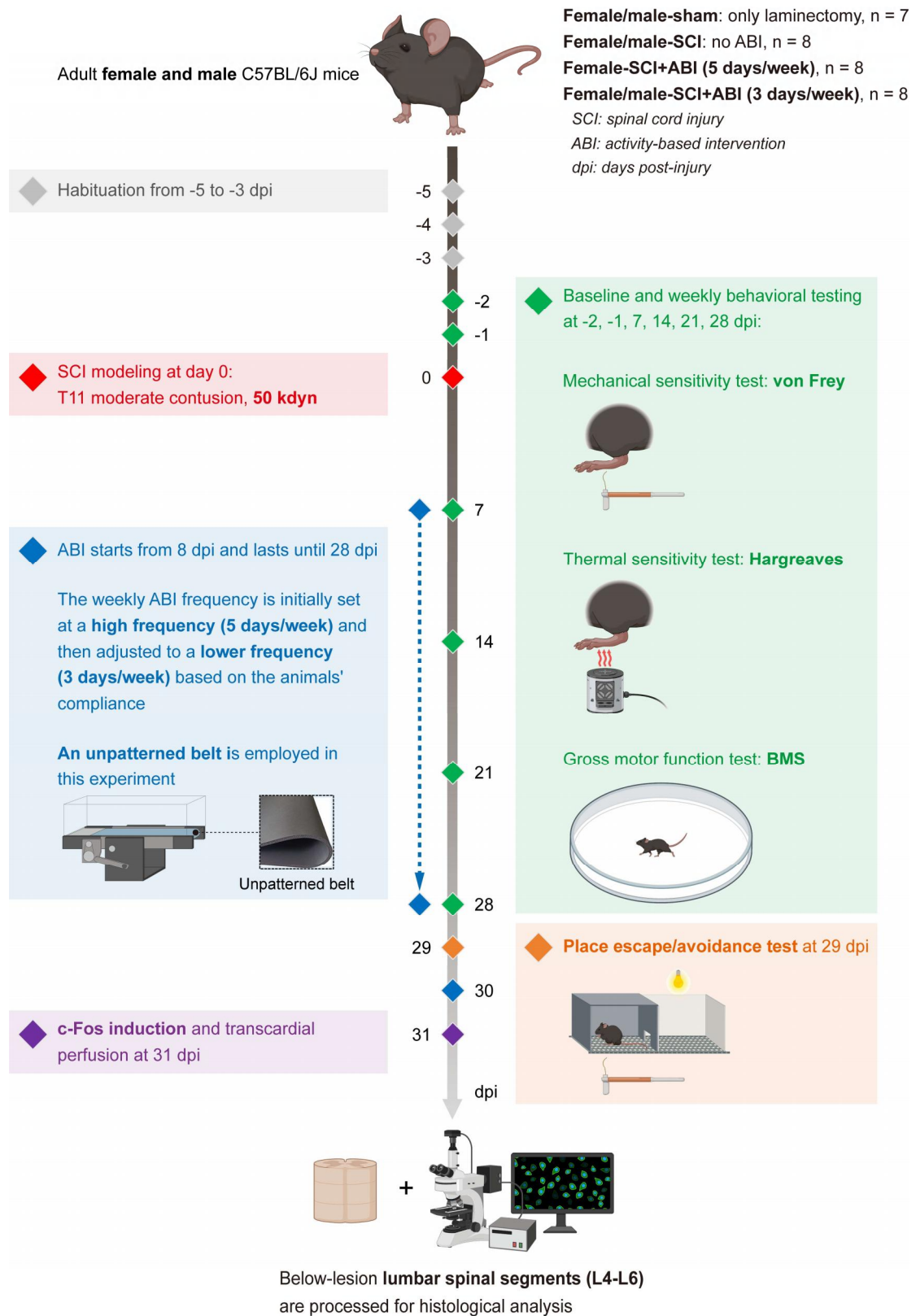


Figure 3, Study 1: Investigating potential sex differences in the development of SCI-NP and its alleviation through ABI

force in females (53.0 ± 1.85 kdyn) and males (53.0 ± 1.51 kdyn), demonstrating consistency between the sexes (Figure 4A). Tissue displacement ranged from 498.0 to 532.7 μm in females and from 495.8 to 574.7 μm in males, indicating stable and consistent contusion modeling outcomes between the sexes (Figure 4B).

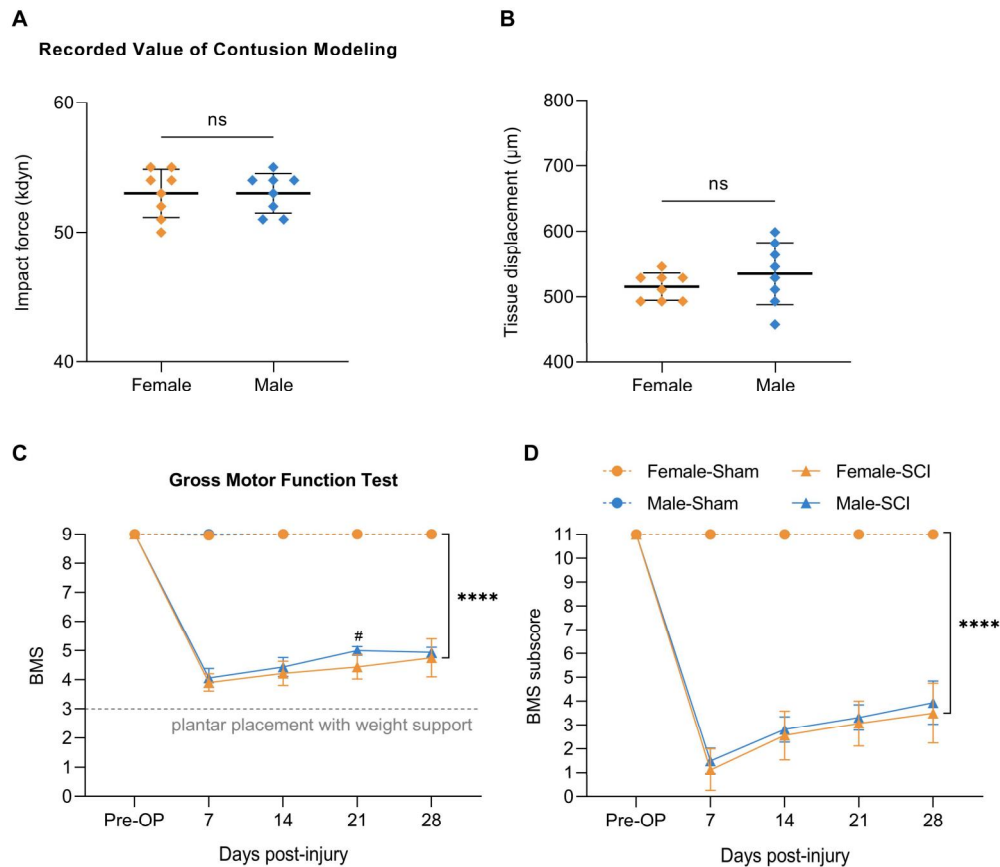


Figure 4: Moderate contusion SCI leads to evident hindlimb gross motor deficits in both sexes of mice.

Recorded values of impact force (A) and tissue displacement (B) during spinal cord T11 moderate contusion modeling (female/male-SCI: $n = 8$). Weekly hindlimb gross motor function BMS (C) and its subscores (D) reveal considerable motor deficits induced by SCI. Overall, except for the time point of 21 dpi when conducting BMS (C), no other statistical differences are observed between the sexes of SCI mice (female/male-sham: $n = 7$; female/male-SCI: $n = 8$). Mean \pm SD. A and B: unpaired t-test, ns: not significant. C and D: Two-way repeated measures ANOVA, group differences, **** $p < 0.0001$; post hoc Tukey test, # $p < 0.05$. * stands for comparisons between sham and SCI groups, and # stands for comparisons between sexes within the sham or SCI group.

The hindlimb motor function was monitored as early as 1 dpi to confirm the successful induction of experimental paralysis immediately following SCI, followed by a series of weekly behavioral tests starting at 7 dpi. SCI resulted in significant impairments in hindlimb gross motor function throughout the study duration in both female and male mice, compared to their respective sham counterparts, as evidenced by the Basso Mouse Scale (BMS) and its subscores (Figure 4, C and D). At 7 dpi, both female and male SCI mice demonstrated a gradual restoration of plantar weight support function ($BMS \geq 3$), enabling the use of the von Frey and Hargreaves tests on the plantar surface to examine below-level sensory functions. By 28 dpi, the average BMS ranged from 4 to 5, indicating recovery of plantar stepping frequencies and hindlimb coordination. At 21 dpi, male SCI mice exhibited a transient higher BMS than their female counterparts (Figure 4C). Except for this, throughout the 3-week post-SCI observational period, there were no other statistically significant differences in the BMS or its subscores between females and males within both the sham and SCI groups.

Next, SCI-induced alternations in the mechanical sensitivity of hindpaws were assessed using the von Frey hair monofilament test. At 7 dpi, both female and male mice with SCI exhibited significantly increased withdrawal responses to non-noxious stimuli delivered by light von Frey hair filaments (0.16 and 0.4 g) compared to their sham counterparts, indicating the onset of below-level mechanical allodynia (Figure 5, A and B). This sensory impairment persisted in SCI mice until the end of the study. Notably, prior to the SCI procedure, male mice allocated to the SCI group exhibited a slightly higher baseline sensitivity to both light filaments compared to their SCI female counterparts (i.e., Pre-OP; Figure 5, A and B). However, following injury, this sex-related sensitivity did not bear significance. To more comprehensively assess the cognitive perception of mechanical allodynia, taking into account the supraspinal processing of NP in both female and male SCI mice, I utilized the Place Escape/Avoidance Paradigm (PEAP, Figure 5, C and D) at 29 dpi. During the initial 2 x 5-minute free exploration phase, devoid of any stimuli, the time each mouse spent on the dark side (preferred side) was recorded to establish each individual's baseline. Subsequently, in the

following 3 x 5-minute testing phase, when the mice remained on the dark side, a non-noxious mechanical stimulus was administered by applying a 0.16 g von Frey hair filament to the plantar surface of the hindpaws, alternating between the left and right paws every 15 seconds (Figure 5C). Comparative analysis with sham animals revealed that SCI mice showed a significant, graded reduction in the time spent in the preferred dark compartment, relative to their respective baselines for each interval (Figure 5D). Consequently, SCI mice exhibited proactive tendencies to escape and/or avoid the dark environment, where they experienced mechanical allodynia in response to normal, non-noxious mechanical stimuli. Additionally, these mice demonstrated a preference for the light side (aversive side), indicative of seeking pain relief. These findings are in alignment with the results obtained from von Frey hair testing alone, highlighting conscious SCI-induced mechanical allodynia presentation.

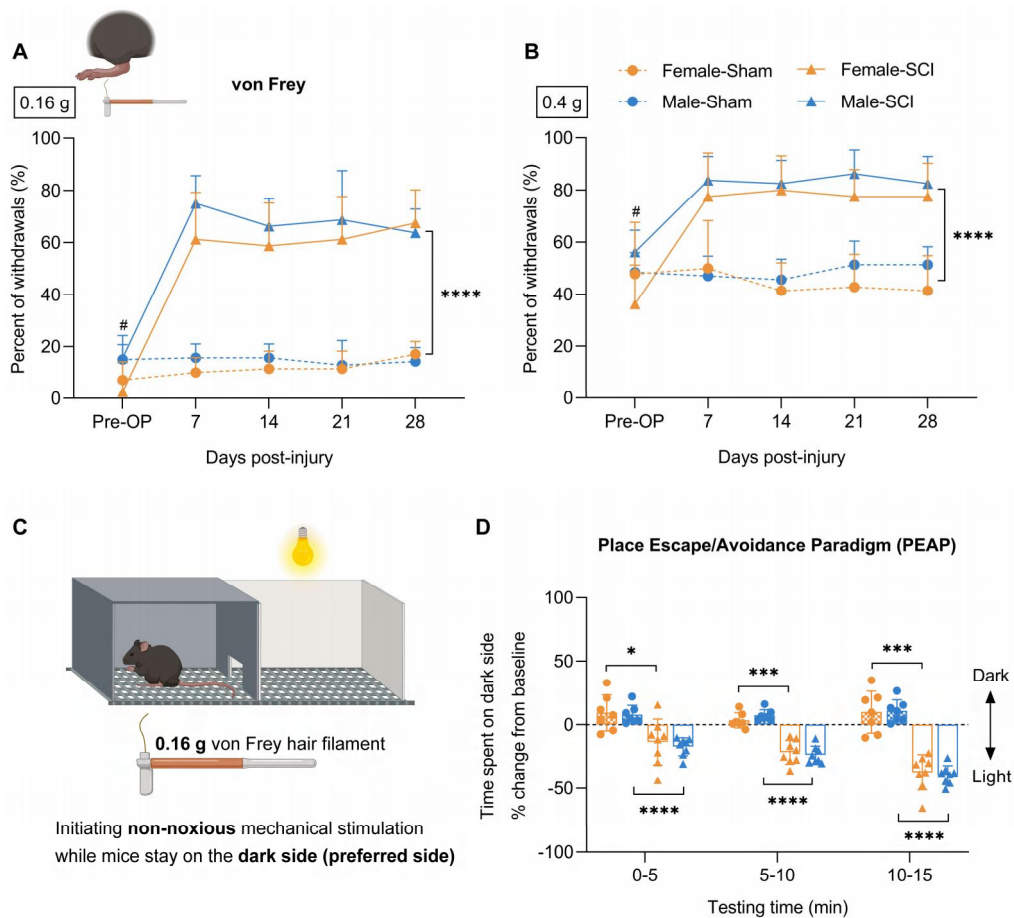


Figure 5: Persistent SCI-induced below-level mechanical allodynia in female and male mice.

SCI mice of both sexes show a significant increase in hindpaw withdrawal responses to non-noxious mechanical stimuli, 0.16 (A) and 0.4 g (B) von Frey hair filaments (female/male-sham: n = 7; female/male-SCI: n = 8). The graphic illustrates the Place Escape/Avoidance Paradigm (PEAP, C), where mice in a preferred dark compartment receive non-noxious stimuli from a 0.16 g von Frey hair filament during the testing phase. Female and male SCI mice demonstrate escape and/or avoidance behaviors to non-noxious stimuli in a dark compartment compared to their baseline behaviors in the absence of stimuli (during the free exploration period), unlike the sham groups, which do not exhibit a change in preference upon stimulation (D). Mean \pm SD. A and B: Two-way repeated measures ANOVA, group differences, **** p < 0.0001; post hoc Tukey test, # p < 0.05. * stands for comparisons between sham and SCI groups, and # stands for comparisons between sexes within the sham or SCI group. D: Two-way repeated measures ANOVA, group differences, p < 0.0001; post hoc Tukey test, * p < 0.05, *** p < 0.001, **** p < 0.0001, * stands for comparisons between sham and SCI groups of each sex.

In contrast to the observations with non-noxious filaments, both sexes of SCI mice exhibited a significant reduction in withdrawal responses to noxious mechanical stimuli (0.6 and 1.4 g von Frey hair filaments) (Figure 6, A and B) compared to their sham counterparts. This sensory deficit was evident as early as 7 dpi and persisted for the duration of the study. These results suggest that SCI led to the initiation and maintenance of below-level mechanical hypoalgesia.

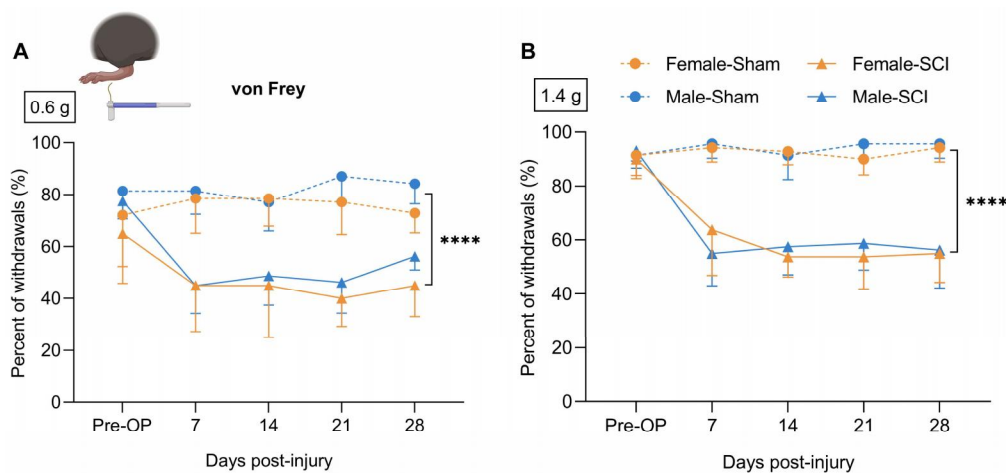


Figure 6: SCI-induced below-level mechanical hypoalgesia in female and male mice.

SCI mice of both sexes exhibit a significant reduction in hindpaw withdrawal responses to noxious mechanical stimuli, 0.6 (A) and 1.4 g (B) von Frey hair filaments (female/male-sham: $n = 7$; female/male-SCI: $n = 8$). Mean \pm SD. Two-way repeated measures ANOVA, group differences, **** $p < 0.0001$.

Moderate contusion SCI resulted in a notable increase in heat sensitivity, as measured by the Hargreaves test, in both sexes of mice throughout the post-operative period (Figure 7). This was indicated by a considerable reduction in withdrawal latency to heat stimuli compared to sham mice. These observations collectively suggest that moderate thoracic SCI induces significant and sustained below-level thermal hyperalgesia in mice of both sexes.

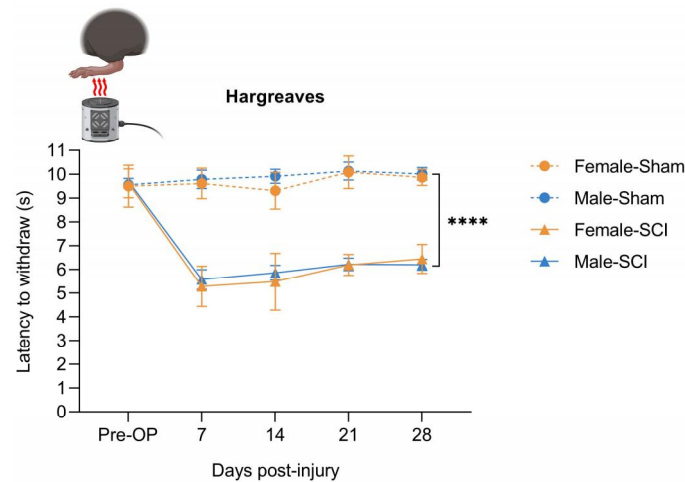


Figure 7: Sustained and robust SCI-induced below-level thermal hyperalgesia in female and male mice.

Both female and male SCI mice demonstrate notably heightened thermal sensitivity to heat stimuli, Hargreaves method (female/male-sham: $n = 7$; female/male-SCI: $n = 8$). Mean \pm SD. Two-way repeated measures ANOVA, group differences, **** $p < 0.0001$.

3.1.2. Female and male mice demonstrate similar progression patterns of NP-associated behaviors following SCI

Female and male mice were specifically investigated for differences in the progression of NP-associated behaviors, including mechanical allodynia and thermal hyperalgesia, over time following SCI. Alterations from each SCI mouse's pre-operative baseline were analyzed and

displayed as proportional changes. Accordingly, SCI-induced mechanical hypersensitivity was represented as a positive change on the graph, reflecting significantly increased withdrawal responses to non-noxious stimuli (Figure 8, A and B). Conversely, thermal hypersensitivity was shown as a negative change, correlating with substantial decreases in withdrawal latency to heat stimuli (Figure 8C).

From 7 to 28 dpi, female SCI mice appeared to exhibit a slightly greater increase in withdrawal responses compared to males, with a significant difference at 14 dpi using a 0.4 g von Frey hair filament (Figure 8B). However, no significant sex differences were noted at other observational time points. Once established at 7 dpi, mechanical hypersensitivity/allodynia remained consistent throughout the study period for both sexes (Figure 8, A and B). Thermal hyperalgesia

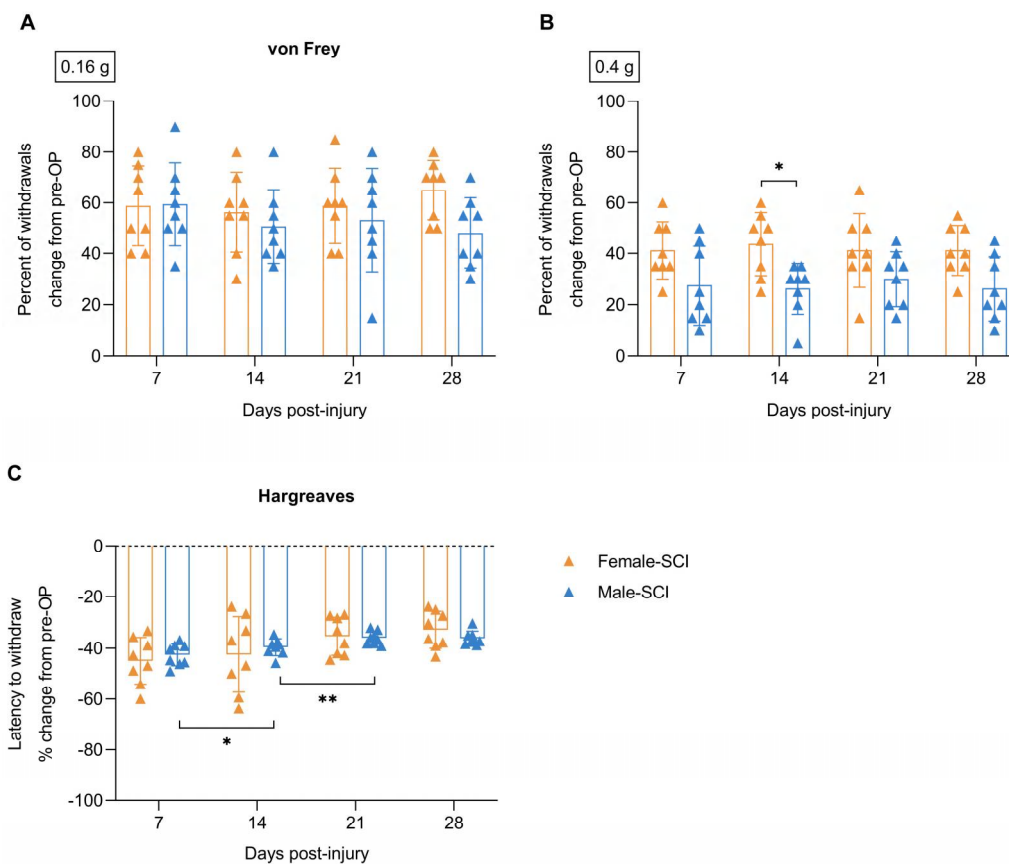


Figure 8: The progression of mechanical and thermal hypersensitivity in female and male mice following the induction of SCI.

Female and male SCI mice exhibit comparable increases in withdrawal rates to non-noxious mechanical stimuli, 0.16 (A) and 0.4 g (B) von Frey hair filaments, as well as similar changes in withdrawal latency to heat stimuli (Hargreaves method, C), from their respective pre-operative level, assessed weekly (female/male-sham: n = 7; female/male-SCI: n = 8). Mean \pm SD. Two-way repeated measures ANOVA: 0.16 g: not significant, 0.4 g: $p_{\text{sex factor}} = 0.0128$, $p_{\text{time factor}} = 0.9054$, Hargreaves: $p_{\text{sex factor}} = 0.8826$, $p_{\text{time factor}} = 0.0031$; post hoc Bonferroni test (B (0.4 g), sex as variable at each time point), $*p < 0.05$; post hoc Tukey test (C (Hargreaves), time point as variable within each sex), $*p < 0.05$, $**p < 0.01$.

persisted in both sexes post-SCI (Figure 8C). Male SCI mice showed a mild, limited reduction in thermal hyperalgesia from 7 to 21 dpi; however, the thermal sensitivity persisted, as at 28 dpi it remained the same as at 21 dpi and did not return to pre-operative levels ($x = 0$). Collectively, these findings confirm no significant sex differences in the behavioral manifestations of SCI-NP.

Taken together, the findings from Section 3.1 highlight that moderate contusion SCI induced comparable hindlimb sensorimotor deficits in both female and male mice. These impairments, including early and persistent gross motor dysfunction, as well as mechanical allodynia/hypoalgesia, and thermal hyperalgesia did not exhibit sex differences over time.

3.2. ABI Mitigates SCI-NP-Associated Symptoms in Both Sexes of Mice

Given the potential sex differences in the neurobiological mechanisms underlying NP (Ghazisaeidi et al. 2023), it is plausible that females and males may exhibit differential responses to various therapeutic interventions. This variance in response could be attributed to differences in the targeted components and mechanisms of these interventions. Therefore, integrating sex as a biological variable in the treatment of activity-based interventions (ABIs) for SCI-NP is essential. In the present study, I consistently utilized the treadmill-based ABI paradigms, which require animals to support their full body weight and alternate their limbs in a rhythmic pattern while running on the belt. Initially, a high-frequency ABI regimen (5

days/week) was employed, followed by a comparison of behavioral outcomes with a lower-frequency regimen (3 days/week). This adjustment in weekly ABI frequency was motivated by observed low compliance among the female animals during the high-frequency regimen in the first experimental cohort, aiming to improve adherence and minimize potential stress-related effects. Both paradigms were initiated from 8 dpi and continued until 28 dpi. Notably, an unpatterned belt made of EVA foam rubber material was used in this experiment (refer to Study 1, Figure 3). Accordingly, the study was extended to include both female and male C57BL/6J mice. The modified protocol was then used to assess the respective responses of female and male mice to ABI. Furthermore, the experiment aimed to evaluate the efficacy of ABI in mitigating SCI-NP-associated symptoms across both sexes.

3.2.1. High-frequency ABI manifests instability in efficacy for alleviating SCI-NP: readout from comparative analysis with lower-frequency ABI

In the experimental design, I initially adopted a high-frequency ABI protocol (5 days/week, 2 x 15 mins/day) due to its proven effectiveness in reducing SCI-NP and its common use in our research setting (Nees et al. 2016; Sliwinski et al. 2018). However, challenges arose with animal compliance, marked by abrupt stops during running that led to entrapment on the treadmill belt. To resolve this, I switched to a less intensive regimen (lower-frequency ABI, 3 days/week, 2 x 15 mins/day), which significantly improved mouse compliance. To further optimize the ABI paradigm, comparative analyses of weekly behavioral tests were conducted to evaluate the efficacy of the protocols in alleviating SCI-NP symptoms. To clarify, the behavioral readouts reported here are exclusively from female mice in the sham, SCI, and both high- and lower-frequency ABI groups utilizing an unpatterned treadmill belt (Study 1, Figure 3), as the high-frequency ABI was initially applied to a cohort of female mice.

Both high- and lower-frequency ABI paradigms were initiated at 8 dpi as an early intervention for SCI-NP. By 14 dpi, mice in the high-frequency ABI group showed a significant reduction in withdrawal responses to non-noxious mechanical stimuli (0.16 and 0.4 g von Frey hair

filaments), whereas the lower-frequency ABI did not exhibit analgesic effects at this time, with withdrawal rates similar to those of the SCI group (Figure 9, A and B). By 21 dpi, however, mice in the high-frequency group exhibited notably increased withdrawal responses to the 0.16 g filament, along with a tendency to increase responses to the 0.4 g filament, suggesting a reversal in the alleviation of mechanical hypersensitivity, even though the response rates were still lower than in untreated SCI mice. By 28 dpi, the high-frequency ABI group showed significantly increased responses to both filaments compared to earlier time points (14 and 21 dpi) and were higher than those in the lower-frequency and sham groups. Nevertheless, they still demonstrated an overall reduction compared to untreated SCI mice when exposed to the 0.16 g filament. Lower-frequency ABI, while not showing the early alleviation of mechanical

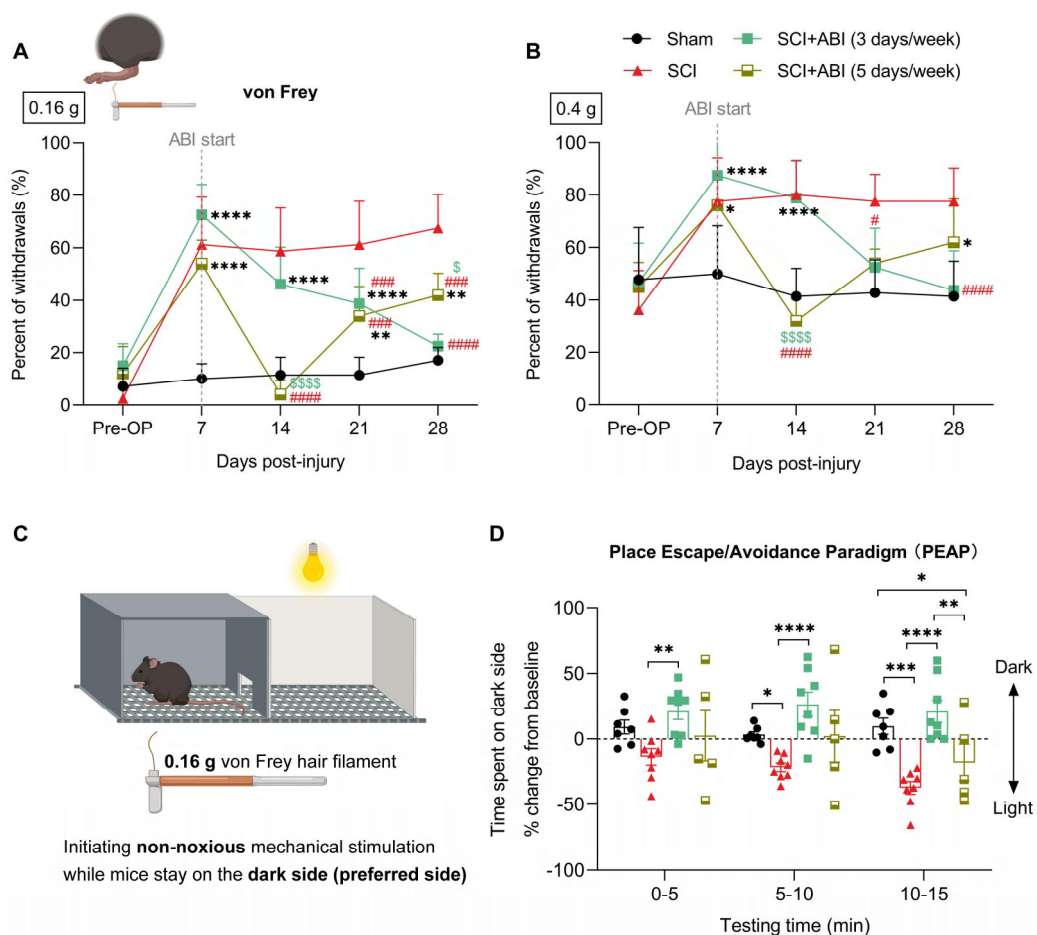


Figure 9: High-frequency ABI exhibits instability in alleviating below-level mechanical hypersensitivity compared to lower-frequency ABI.

Hindpaw withdrawal responses in mice to non-noxious mechanical stimuli, 0.16 (A) and 0.4 g (B) von Frey hair filaments. The high-frequency ABI group exhibits fluctuating and limited mitigation of mechanical allodynia. In contrast, the lower-frequency ABI consistently alleviates this condition (female, sham: $n = 7$; SCI: $n = 8$; SCI+ABI (lower-frequency 3 days/week): $n = 8$; SCI+ABI (high-frequency 5 days/week): $n = 5$). Graphic illustration of the Place Escape/Avoidance Paradigm (PEAP, C). Mice subjected to high-frequency ABI actively escape and/or avoid painful sensations upon receiving non-noxious mechanical stimuli in the preferred dark environment (D). In comparison, mice receiving lower-frequency ABI do not demonstrate a place preference for the light environment after receiving the stimuli, similar to sham animals. Mean \pm SD. Two-way repeated measures ANOVA, group differences, $p < 0.0001$; post hoc Tukey test. Symbols in A and B indicate group comparisons: * (black) shows differences from the sham group, # (red) from the SCI group, and \$ (light green) marks differences between high-frequency and lower-frequency ABI groups. In D, * (black) denotes statistical differences between the specified groups. $*p < 0.05$, $**p < 0.01$, $***p < 0.001$, $****p < 0.0001$; $\#p < 0.05$, $###p < 0.001$, $####p < 0.0001$; $\$p < 0.05$, $$$$$p < 0.0001$.

allodynia as observed with high-frequency ABI at 14 dpi, led to a gradual decrease in withdrawal responses over time, aligning with the sham group by the end of the study (i.e., 28 dpi; Figure 9, A and B). The PEAP results (Figure 9D) indicated that mice in the high-frequency ABI group displayed behaviors suggesting active escape and/or avoidance of pain, preferring light environments indicative of seeking pain relief similar to SCI animals. In contrast, low-frequency ABI mice did not develop a place preference for the light side, behaving similarly to sham animals. These findings suggest that while high-frequency ABI initially reduced symptoms, its effects were less stable over time compared to the consistent improvements seen with lower-frequency ABI.

Comparative analyses of other behavioral responses revealed no significant differences between the mice subjected to high-frequency ABI and those treated with lower-frequency ABI (Supplementary Figure 1/Figure S1).

Considering both the well-being of the animals and the consistent efficacy of ABI in mitigating SCI-NP, the lower-frequency ABI paradigm emerged as a more optimal treatment compared to the high-frequency paradigm. Therefore, subsequent experiments continued to apply the modified protocol to SCI+ABI mice.

3.2.2. Female and male SCI mice demonstrate comparable responses to ABI and present amelioration of mechanical allodynia

To investigate potential differences in the response to ABI between female and male SCI mice, I conducted multiple sensorimotor behavioral tests at multiple post-operative timepoints immediately following SCI. Specifically, a treadmill-based ABI paradigm was administered on an unpatterned running belt (3 days/week, 2 x 15 mins/day) to both sexes of SCI mice, starting in the subacute phase (8 dpi) and continuing until 28 dpi, the intermediate phase of SCI (refer to Study 1, Figure 3). As SCI mice gradually recover partial hindlimb motor function, I increased the daily ABI velocity based on their daily performance to ensure the animals ran in the middle area of the running belt, indicative of "moderate intensity". Both female and male mice were trained at consistent velocities each day the ABI was applied (Figure 10).

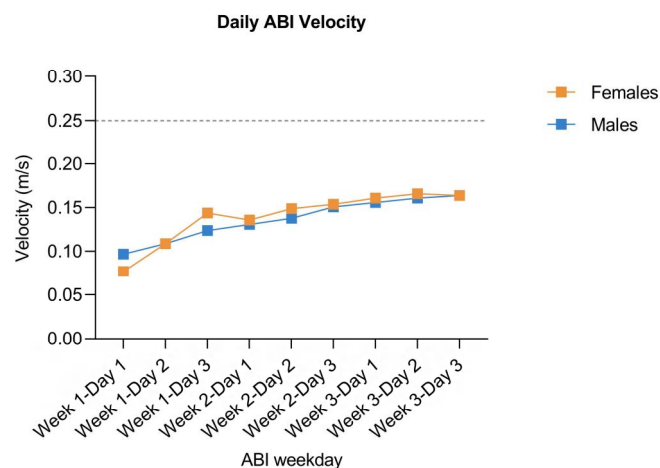


Figure 10: Daily ABI velocity recordings for female and male mice.

The dotted line indicates the maximum velocity setting for the ABI.

From 14 to 28 dpi, SCI+ABI mice of both sexes showed a gradual decrease in withdrawal responses to non-noxious mechanical stimuli, as tested with 0.16 and 0.4 g von Frey hair filaments (Figure 11, A-D). At 21 dpi, a significant alleviation of mechanical allodynia was observed in both female and male SCI mice with ABI. By the end of the study, the withdrawal rates of SCI+ABI mice, across both sexes, were comparable to those of the sham group, suggesting that ABI successfully reversed SCI-induced below-level mechanical allodynia.

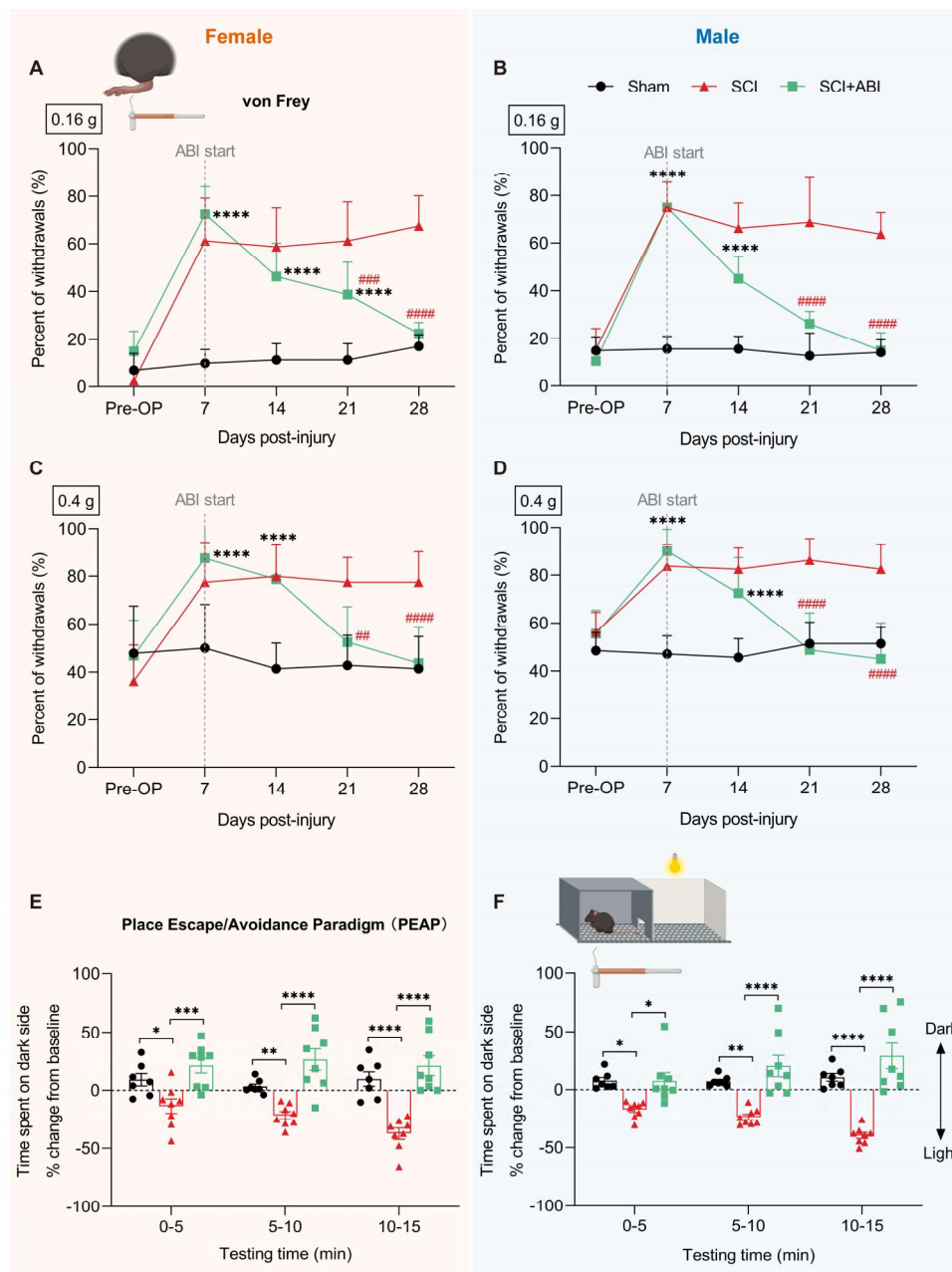


Figure 11: ABI mitigates SCI-induced below-level mechanical allodynia in both female and male mice.

A gradual and significant reduction in hindpaw withdrawal responses to non-noxious mechanical stimuli, applied with 0.16 and 0.4 g von Frey hair filaments, is observed in both female (**A** and **C**) and male (**B** and **D**) SCI+ABI mice (female/male-sham: n = 7; female/male-SCI: n = 8; female/male-SCI+ABI: n = 8). The Place Escape/Avoidance Paradigm (PEAP, **E** and **F**) confirms that SCI+ABI mice of both sexes do not escape and/or avoid sensations upon receiving non-noxious mechanical stimuli (0.16 g filament) in the dark environment. Mean \pm SD. Two-way repeated measures ANOVA, group differences, $p < 0.0001$; post hoc Tukey test. Symbols in **A-D** indicate group comparisons: * (black) denotes differences from the sham group, # (red) from the SCI group. In **E** and **F**, * (black) signifies statistical differences between specified groups. * $p < 0.05$, ** $p < 0.01$, *** $p < 0.001$, **** $p < 0.0001$; ## $p < 0.01$, ### $p < 0.001$, #### $p < 0.0001$.

The Place Escape/Avoidance Paradigm (PEAP) conducted on both female and male SCI+ABI mice revealed that they did not escape and/or avoid when exposed to a 0.16 g mechanical stimulus in a dark compartment (Figure 11, **E** and **F**). This response was consistent with that observed in their sex-matched, sham counterparts. In contrast, mice with SCI alone, regardless of sex, exhibited a significant decrease in time spent on the dark side during the testing period (when exposed to a non-noxious mechanical stimulus) compared to the free exploration period (when no stimulus was present). Taken together, these results indicate that ABI mitigates SCI-induced below-level mechanical allodynia, with this effectiveness being independent of sex.

However, neither female nor male mice exhibited any improvement in response to noxious mechanical stimuli with ABI (Figures 12A-D). This observation is consistent with previous findings from our laboratory (Nees et al. 2016; Sliwinski et al. 2018), collectively indicating that ABI has no beneficial effect on SCI-induced mechanical hypoalgesia in either sex. In addition, throughout the short-term study period, ABI did not effectively alleviate below-level thermal hyperalgesia in SCI mice of both sexes (Figure 12, **E** and **F**). This observation is similar to findings previously reported by our laboratory, where an early short-term ABI (5 weeks), initiated at 7 dpi, did not effectively alleviate thermal hyperalgesia in SCI mice (Nees et al. 2016). However, my colleague found that a 4-week continuous ABI, initiated at 42 dpi,

effectively mitigated thermal hypersensitivity (Sliwinski et al. 2018). This discrepancy highlights the critical importance of the timing and duration of ABI for its efficacy in alleviating SCI-NP.

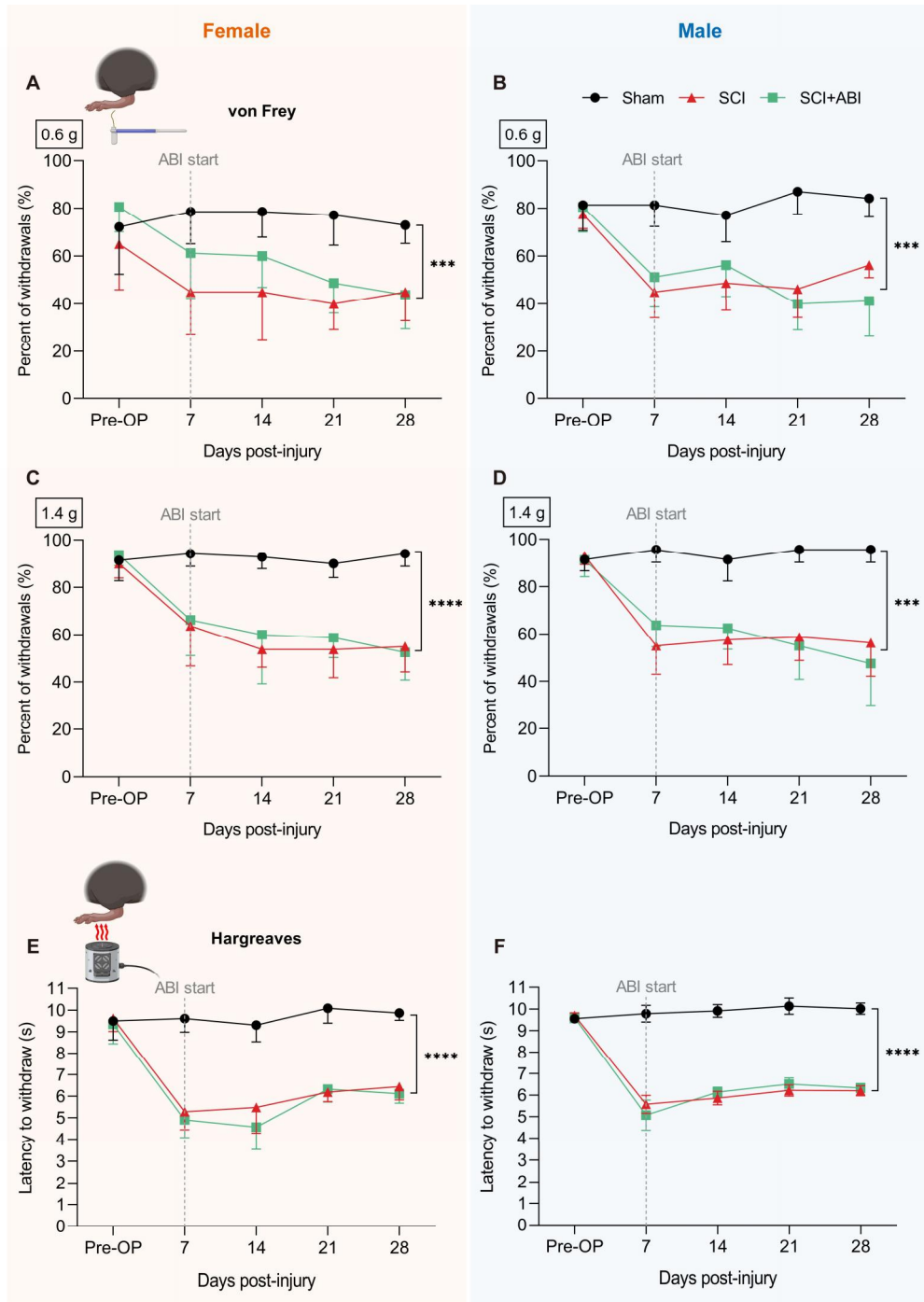


Figure 12: Lack of improvement in SCI-induced mechanical hypoalgesia and thermal hyperalgesia in mice of both sexes following ABI.

ABI does not reverse the SCI-induced reduction in hindpaw withdrawal responses to noxious mechanical stimuli applied with 0.6 and 1.4 g von Frey hair filaments in both female (**A** and **C**) and male (**B** and **D**) mice. SCI mice of both sexes subjected to ABI show no improvement in SCI-induced thermal hyperalgesia as tested by the Hargreaves method (**E** and **F**) (female/male-sham: $n = 7$; female/male-SCI: $n = 8$; female/male-SCI+ABI: $n = 8$). Mean \pm SD. Two-way repeated measures ANOVA, group differences, $***p < 0.001$, $****p < 0.0001$.

All SCI groups showed slight recovery in hindlimb gross motor function, as evaluated by BMS and its subscores (Figure 13, A-D). However, the ABI paradigm did not lead to any enhancement of gross motor recovery in the hindlimbs among mice of either sex.

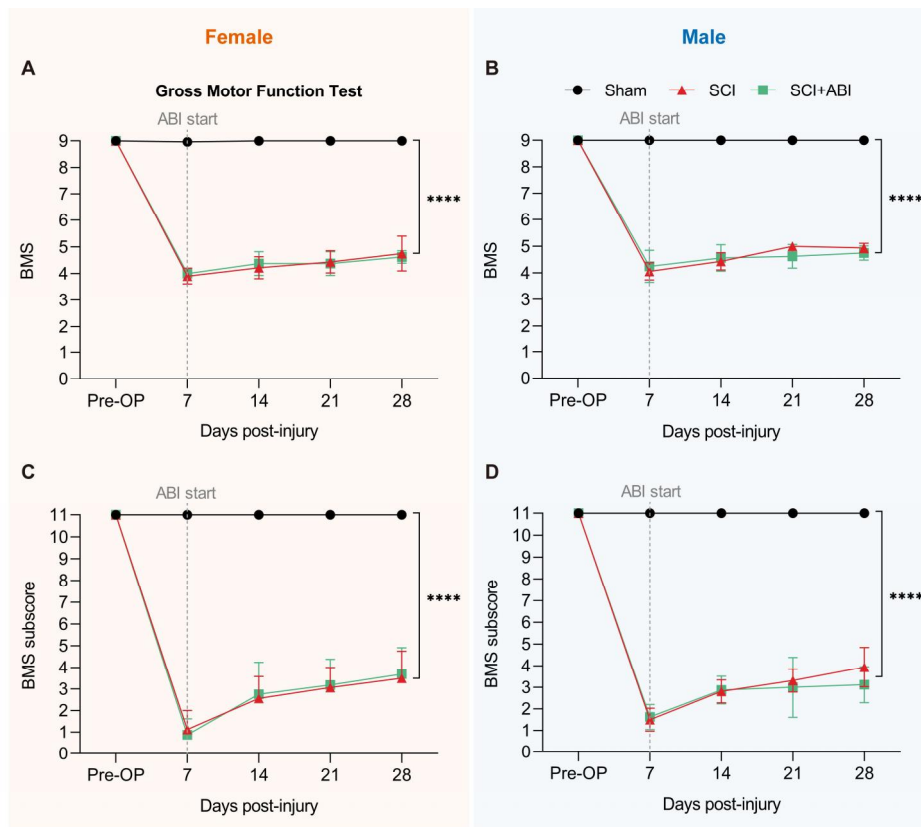


Figure 13: No promotion of hindlimb gross motor recovery induced by ABI observed in mice of both sexes.

Hindlimb gross motor function, assessed weekly using BMS and subscores reveals no enhanced recovery by ABI in both female (**A** and **C**) and male (**B** and **D**) SCI mice, respectively (female/male-sham: $n = 7$;

female/male-SCI: n = 8; female/male-SCI+ABI: n = 8). Mean \pm SD. Two-way repeated measures ANOVA, group differences, **** $p < 0.0001$.

Overall, female and male SCI mice exhibited parallel behavioral responses to ABI, demonstrating a significant amelioration of below-level mechanical allodynia.

3.3. ABI on a Patterned Treadmill Belt Promotes Faster SCI-NP

Reduction Compared to an Unpatterned Treadmill Belt

To assess whether varying intensities of mechanoreceptive and proprioceptive inputs during ABI differentially affect the efficacy in alleviating symptoms associated with SCI-NP, a study was proposed. I anticipate this investigation to provide foundational insights for tailoring ABI modifications to meet clinical needs. In this experiment, ABI paradigms administered on either an unpatterned or patterned treadmill belt were applied to female mice starting from the subacute phase of SCI (8 dpi). Notably, since female ABI mice trained on an unpatterned belt, the sham control group, and the SCI untreated group were already included in my study settings in the previous sections, I only added a new cohort of 8 female SCI mice trained on the patterned belt to minimize the use of experimental animals (refer to Study 2, Figure 14).

An unpatterned belt (UPB) offers a smooth, consistent surface for mice, presenting minimal mechanoreceptive/proprioceptive challenges. In contrast, a patterned belt (PB), equipped with "acupressure points", is designed to deliver increased mechanoreceptive stimuli as mice navigate its surface. Moreover, the irregular patterns are expected to demand greater effort to maintain balance, potentially enhancing proprioceptive input from the joint capsules and muscle spindles in the hindlimbs (Figure 15).

To ensure control of variables, the daily ABI velocity was standardized for mice trained on both unpatterned and patterned belts (Figure 16).

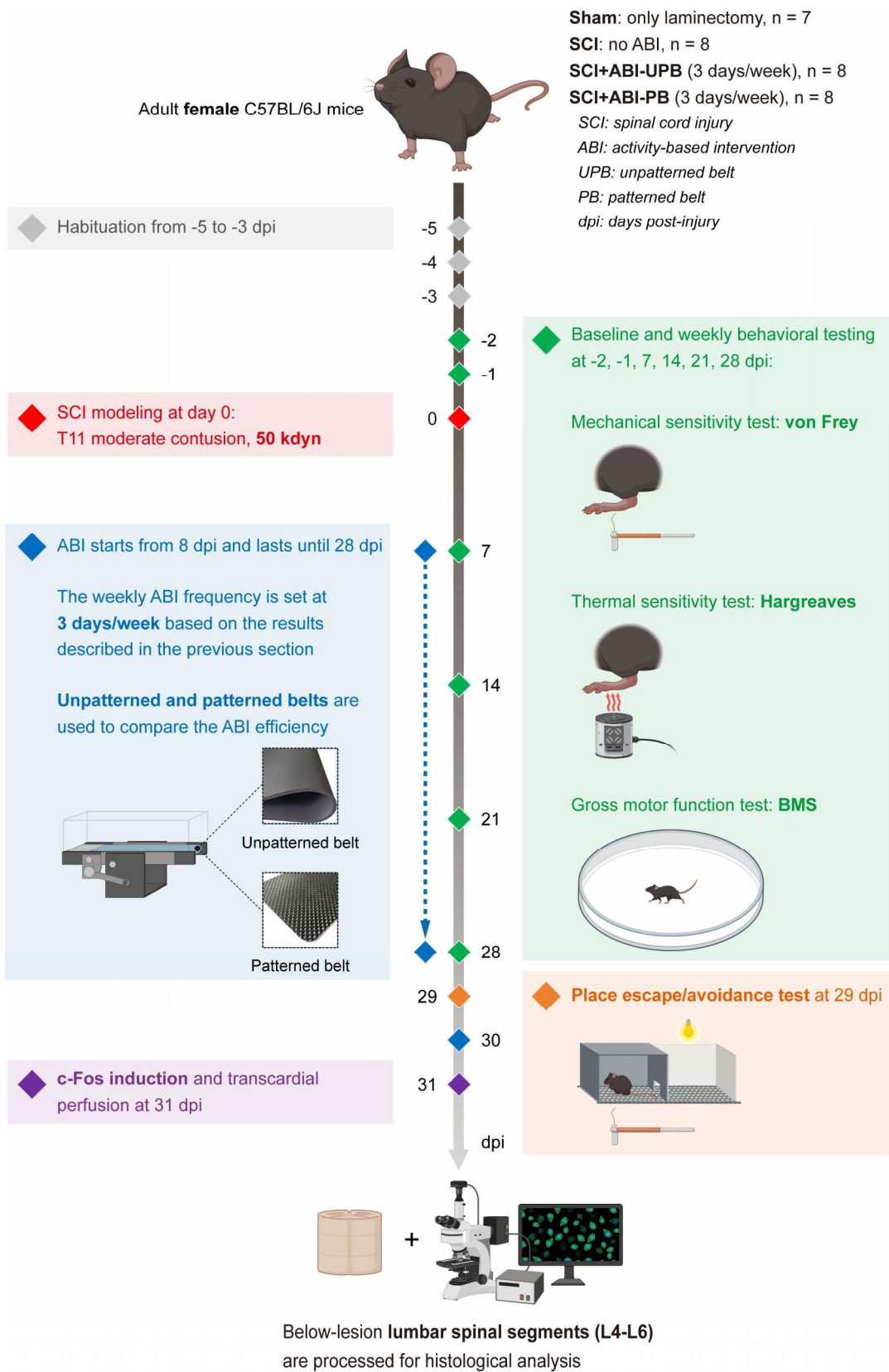


Figure 14, Study 2: Examining the role of increased sensory input during ABI in improving its efficacy in mitigating SCI-NP.

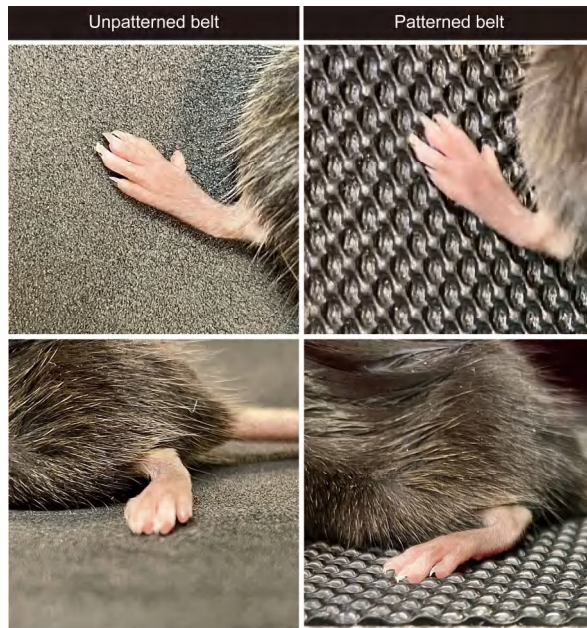


Figure 15: Representative images of an unpatterned belt and a patterned belt.

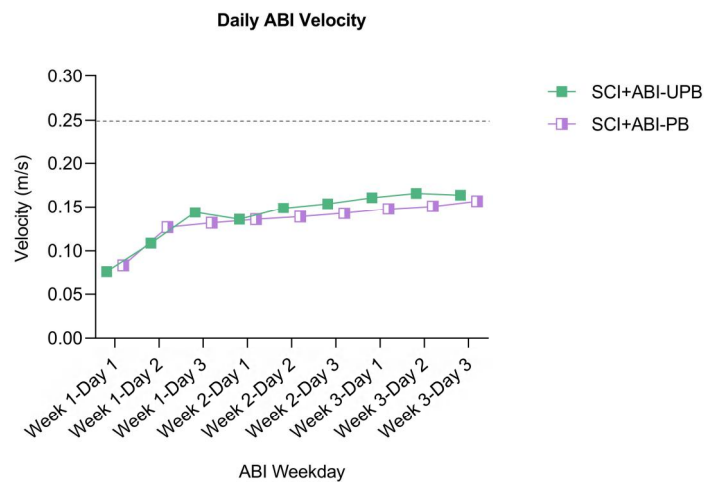


Figure 16: Daily ABI velocity recordings for female mice trained on an unpatterned belt or a patterned belt.

The dotted line indicates the maximum velocity setting for the ABI.

From 14 to 28 dpi, ABI paradigms using both unpatterned (ABI+UPB) and patterned belts (ABI+PB) gradually alleviate SCI-induced mechanical allodynia in mice. This observation was evidenced by the progressive decrease in withdrawal responses to 0.16 and 0.4 g non-noxious

von Frey hair filaments (Figure 17, A and B). Interestingly, at 14 dpi, SCI mice trained on a patterned belt exhibited significantly reduced withdrawal responses compared to those without ABI, while those on an unpatterned belt did not show improvements. By 21 dpi, the ABI paradigm with a patterned belt significantly reduced withdrawal responses, closely matching those of sham animals, unlike the paradigm using an unpatterned belt, which showed less improvement. By the end of the study, between ABI-treated groups (both UPB and PB) and the sham group, no statistical differences were found in the withdrawal responses to both non-noxious filaments (i.e., 28 dpi; Figure 17, A and B). This result highlights the efficacy of the ABI approach in alleviating SCI-induced mechanical allodynia, independent of the belt pattern utilized. The absence of mechanical allodynia in animals undergoing ABI was confirmed via

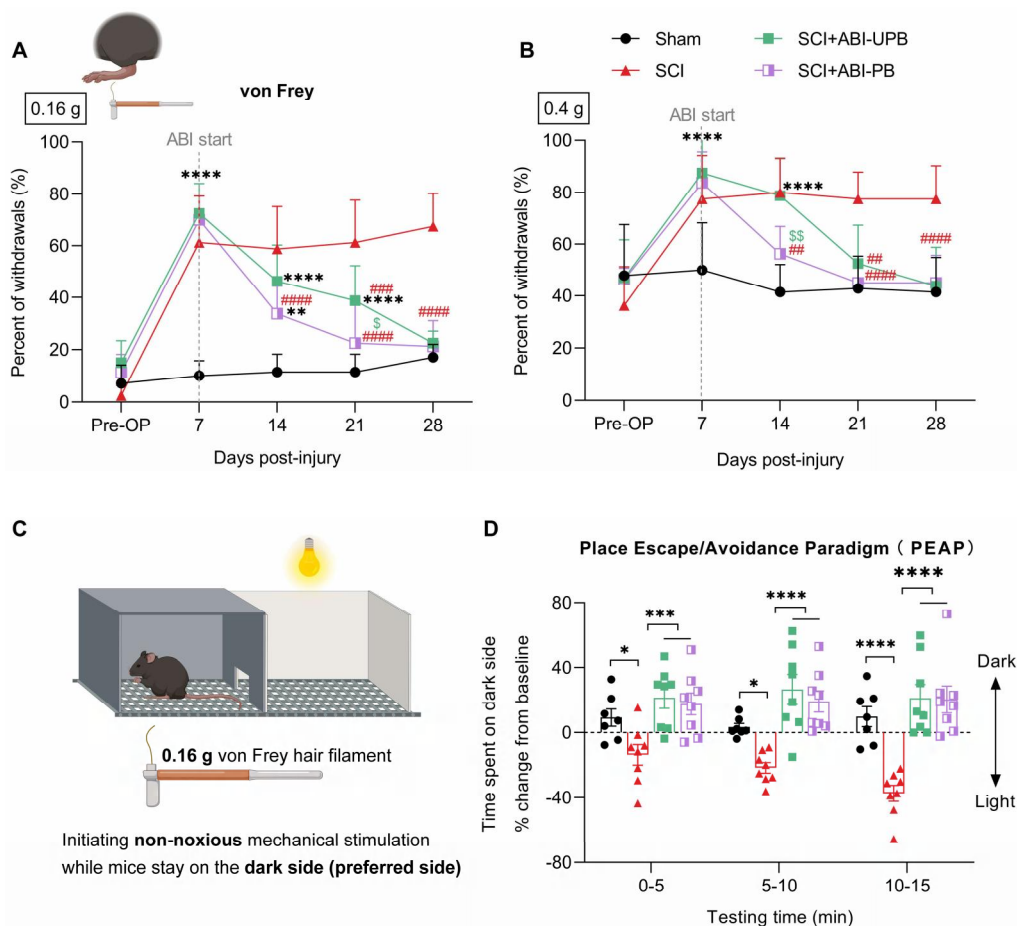


Figure 17: Patterned ABI exhibits higher efficiency in mitigating SCI-induced mechanical allodynia compared to unpatterned ABI.

Hindpaw withdrawal responses in mice to non-noxious mechanical stimuli applied with 0.16 (A) and 0.4 g (B) von Frey hair filaments show that ABI+PB (patterned belt) exhibits higher speed of efficiency in alleviating SCI-induced mechanical allodynia than ABI+UPB (unpatterned belt) (female, sham: n = 7; SCI: n = 8; SCI+ABI-UPB: n = 8; SCI+ABI-PB: n = 8). The Place Escape/Avoidance Paradigm Graphic (C) demonstrates that SCI mice subjected to either ABI paradigm do not develop a place preference for the light environment after receiving non-noxious stimuli, similar to sham animals at the end of the study (D). Mean \pm SD. Two-way repeated measures ANOVA, group differences, $p < 0.0001$; post hoc Tukey test. Symbols in A and B indicate group comparisons: * (black) indicates differences from the sham group, # (red) from the SCI group, and \$ (light green) marks differences between unpatterned and patterned ABI groups. In D, * (black) denotes statistical differences between specified groups. * $p < 0.05$, *** $p < 0.001$, **** $p < 0.0001$; ### $p < 0.001$, #### $p < 0.0001$; \$ $p < 0.05$, \$\$ $p < 0.01$.

their performance during PEAP testing, where ABI-treated mice behaved similarly to sham animals, not avoiding the dark environment when exposed to a 0.16 g filament (Figure 17, C and D).

The use of a patterned belt did not alter outcomes in ABI-related treatments for other SCI-induced sensorimotor deficits such as mechanical hypoalgesia, thermal hyperalgesia, and hindlimb gross motor dysfunction. This aligns with observations detailed in Section 3.2. The evidence comes from weekly behavioral tests assessing mechanical sensitivity with 0.6 and 1.4 g von Frey hair filaments (Figure S2, A and B), thermal sensitivity via the Hargreaves test (Figure S2C), and gross motor function using the BMS and its subscores (Figure S2, D and E).

Taken together, these findings suggest that patterned ABI, which provides increased mechanoreceptive and proprioceptive input compared to ABI with an unpatterned belt, enhances the speed of efficiency in the amelioration of below-level SCI-NP-associated symptoms.

3.4. ABI Inhibits Maladaptive Plasticity of CGRP-Expressing Nociceptors into the Deeper Dorsal Horn

The dorsal horn of the spinal cord, containing a complex array of functionally distinct laminae, serves as the primary locus for sensory processing within the central somatosensory nervous system before sensory information is relayed to the brain. Superficial laminae I and II specifically process nociceptive information; herein, local projection neurons become activated by noxious stimuli, which are mediated by C- and A δ -fibers (Figure 18). Peptidergic nociceptive fibers, characterized by calcitonin gene-related peptide-positive (CGRP+) expression, predominantly terminate in lamina I and the outer portion of lamina II (IIo), while isolectin B4 (IB4)-expressing non-peptidergic projections primarily terminate in the inner segment of lamina II (IIi). Intermediate laminae III-IV, conversely, receive mainly non-noxious sensory input, with synapses in this region being registered by A β -fibers.

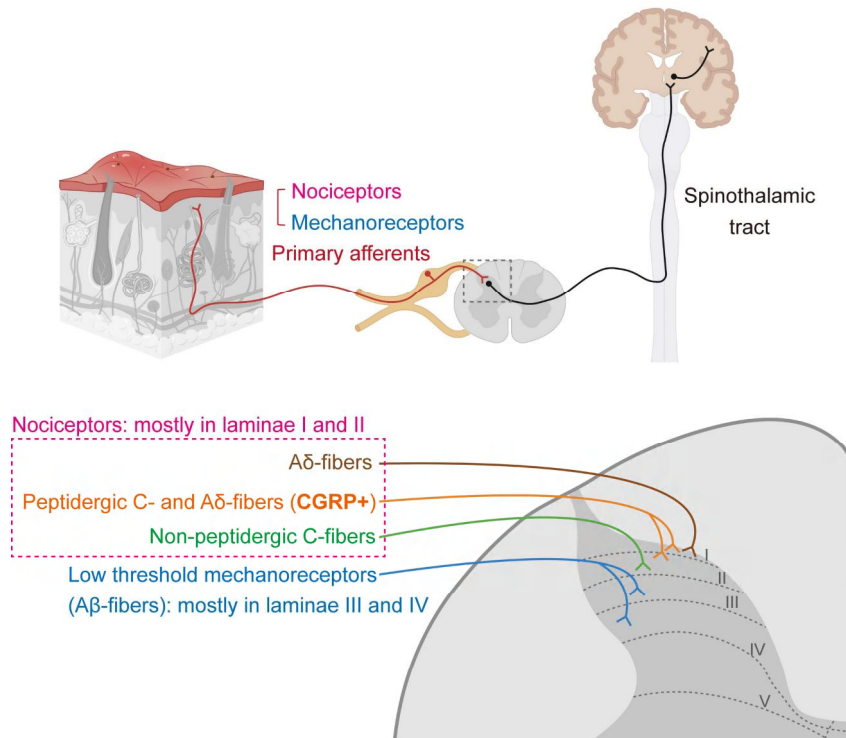


Figure 18: The projection patterns of nociceptors and mechanoreceptors into the dorsal horn of the spinal cord.

This diagram illustrates the distinct central termination zones of nociceptors and mechanoreceptors within the dorsal horn of the spinal cord and highlights the layered structure of the dorsal horn and the precision with which it processes different sensory modalities. Nociceptors, which are essential for the transmission of pain and temperature sensations, send their axons to the outer layers of the dorsal horn (laminae I and II), underscoring their crucial role in the perception of harmful stimuli. Meanwhile, mechanoreceptors, responsible for detecting touch and pressure, project their axons to the deeper layers (laminae III-V).

Subsequent to SCI, functional and structural changes within the dorsal horn have been observed to correlate with the emergence of SCI-NP-associated behaviors in the current studies. For example, alterations in the activity of nociceptive fibers can lead to maladaptive plasticity beyond their original site of termination. As depicted in Figure 19, A-C, compared to the sham groups, mice of both sexes subjected to SCI without ABI exhibited a marked increase in the sprouting of CGRP-expressing nociceptors within laminae III-IV of the lumbar spinal segments L4-L6. This increase is highly correlated with behavioral indicators of below-level mechanical allodynia. Specifically, there is a strong positive correlation between CGRP-labeling density in laminae III-IV and the withdrawal frequency to a non-noxious 0.16 g von Frey hair filament (Figure 19, D and E). In contrast, in the ABI groups—where SCI mice of both sexes underwent a lower-frequency ABI protocol (3 days/week on an unpatterned belt)—there was a significantly reduced density of CGRP+ nociceptors in the deeper laminae III-IV compared to those without ABI. Notably, both female and male SCI mice receiving ABI showed a CGRP labeling density similar to that of the sham controls. These findings are consistent with results from previous research by our laboratory, which indicated comparable outcomes whether ABI (administered 5 days/week) was implemented early (7 dpi) or during the chronic phase (42 dpi) of SCI in female mice (Nees et al. 2016; Sliwinski et al. 2018). Additionally, ABI on a patterned belt exhibited an effect similar to that when trained on an unpatterned belt (Figure S3). These results indicate that the maladaptive sprouting of CGRP+ nociceptors plays a pivotal role in the initiation and perpetuation of SCI-NP and suggest that ABI treatment mitigates mechanical allodynia by reducing the abnormal sprouting of CGRP+ nociceptors into laminae III-IV.

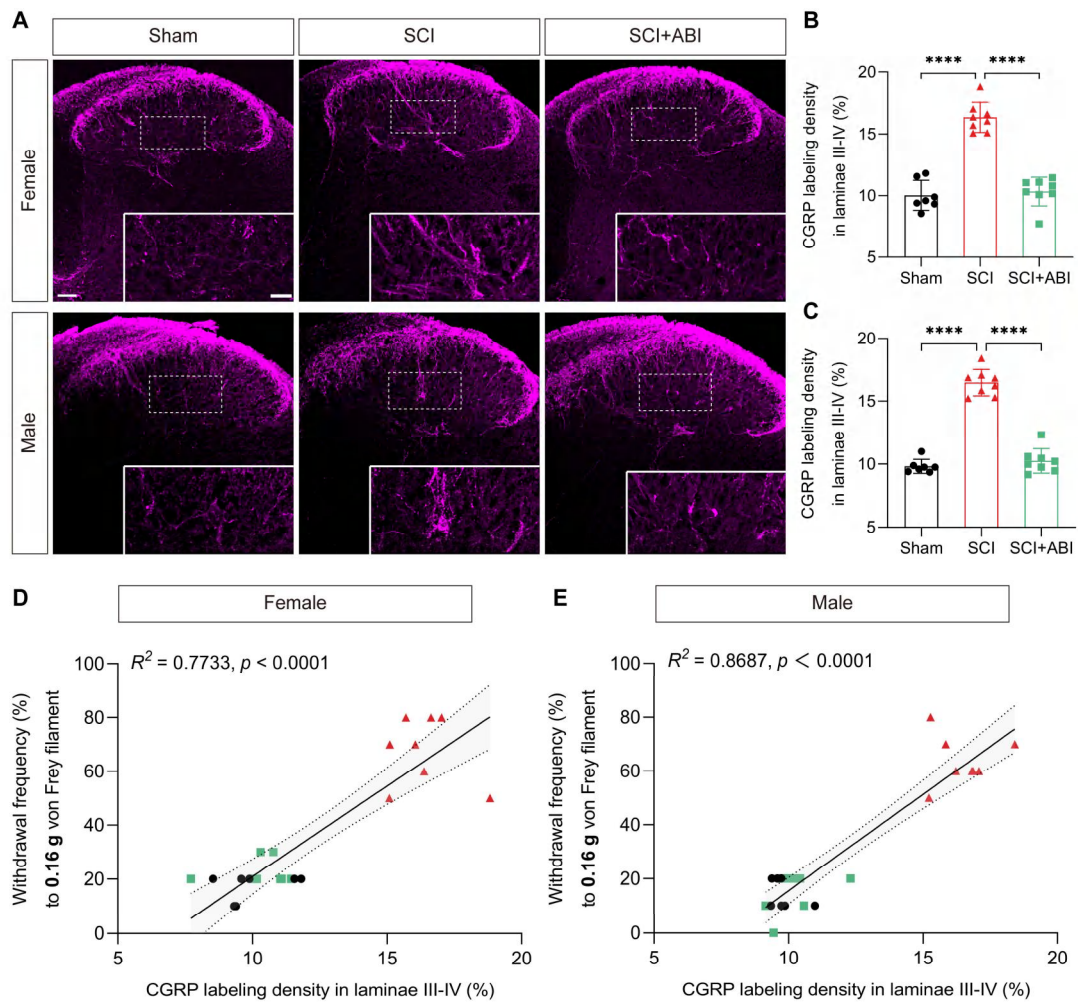


Figure 19: ABI inhibits the aberrant sprouting of CGRP-expressing nociceptive fibers into laminae III-IV induced by SCI.

Immunofluorescence staining of lumbar spinal cord sections shows CGRP-positive expression (A, scale bars in main images: 50 μm, in magnified images: 20 μm). Quantification of the percentage of CGRP-labeled area in laminae III-IV of the spinal cord dorsal horn of female (B) and male (C) mice. SCI leads to a significant increase in the sprouting of CGRP+ nociceptors within laminae III-IV, whereas ABI effectively inhibits this aberrant sprouting in both sexes of SCI mice. (ABI is applied on an unpatterned belt as shown in Study 1, Figure 3. For each sex: sham: n = 7; SCI: n = 8; SCI+ABI: n = 8). Mean ±SD. Ordinary one-way ANOVA ($p < 0.0001$), post hoc Tukey test: **** $p < 0.0001$. Scatter plots in D and E showing the relationship between CGRP labeling density in laminae III-IV and withdrawal frequency to a non-noxious 0.16 g von Frey hair filament. Each point represents an individual observation. The regression lines are shown with the equations $Y = 6.724X - 46.37$ for females and $Y = 7.149X - 56.02$ for males. The Pearson correlation

coefficients are $r = 0.8793$ for females and $r = 0.9320$ for males. The R-squared values are $R^2 = 0.7733$ for females and $R^2 = 0.8687$ for males, indicating that a high proportion of the variance in withdrawal frequency is explained by CGRP labeling density. The relationship is statistically significant ($p < 0.0001$). Higher CGRP labeling density in laminae III-IV is associated with a higher withdrawal frequency to the non-noxious 0.16 g filament, which is linked with mechanical allodynia.

3.5. ABI Depresses Heightened Neuronal Activity in the Spinal Cord

Dorsal Horn after SCI

Considering the potential link between SCI-induced mechanical allodynia and the altered pattern of neuronal activation in the spinal cord dorsal horn, I devised an experiment to examine the activation of c-Fos neuronal cells (Figure S4A) triggered by a non-noxious mechanical stimulus (0.16 g von Frey hair filament) applied to the plantar surface of the mouse's hindpaws. This investigation aimed to clarify the alternations in the patterns of neuronal activation associated with SCI-NP, evaluate the impact of ABI, and delineate the laminar distribution of activated c-Fos cells within the spinal cord dorsal horn in both sexes.

In both female and male sham mice, pronounced c-Fos activation was observed in the spinal cord dorsal horn following exposure to a non-noxious mechanical stimulus. Notably, in sham mice there was a higher prevalence of c-Fos-positive cells in the deeper laminae III-V compared to the superficial laminae I and II (Figure 20, A, D, and F). This distribution reflects the specialized activation pattern of dorsal horn neurons for processing innocuous stimuli, highlighting their distinct functional roles within these laminae. SCI mice of both sexes exhibited a significantly enhanced activation of dorsal horn neurons in response to the innocuous stimuli, as evidenced by a marked increase in the total number of c-Fos+ cells compared to sham animals (Figure 20, A-C). The increase in neuronal activation was observed in both the superficial laminae I-II and the deeper layers of laminae III-V (Figure 20, D and F). This pattern suggests that SCI enhances stimulus-induced neuronal activation not only in the regions typically responsible for processing innocuous stimuli (laminae III-V) but also in areas

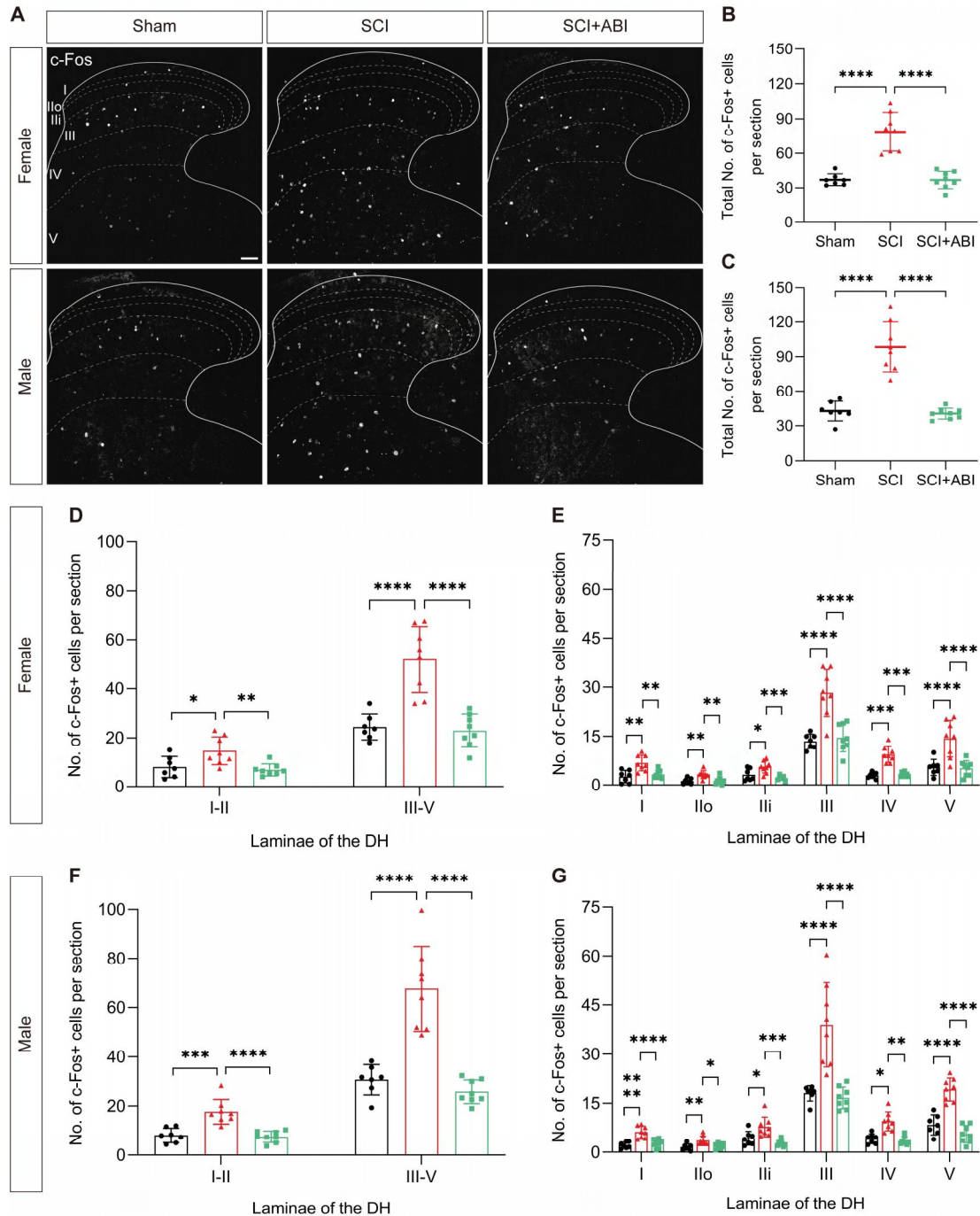


Figure 20: ABI diminishes touch-evoked SCI c-Fos neuronal activation in the dorsal horn.

Immunofluorescence staining of lumbar spinal cord sections showing c-Fos expression (A, scale bars: 50 μ m). Quantification of the number of c-Fos+ cells triggered by a non-noxious mechanical stimulus (0.16 g von Frey hair filament) in the spinal cord dorsal horn of female (B, D, and E) and male (C, F, and G) mice. SCI leads to a significant increase in touch-evoked neuronal activation in the spinal cord dorsal horn, especially within laminae III-IV, whereas ABI effectively depresses this aberrant enhancement in both sexes

of SCI mice (ABI is applied on an unpatterned belt as shown in Study 1, Figure 3. For each sex: sham: n = 7; SCI: n = 8; SCI+ABI: n = 8). Mean \pm SD. Ordinary one-way ANOVA ($p < 0.0001$), post hoc Tukey test: $*p < 0.05$, $**p < 0.01$, $***p < 0.001$, $****p < 0.0001$.

primarily involved in transmitting nociceptive information (laminae I-II). This widespread neuronal activation may then contribute to the maladaptive processing of non-noxious mechanical stimuli, leading to mechanical allodynia. The ABI paradigm (utilizing an unpatterned belt as shown in Figure 3) effectively reversed the heightened c-Fos activation in SCI mice of both sexes to levels comparable to their sham controls (Figure 20, B and C). This reduction in neuronal activation was consistent across all laminae, from I to V (Figure 20, E and G). Similarly, when the ABI was implemented using a patterned treadmill belt, the same modulatory effects were observed (Figure S4, B-D). Overall, these results demonstrate that SCI induces significant increase in neuronal activation evoked by innocuous stimuli within the spinal cord dorsal horn, which is closely linked to the development of mechanical allodynia in both female and male mice (Figure 21, A-F). The ABI paradigms prove to be effective in suppressing this enhanced neuronal activation and reversing mechanical hypersensitivity in SCI mice of both sexes.

Interesting, the increased plasticity of CGRP+ nociceptors following SCI was notably observed in the deeper layers of the dorsal horn, as detailed in Section 3.4. Through the implementation of ABI paradigms, the sprouting of CGRP+ nociceptors was effectively inhibited, which coincided with reduced neuronal activation as evidenced by c-Fos labeling. These findings suggest potential interactions between the sprouted nociceptors and altered neuronal activity in the deeper dorsal horn under conditions of SCI-NP.

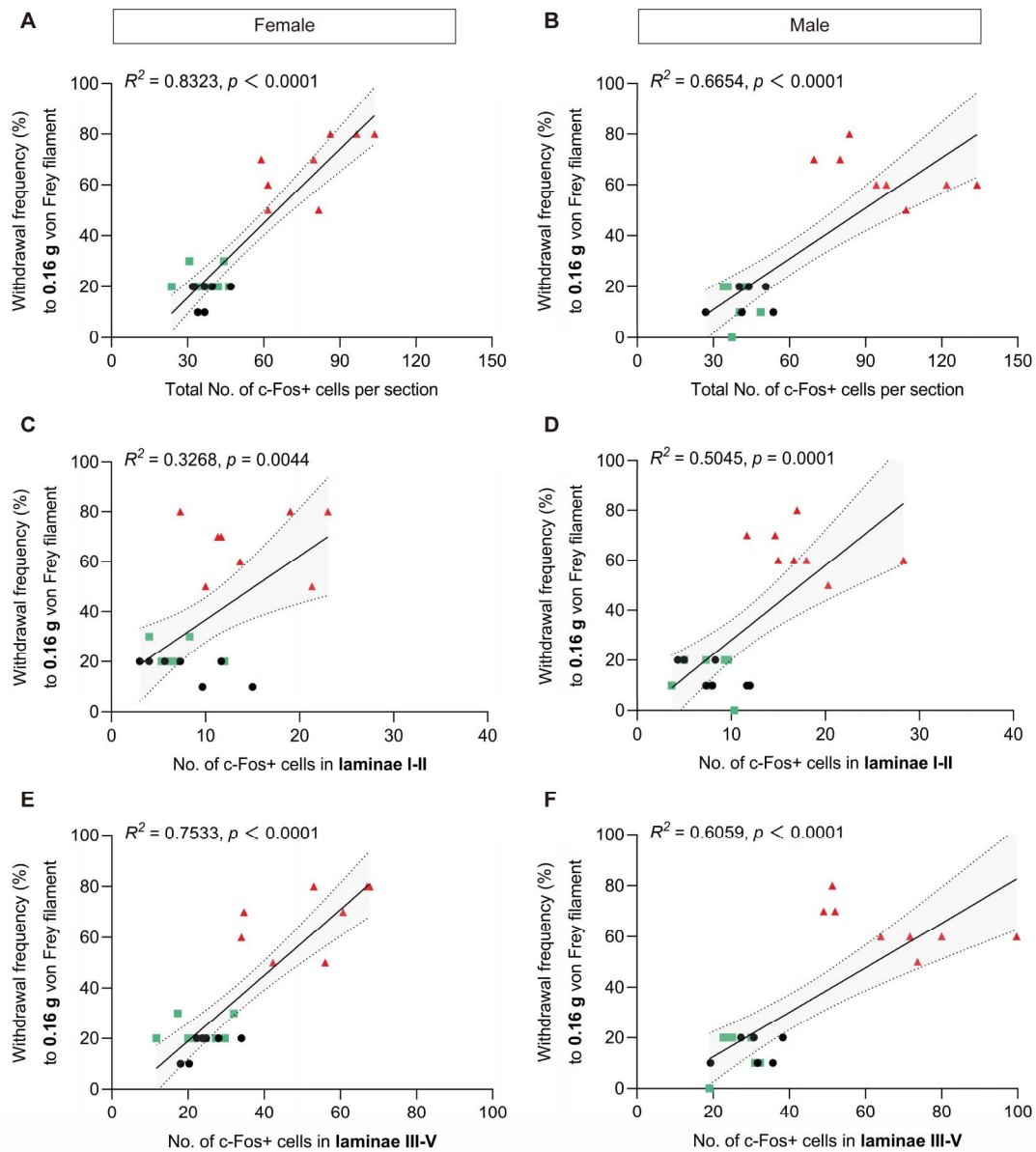


Figure 21: Touch-induced c-Fos neuronal activation in the dorsal horn exhibit a strong connection with the development of below-level mechanical allodynia.

Scatter plots showing the relationship between the number of c-Fos+ cells in different regions of the spinal cord dorsal horn and withdrawal frequency to a non-noxious 0.16 g von Frey hair filament in females (**A**, **C**, and **E**) and males (**B**, **D**, and **F**). Each point represents an individual observation (for each sex: sham: $n = 7$; SCI: $n = 8$; SCI+ABI: $n = 8$). The regression lines are shown with the equations for females and males: **A**: $Y = 0.9723X - 13.47$, **B**: $Y = 0.6612X - 8.778$; **C**: $Y = 2.560X + 11.11$, **D**: $Y = 2.985X - 1.831$; **E**: $Y = 1.299X - 6.966$, **F**: $Y = 0.8794X - 5.057$. The Pearson correlation coefficients are $r = 0.9123$ in **A**, 0.8157 in

B, 0.5717 in **C**, 0.7103 in **D**, 0.8679 in **E**, and 0.7784 in **F**. The R-squared values are $R^2 = 0.8323$ in **A**, 0.6654 in **B**, 0.3268 in **C**, 0.5045 in **D**, 0.7533 in **E**, and 0.6059 in **F**, indicating that a generally high proportion of the variance in withdrawal frequency is explained by the number of c-Fos+ cells. The relationships are statistically significant ($p < 0.0001$). A higher number of c-Fos+ cells is associated with a higher withdrawal frequency to the non-noxious 0.16 g filament, indicating increased mechanical sensitivity.

3.6. ABI Subsides SCI-Induced Enhancement of Activation in Dorsal

Horn PKC γ -Expressing Interneurons

To investigate the role of PKC γ -expressing excitatory interneurons in the development and alleviation of SCI-NP-associated behaviors, I examined the reactivity of dorsal horn PKC γ + neurons (Figure S5A) below the level of injury (lumbar spinal cord segments L4-L6) in response to SCI and subsequent ABI treatment in mice of both sexes.

Both female and male SCI mice demonstrated significantly increased dorsal horn PKC γ immunoreactivity, characterized by elevated PKC γ immunodensity (Figure 22, A-C). Additionally, these subjects exhibited an augmented number of visible PKC γ + interneurons beneath lamina Iii (Figure 22, A, D and E), a region where these interneurons are predominantly located (Miraucourt et al. 2011; Neumann et al. 2008). SCI+ABI animals of both sexes, subjected to an unpatterned belt, showed significantly reduced PKC γ immunodensity and fewer visible PKC γ + cells below lamina Iii, with no significant differences observed compared to the sham groups. Interestingly, ABI administered using a patterned belt was also demonstrated to effectively reduce the SCI-induced increase in reactivity of dorsal horn PKC γ + interneurons below the level of injury with a higher efficiency compared to ABI on an unpatterned belt (Figure S5, B-D). Collectively, these findings suggest that the development of below-level mechanical allodynia following SCI is closely linked to the increased reactivity of PKC γ + interneurons in the spinal cord dorsal horn (Figure 22, F and G). Furthermore, ABI appears effective in mitigating SCI-induced mechanical hypersensitivity by reducing the heightened reactivity of PKC γ + neurons triggered by the injury.

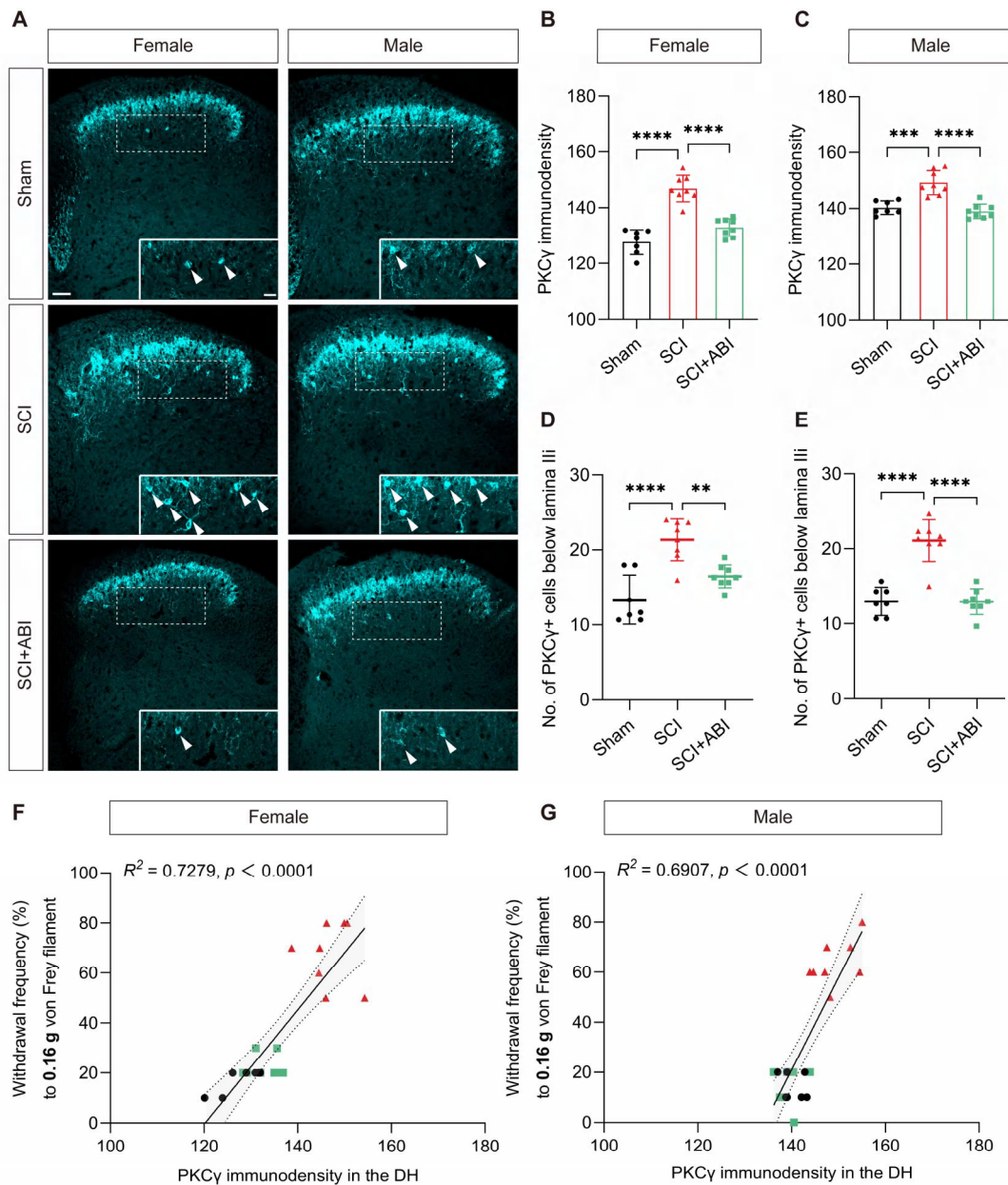


Figure 22: ABI reduces SCI-induced heightened reactivity of PKC γ -expressing interneurons in the below-lesion spinal cord dorsal horn.

Immunofluorescence staining of lumbar spinal cord sections showing PKC γ expression (A, scale bar in main image: 50 μ m, in magnified image: 20 μ m). Quantification of PKC γ immunoreactivity in the spinal cord dorsal horn reveals that SCI leads to significantly increased PKC γ immunodensity (B and C), as well as a greater number of PKC γ + cells below lamina III (D and E) in SCI mice of both sexes, which are then reversed by ABI treatment (ABI is applied on an unpatterned belt as shown in Study 1, Figure 3. For each sex: sham: n = 7; SCI: n = 8; SCI+ABI: n = 8). Mean \pm SD. Ordinary one-way ANOVA ($p < 0.0001$), post hoc Tukey

test: $**p < 0.01$, $***p < 0.001$, $****p < 0.0001$. Scatter plots showing the relationship between PKC γ immunoreactivity in the spinal cord dorsal horn and withdrawal frequency to a non-noxious 0.16 g von Frey hair filament in females (**F**) and males (**G**). The regression equations are **F**: $Y = 2.287X - 274.9$ with $r = 0.8532$ and $R^2 = 0.7279$; and **G**: $Y = 3.686X - 495.1$ with $r = 0.8311$ and $R^2 = 0.6907$. The relationships are statistically significant ($p < 0.0001$). Higher PKC γ immunoreactivity in the dorsal horn is highly correlated with a higher withdrawal frequency to the non-noxious 0.16 g filament, indicating greater mechanical sensitivity.

The enhanced reactivity of dorsal horn PKC γ^+ excitatory interneurons in SCI-NP mice may suggest that these neurons gain access to transmit excitation to dorsally-located nociceptive-specific neurons in superficial laminae I and II. This hypothesis is supported by conducting c-Fos induction detailed in Section 3.5, where SCI-NP mice demonstrated increased neuronal activation in the superficial laminae I-II in response to innocuous stimuli, potentially due to receiving excitation signals from PKC γ^+ excitatory interneurons. However, during the peak period for detecting most c-Fos activation, which occurs 1 hour post-stimuli, I did not observe c-Fos activation in PKC γ^+ neurons. This absence might be attributable to missing or not reaching the optimal time window for detecting activation of PKC γ interneurons in response to non-noxious mechanical stimuli, as it may occur immediately after stimulation.

On the other hand, in these lumbar spinal cord sections, PKC γ expression was also shown in the region of dorsal corticospinal tract (CST), which originates from corticospinal neurons in layer 5 of the motor and somatosensory cortices and innervates all segments of the spinal cord. Disruption of CST axons leads to motor functional deficits following traumatic injuries such as SCI (Chen and Zheng 2014; Liu et al. 2017). At the end of the study, the CST-related anatomical alterations in mice following SCI and ABI were assessed by examining PKC γ^+ dorsal axons below the lesion level (Figure 23). As expected, mice subjected to SCI demonstrated a considerable loss in dorsal CST innervation. ABI paradigms did not alter the volume of PKC γ^+ axons within the dorsal CST following SCI. These observations are

consistent with the substantial impairment of hindlimb gross motor functions due to SCI, which was not improved by ABI paradigms.

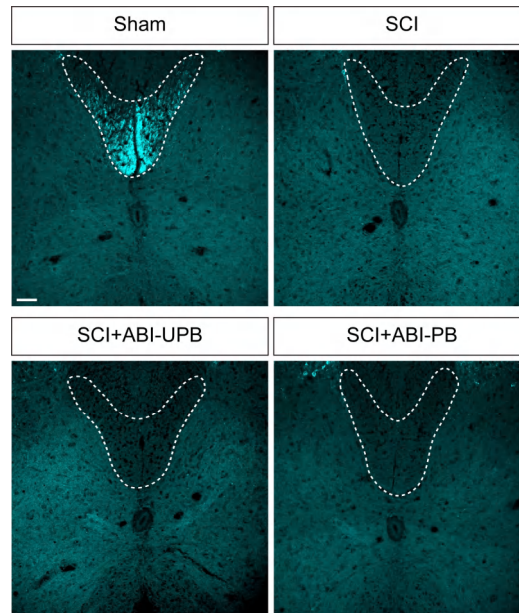


Figure 23: ABI paradigms do not promote axonal regeneration of the dorsal corticospinal tract below the level of injury.

Immunofluorescence staining of lumbar spinal cord sections showing PKC γ ⁺ expression of dorsal CST (scale bar: 50 μ m). This part of the immunostaining work was only performed in female mice from all four groups, including sham, SCI, ABI on an unpatterned belt, and ABI on a patterned belt (sham: n = 7; SCI: n = 8; SCI+ABI-UPB: n = 8; SCI+ABI-PB: n = 8).

3.7. Neuroglial Reaction Does Not Differ in the Dorsal Horn of Below-Lesion Spinal Cord

To determine whether SCI-induced below-level mechanical allodynia is associated with inflammatory-related responses within the spinal cord dorsal horn, I conducted histological analysis of neuroglia responses at the corresponding dermatome level of lumbar spinal segments (L4-L6). I used the glial fibrillary acidic protein (GFAP) to label astrocytes, and the ionized calcium-binding adapter molecule 1 (Iba1) for staining microglia to examine if they

were reactivated in SCI-NP mice. It is worth noting that this part of the immunohistochemistry work was only performed in female mice from all groups, including sham, SCI, ABI on an unpatterned belt, and ABI on a patterned belt.

At the conclusion of the study (31 dpi), female mice from all four experimental groups displayed similar levels of GFAP (Figure 24, A and B) and Iba1 (Figure 25, A and B) intensity within the dorsal horn of the spinal cord. This similarity in intensity levels suggests that during the intermediate phase of the injury, SCI did not exhibit below-level inflammatory responses from astrocytes and microglia. Furthermore, the administration of ABI paradigms appeared to have no significant impact on the reactivity of either astrocytes or microglia.

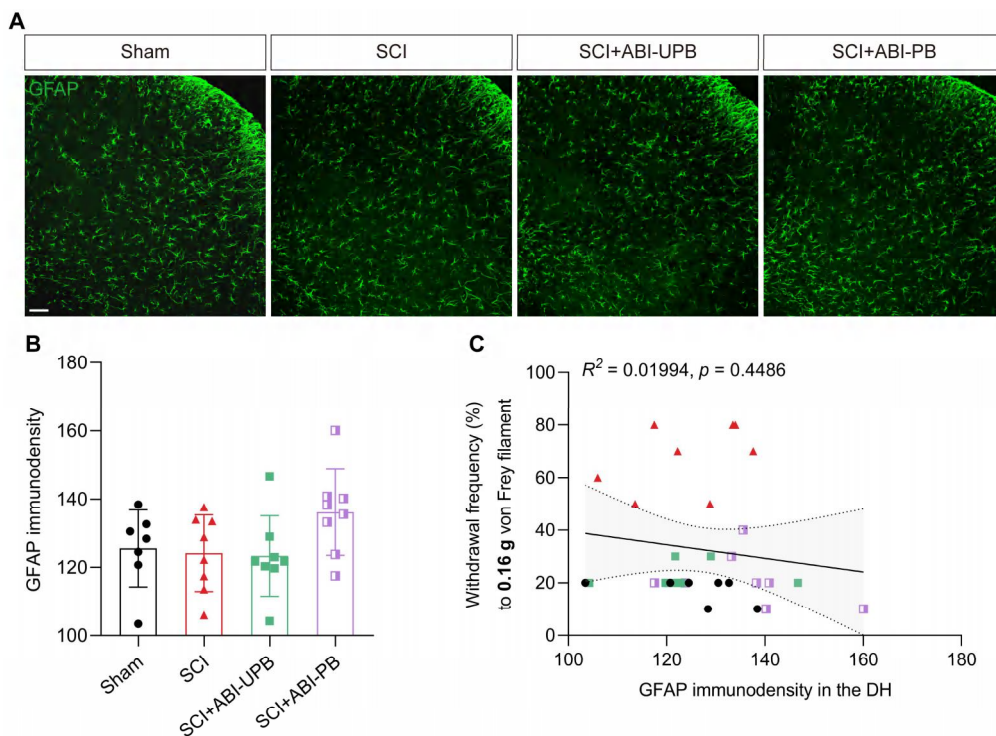


Figure 24: Astrocytes do not exhibit alterations in the dorsal horn of the below-level spinal cord in response to SCI or ABI paradigms.

Immunofluorescence staining of lumbar spinal cord sections showing GFAP expression (A, scale bar: 50 μ m). Quantification of GFAP immunodensity in the spinal cord dorsal horn shows no statistical difference

among the four groups (**B**) (female, sham: n = 7; SCI: n = 8; SCI+ABI-UPB: n = 8; SCI+ABI-PB: n = 8). Mean \pm SD. Ordinary one-way ANOVA, $p = 0.1265$. Combined analysis of Pearson correlation and linear regression indicates there is no statistically significant relationship between GFAP immunodensity in the dorsal horn and mechanical sensitivity/hypersensitivity ($p = 0.4486$, $r = -0.1412$, $R^2 = 0.01994$, as indicated by withdrawal frequency to a 0.16 g von Frey hair filament).

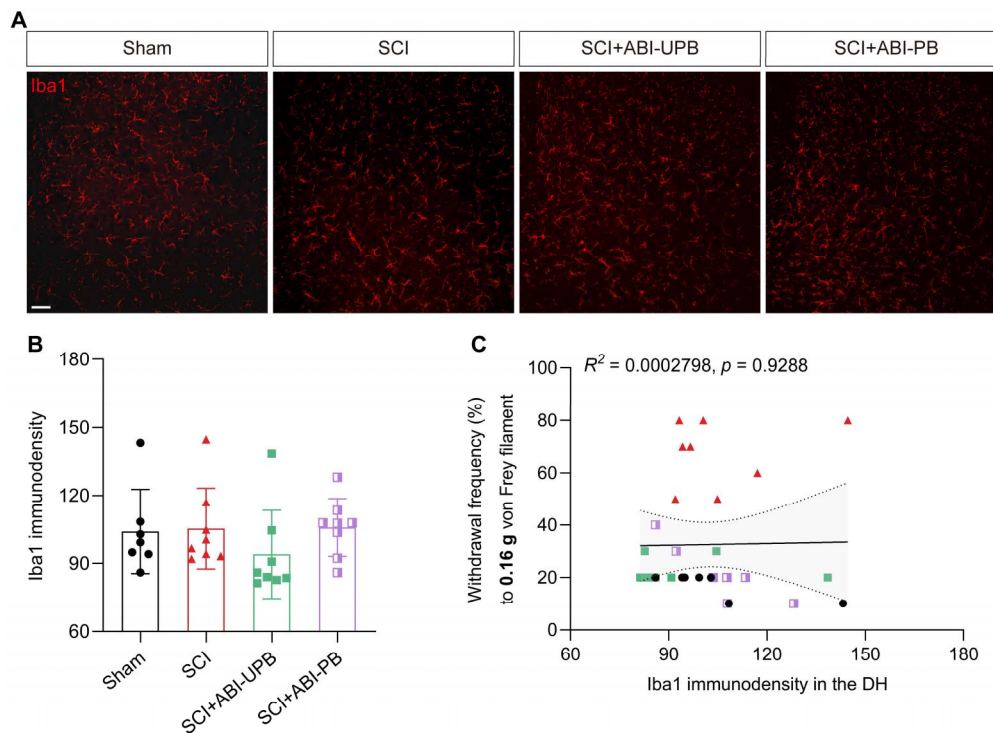


Figure 25: Microglia do not demonstrate changes in the dorsal horn of the spinal cord below the lesion in response to SCI or ABI paradigms.

Immunofluorescence staining of lumbar spinal cord sections showing Iba1 expression (**A**, scale bar: 50 μ m). Quantification of Iba1 immunodensity in the spinal cord dorsal horn shows no statistical difference among the four groups (**B**) (female, sham: n = 7; SCI: n = 8; SCI+ABI-UPB: n = 8; SCI+ABI-PB: n = 8). Mean \pm SD. Ordinary one-way ANOVA, $p = 0.4827$. Combined analysis of Pearson correlation and linear regression indicates there is no statistically significant relationship between dorsal horn Iba1 immunodensity and below-level mechanical sensitivity/hypersensitivity ($p = 0.9288$, $r = 0.01673$, $R^2 = 0.0002798$), as indicated by withdrawal frequency to a 0.16 g von Frey hair filament.

It is important to note that the staining work for male mice will be conducted in the near future to examine if the male SCI and ABI mice present differently in the inflammatory-related responses from my current observations in their female counterparts. Overall, alternations in neuroglial responses below the level of injury were not observed in female mice during the intermediate phase of SCI, suggesting that they do not serve as key factor in driving below-level SCI-NP in this phase (Figure 24C and 25C).

4. Discussion

4.1. Sex Does Not Act as a Significant Variable in the Development of SCI-NP and Its Amelioration by ABI

The present work provides insights into how both sexes of mice develop NP-associated behaviors below the level of injury early after a spinal cord T11 moderate contusion, and how they respond to ABI treatment initiated subacutely after SCI. Both female and male mice developed persistent mechanical allodynia and thermal hyperalgesia below the injury level in a comparable manner following SCI. These findings align with previous observations in mice using a thoracic contusion SCI model with an impact force of 75 kdyn (Gensel et al. 2019; McFarlane et al. 2020) and in rats subjected to a moderate thoracic contusion using a weight drop method (10 g weight, 12.5 mm height) (Walker et al. 2019). However, studies using a severe thoracic contusion SCI model in rats have shown that males are more likely to develop mechanical allodynia at (Hubscher et al. 2010) or below (Gaudet et al. 2017) the injury level. Additionally, research employing a photochemical SCI model at the L4/L5 spinal cord segment found increased below-level mechanical hypersensitivity in females compared to males (Dominguez et al. 2012). A recent study using a moderate thoracic contusion model (60 kdyn) reported more pronounced mechanical and thermal hypersensitivity in female mice than in males (Lee et al. 2023). These contrasting findings suggest that sex differences in SCI-NP-associated behaviors may result from the variety of species, injury models, and severity levels used in these experiments. Moreover, the exclusive reliance on reflex-based assays such as von Frey and Hargreaves tests in previous studies indicates that the observed discrepancies might also arise from variability in the reflex-based methodologies employed and the evaluators' experience in assessing SCI-NP-associated behaviors across different laboratories.

In the current study, I expanded the evaluation beyond reflex-based assays to include the supraspinal processing of nociception using the Place Escape/Avoidance Paradigm (PEAP). By

the conclusion of the study, both female and male SCI mice demonstrated similar behaviors in escaping and/or avoiding nociceptive stimuli, alongside exhibiting preferences for locations offering pain relief. Incorporating this method provided more comprehensive insights into not only how each sex interprets nociceptive stimuli but also their cognitive perceptions of pain. Consequently, there is a need for subsequent research to incorporate multi-conceptual evaluations of SCI-NP-associated behaviors, aiming to provide a more thorough understanding of potential differences in the perception and interpretation of SCI-NP between females and males. Additionally, the incorporation of sham controls throughout the study facilitated the demonstration of comparable baselines in mechanical and thermal sensitivity across sexes. It also enabled comparisons of changes in SCI-NP-associated behaviors with those observed in sham animals, as well as with the pre-operative levels of SCI animals. This approach significantly enhanced the reliability of the reported results.

Previously, these studies investigating sex differences in the behavioral manifestation of NP following SCI have not further explored the potential differences in the mechanisms mediating pain. Research focusing on NP mechanisms triggered by PNI has revealed sex differences in pain signaling pathways. A recent review article highlighted the significant impact of sex differences on the functions of microglia and T cells in exacerbating pain hypersensitivity. In contrast, the roles of macrophages, primary sensory neurons, and spinal dorsal horn neurons appear to be consistent across sexes (Ghazisaeidi et al. 2023). This suggests a complex interaction of cellular mechanisms involved in pain signaling. While females and males exhibit similar NP-associated behaviors and comparable mechanistic alterations following injury, their responses to specific mechanism-targeted treatments have been shown to differ. For example, research has demonstrated a male dominance in microglial signaling in NP, although both sexes display identical NP-associated behaviors and morphological reactivity of microglia (i.e., microgliosis) after nerve injury (Chen et al. 2018; Mapplebeck et al. 2017; Mapplebeck et al. 2018; Sorge et al. 2011; Sorge et al. 2015). Specifically, chemogenetic activation of spinal microglia leads to enhanced pain sensitivity in male mice only. Strategies aimed at inhibiting

or eliminating microglia reverse mechanical hypersensitivity exclusively in males, not in females, suggesting that the disparity may stem from inherent sex differences in the activation of receptors within the neuroimmune system (Saika et al. 2021; Saika et al. 2020). Given the potential sex differences in the neurobiological mechanisms underlying pain signaling pathways in SCI-NP, it is crucial to investigate the potential disparities in treatment effectiveness between sexes.

In this study, I show that the histological analysis of CGRP, c-Fos, and PKC γ in the spinal cord dorsal horn below the injury level in sham and SCI mice of both sexes confirms that the presence of mechanical allodynia is associated with maladaptive structural and functional changes mediated by CGRP-expressing nociceptors, patterns of neuronal activation, and PKC γ -positive excitatory interneurons. Following ABI treatment, both female and male SCI mice exhibited a significant reduction in below-level mechanical allodynia, comparable to that of sham controls. Moreover, the modulatory effect of ABI on these mechanistic components appears to be sex-independent, suggesting that the mechanisms mediating NP following SCI are analogous across the sexes. This work underscores the complexity of NP mechanisms post-SCI and highlights the potential of ABI as a therapeutic strategy that is effective regardless of sex differences.

4.2. Increasing Mechanoreceptive and Proprioceptive Input Enhances

ABI Efficiency in Mitigating SCI-NP

The implementation of ABI paradigms on the treadmill provides consistent and direct sensory feedback through the neural structures associated with the limbs of mice. This intervention specifically targets mechanoreceptors embedded in the skin, which are stimulated by tactile contact, pressure, vibrational forces, and rotational movements linked to changes in position and motion dynamics (Ergen and Ulkar 2007; French and Torkkeli 2009). Additionally, proprioceptors are engaged by the stretching and kinetic activities of muscles and joints, which exert tension and stress on the musculoskeletal system (Proske 2015). Studies have shown that

treadmill-based ABI induces extensive neuronal activation in the most medial parts of laminae IV, V, and VII within the spinal cord, aligning with the dermatomal mapping of both the forelimbs and hindlimbs in the studied animals (Ahn et al. 2006). This implies that the neuronal activation induced by ABI is effectively transmitted through the central somatosensory nervous system, forming the basis for ABI's effect on modulating SCI-NP by influencing somatosensory processing within the spinal cord.

In the current study, I devised experimental designs that varied the degree of mechanoreceptive and proprioceptive inputs delivered to the mouse hindlimbs during ABI by utilizing both patterned and unpatterned treadmill running belts (Figure 15). The objective was to investigate if variations in the treadmill surface could influence the therapeutic outcomes in the ABI treatment of below-level SCI-NP. The patterned belt is relatively stiff and uneven, featuring diamond patterns on its surface. Since the area of each pattern is smaller than the plantar surface of the mouse hindpaw, the mice can run steadily on the belt while experiencing intensified mechanical pressure or distortion on the hindpaw surface, necessitating augmented muscular and joint efforts for balance maintenance. In contrast, the unpatterned belt was designed to reduce sensory stimulation with its flat and regular surface. Interestingly, ABI on a patterned belt demonstrated higher efficiency in mitigating SCI-NP, achieving significant pain relief within 7 days post-ABI, whereas ABI on an unpatterned belt required 14 days to achieve similar results (Figure 17, A-D). This finding highlights the crucial role of sensory input modulation in enhancing the efficacy of ABI therapies. By adjusting the physical environment of the treadmill, the increased sensory stimulation from the patterned belt appears to more effectively activate neuroplastic mechanisms essential for pain modulation and recovery in SCI-NP conditions. Additionally, it would be worthwhile to conduct a timed experiment ending at the point where the two paradigms show significantly different effect on SCI-NP (e.g., 7 days post-ABI based on current findings). This would allow for further investigation into the differences in the effect of ABI using unpatterned and patterned belts.

In the review article I published in 2022, the comparison of SCI-NP-associated behavioral readouts from the included studies indicated that "full weight-bearing rhythmic ABI" (such as treadmill training alone, wheel running, free walking) is more beneficial for alleviating SCI-NP than "non-full weight-bearing rhythmic ABI" (e.g., treadmill training with a body weight support system, swimming, standing with a support system) (Chen et al. 2022). The term "full weight-bearing rhythmic ABI" refers to intervention methods that require animals to carry their full body weight and alternate their limbs in a rhythmic pattern. I hypothesized that this type of ABI would likely induce greater activation of proprioceptive and mechanoreceptive sensory neurons due to its inherent properties. A study that included two different full weight-bearing rhythmic ABI paradigms, treadmill training and free-access wheel running, reported that the free-access wheel, which allowed unlimited running times during the day, was more effective in mitigating below-level SCI-NP and showed stronger proprioceptive vesicular glutamate transporter 1 (VGluT1) immunoreactivity in the below-level spinal cord compared to treadmill training, which provided limited running times. Additionally, the same study showed that a locked wheel, designed to reduce movement, had no effect on SCI-NP amelioration (Sanchez-Ventura et al. 2021). These findings provide indirect evidence that the intensity of sensory stimulation during ABI influences its effectiveness in improving NP conditions following SCI. Together with my findings, which directly compare the same ABI paradigms while varying the intensity of sensory input, these results may help to modify clinical methods for improving NP state in SCI patients by integrating methods that enhance sensory stimulation to the affected extremity.

4.3. Reversing SCI-Increased Neuronal Activation in Spinal Cord

Dorsal Horn through the ABI Paradigm

In the present study, I used c-Fos expression as a biomarker to track neuronal activation within the below-lesion spinal cords (lumbar spinal cord segments L4-L6) following the application of non-noxious mechanical stimuli to the mouse hindpaws. This approach facilitated a detailed examination of the specific neuronal activation patterns associated with sensory transmission

and processing of innocuous stimuli under both physiological and SCI-NP conditions. Given that the moderate thoracic contusion SCI model reliably produces significant and persistent below-level mechanical allodynia, the observed changes in neuronal activation patterns induced by innocuous stimuli in SCI mice, as compared to sham controls, are found to correlate strongly with the behavioral manifestations of mechanical allodynia. Furthermore, comparative analysis of neuronal activation patterns across sham, SCI, and SCI+ABI groups demonstrated how ABI modulates and reverses SCI-induced alternations in neuronal activation.

Previous studies have demonstrated that, under physiological conditions, non-noxious mechanical stimuli such as brushing or touching of the hindpaws predominantly activate neurons within laminae III, IV, and V of the lumbar spinal cord in mice and rats. Notably, the most significant neuronal activation is observed in lamina III (Berrocal et al. 2007; Bourane et al. 2015; Gatto et al. 2021; Hunt et al. 1987). In the current study, sham animals exhibited significantly higher counts of c-Fos⁺ cells in the deeper laminae III-V compared to the superficial laminae I and II. This observation aligns with the well-established understanding that the deeper laminae III-V receive innervation primarily from non-nociceptive, low-threshold mechanoreceptors and are responsible for further processing of such non-noxious stimuli. Conversely, in the superficial laminae I and II, which serve as the predominant termination sites for C- and A δ -nociceptors, where nociceptive-specific neurons are primarily located, there was no considerable neuronal activation observed in the sham mice, confirming the stimulus used was indeed a non-noxious stimulus in physiological situations .

It has been reported that neuronal cells within laminae III-V of the spinal cord are crucial for processing both pain-related and tactile sensory information. Specifically, lamina III is composed of a mixture of excitatory and inhibitory interneurons that process mechanical nociception and non-nociceptive, mechanoreceptive information (Todd 2010). Lamina IV neurons are predominantly involved in processing non-nociceptive tactile and proprioceptive information, with a significant presence of projection neurons that convey sensory information

to higher supraspinal centers (Abraira and Ginty 2013). Lamina V contains wide dynamic range (WDR) neurons that respond to both nociceptive and non-nociceptive stimuli. These WDR neurons are pivotal in pain perception and are implicated in the integration of sensory information from both local interneurons and descending fibers from the brain (Peirs and Seal 2016). Therefore, these deeper laminae, which consist of functionally distinct neurons for processing a variety of sensory inputs, can be extensively activated in response to innocuous stimuli, as I observed in sham mice. Moreover, part of the intense c-Fos cells in lamina III is presumed to be from postsynaptic dorsal column (PSDC) cells. PSDC cells receive cutaneous mechanical and/or noxious visceral information received from primary afferents (Westlund 2007). The information is relayed by PSDC axons ascending through the dorsal column to innervate the dorsal column nuclei in the dorsal midline of the caudal medulla.

SCI led to increased neuronal activation (induced by innocuous stimuli) in the superficial lamina I-II and the deeper laminae III-V in both female and male mice when compared to their respective sham counterparts. The overall heightened neuronal activation signifies a disruption in sensory processing resulting from altered patterns of neuronal activation, potentially leading to anatomical reorganization of spinal cord circuitry associated with the presence of mechanical allodynia post-SCI. This observation is corroborated by prior studies demonstrating elevated c-Fos expression rostral to the SCI site, which correlates with the manifestation of mechanical allodynia at and/or above the level of injury (Siddall et al. 1999).

In the deeper laminae III-V, the increase in neuronal activation suggest that neurons for transmitting and processing nociceptive information were erroneously activated under SCI conditions, resulting in the sensation of pain upon receiving non-noxious stimuli. Under SCI conditions, the enhanced activity of DRG sensory neurons (peripheral sensitization) may lead to the growth of their axons (Mesquida-Veny et al. 2022; Walters 2012; Wu et al. 2020), as indicated by the findings from the present study that hyperactivated CGRP+ nociceptors sprouted into deeper laminae III-IV of the dorsal horn in SCI-NP mice. This aberrant sprouting

of nociceptive fibers is likely a result of STT damage, necessitating a rerouting of information (Walters 2012), with growth down to the WDR neurons allowing for signal transmission of pain to still occur. Specifically, the aberrant growth of nociceptors into the deeper dorsal horn facilitates direct interactions with WDR neurons located in these layers. These interactions may lead to the maladaptive activation of WDR neurons, causing them to transmit predominantly nociceptive information to supraspinal centers, thus contributing to the development of NP conditions (Gwak et al. 2007). This hypothesis is further supported by my findings indicating that SCI enhances neuronal activation in the deeper laminae in response to non-noxious stimuli; however, in ABI mice, the sprouting of CGRP+ nociceptive fibers into laminae III-IV was inhibited. Consequently, these mice exhibited neuronal activation patterns similar to sham controls in these deeper laminae. It is promising to further examine the activity of DRG nociceptors in the ABI group compared to the SCI-only group in future experiments. This will help determine if ABI modulates the hyperactivity state of these primary sensory neurons, potentially leading to a reduction in the central sprouting of their fibers.

Furthermore, even though innocuous stimuli primarily activate the neurons in the deeper laminae, a few c-Fos+ neurons were also observed in the superficial laminae in sham animals. Moreover, SCI led to enhanced neuronal activation induced by innocuous stimuli in the superficial laminae I and II of female and male mice. This suggests that nociceptive-specific neurons, which are originally not responsible for non-nociceptive signaling, may undergo maladaptive activation in response to non-noxious mechanical stimuli, thereby transmitting pain information within the central somatosensory nervous system. This might be linked to the enhanced reactivity of PKC γ excitatory interneurons following SCI. As detailed in Section 3.6, under SCI-NP conditions, the activated PKC γ interneurons may acquire the ability to transmit excitation to dorsally located nociceptive-specific neurons, leading to pain sensations.

On the other hand, considering the impairment of inhibitory functions following SCI, excitatory interneurons involved in either nociceptive or non-nociceptive signaling might be

globally activated as a result of disinhibition. It has been demonstrated that in a mouse model of spared nerve injury-induced mechanical allodynia, mice exposed to innocuous mechanical stimulation of the hindpaw skin by walking at a slow pace on a treadmill recruit extensively increased c-Fos⁺ cells in the dorsal horn, extending from lamina I to VI. During the persistent pain state, approximately 70% of these activated neuronal cells induced by non-noxious mechanical stimuli are Pax2-negative, suggesting that about two-thirds of the neuronal cells recruited in this spinal circuit are excitatory (Peirs et al. 2015). Co-labeling of c-Fos with neuronal markers and anterograde tracing further reveals that these activated deep dorsal horn neurons, mostly from lamina III, transiently express vesicular glutamate transporter 3 (VGLUT3). Neighboring cells in lamina III receive input from transient VGLUT3 neurons and relay the signal to lamina II cells including PKC γ ⁺ excitatory interneurons, which act to refine the excitability of the circuit, leading to pain states (Peirs et al. 2015).

ABI reversed SCI-induced increases in c-Fos⁺ cells across laminae I-V, indicating a significant effect of ABI on modulating SCI-induced alterations in neuronal activation that contribute to mechanical allodynia. Previous studies have shown that ABI paradigms exhibit anti-inflammatory effects by attenuating immune cell activation and regulating pro-inflammatory and neurotrophic factors in the spinal cord below the injury level (Cheng et al. 2022; Chhaya et al. 2019; Dugan et al. 2020; Dugan et al. 2021). Such modulation of the neuroimmune processes may reduce neuronal hyperexcitability along the peripheral and central somatosensory pathways induced by SCI, thereby alleviating mechanical allodynia. Furthermore, ABIs contribute to restoring the physiological balance of endogenous GABAergic inhibition within the spinal cord dorsal horn pain pathway (Dugan et al. 2020; Dugan et al. 2021; Li et al. 2020; Tashiro et al. 2018; Tashiro et al. 2015). This restoration of inhibition consequently reduces aberrant neuronal activation within the dorsal horn, facilitating the functional organization of sensory processing and ultimately alleviating mechanical allodynia. These mechanisms will be further examined in future studies.

4.4. Regulating Enhanced Activation of PKC γ -Positive Neurons in Spinal Cord Dorsal Horn Following SCI by ABI

The immunostaining of PKC γ in the spinal cord dorsal horn specifically highlights populations of excitatory interneurons that express the PKC γ enzyme, which plays a crucial role in signal transduction. These PKC γ -immunoreactive interneurons primarily exhibit a fusiform morphology and form a dense plexus in the inner part of superficial lamina II, demonstrating strong immunoreactivity. In contrast, their distribution in lamina I, IIo, and III features a scattering of cells with weak to moderate immunoreactivity. Immunostaining also reveals the cell bodies and dendritic trees of PKC γ -positive neurons (Mermet-Joret et al. 2017; Peirs et al. 2014; Polgar et al. 1999). Polgar et al. noted that many PKC γ ⁺ neurons in lamina II possess rostrocaudally-oriented dendrites and resemble small islet cells, whereas some in lamina II and many in lamina III exhibit dendrites oriented dorsally or ventrally (Polgar et al. 1999).

In the present work, the emergence of below-level mechanical allodynia following SCI is associated with increased expression of PKC γ in the dorsal horn neurons of the lumbar spinal cord regions. This enhancement in PKC γ ⁺ neuron activation is primarily evidenced by elevated PKC γ immunoreactivity and an increase in the number of discernible PKC γ -immunoreactive cells in the deeper laminae (below lamina III). As previously mentioned, across different laminae in the dorsal horn, PKC γ ⁺ neurons exhibit varying degrees of immunoreactivity. Therefore, the observed increase in the number of PKC γ ⁺ cells might be attributable to these cells exhibiting enhanced expression of PKC γ in cells upon activation in response to SCI, which then makes them more visible. A similar finding was reported in a mouse model of severe thoracic contusion injury (with the presence of at-level tactile allodynia), where there was a significant increase in the number of PKC γ ⁺ neurons outside of lamina III, appearing in the deeper laminae III-V of the spinal cord caudal to the lesion (Kerr and David 2007). It has been reported that PKC-mediated phosphorylation of glutamate receptors may facilitate long-term changes in neuronal excitability and enhance NMDA-activated currents, thereby exacerbating

neuronal excitability (Chen and Huang 1992; Raymond et al. 1993). This hypothesis is further supported by studies demonstrating that selective inhibition of PKC γ and selective blockade of glutamate NMDA receptors in the superficial dorsal horn prevent both the activation of the nociceptive circuit and the development of mechanical allodynia (Martin et al. 2001; Mirauccourt et al. 2007).

Moreover, research using a rat model of peripheral inflammatory injury has demonstrated a significant increase in dorsal horn PKC γ expression, accompanied by a significant translocation of PKC γ from the nucleus and cytosol to the plasma membrane. This translocation regulates both the input to and output from the nociceptive-specific neurons of the superficial dorsal horn, particularly through actions on their dorsally projecting dendritic arbors (Martin et al. 1999). These findings, along with my observations, suggest that the observed increase in the number of PKC γ + cells below lamina III is likely due to enhanced PKC γ expression within these cells. Coupled with increased PKC γ expression in lamina III, this leads to heightened overall dorsal horn PKC γ immunoreactivity. Furthermore, in a mouse model of moderate contusion of the cervical spinal cord (C5/6), SCI was shown to significantly increase the activation of PKC γ + interneurons in the spinal cord dorsal horn caudal to the injury level, together with signs of below-level SCI-NP (Brown et al. 2022). Taken together, these findings suggest that below the injury level, the enhanced expression of PKC γ in dorsal horn excitatory interneurons serves as an important driver for the induction and maintenance of central sensitization, contributing to mechanical allodynia following SCI.

Although the function of dorsal horn PKC γ has not been extensively examined in SCI conditions, the maladaptive activation and the selective inhibition or deletion of PKC γ + neurons have been reported in various neuropathic conditions following PNI, to explore their role in nociceptive transmission. Research has demonstrated that mice with a deletion of the gene encoding PKC γ , resulting in the absence of the PKC γ isoenzyme, exhibit reduced signs of NP following sciatic nerve ligation (Malmberg et al. 1997). Furthermore, pharmacological

inhibition of PKC γ kinase has been shown to significantly alleviate mechanical allodynia in mice after sciatic nerve injury (Petitjean et al. 2015). The findings from the current study, together with these observations from previous research, suggest that PKC γ plays a critical role in the development of NP and that its inhibition may represent a promising therapeutic strategy for managing this condition following SCI.

On the other hand, spinal cord glycinergic inhibitory interneurons directly synapse with PKC γ + excitatory interneurons. Their disinhibition, induced by both SCI and PNI, has been shown to significantly increase the activation of PKC γ + neurons and contribute to below-level mechanical allodynia (Brown et al. 2022; Lu et al. 2013). The suppressed postsynaptic glycinergic inhibition of PKC γ + neurons is accompanied by increased levels of intracellular Cl⁻ concentration, which impairs the function of inhibitory receptors such as the GABA_A receptor, allowing Cl⁻ to enter the cells. This disrupts the generation of functional hyperpolarization that normally inhibits neuronal activity (Bardoni et al. 2013; Braz et al. 2014; Fiumelli and Woodin 2007; Kaila et al. 2014; Lu et al. 2013; Zheng et al. 2010). The intracellular chloride concentration is largely determined by the expression and function of chloride co-transporters, such as the K⁺- Cl⁻ cotransporter (KCC2) (Fiumelli and Woodin 2007), it has been shown that functional GABA and glycine inhibition in the spinal cord crucially depends on the expression of KCC2 (Blaesse and Schmidt 2015; Hubner et al. 2001). In SCI and PNI models, the overall loss of dorsal horn inhibitory signaling, as measured by decreased GABA, GAD, and KCC2 expression, leads to NP-associated behaviors (Drew et al. 2004; Dugan et al. 2020; Dugan et al. 2021; Ibuki et al. 1997; Kami et al. 2016; Tashiro et al. 2018; Tashiro et al. 2015). The ABI paradigms in my current study are demonstrated to reduce the SCI-induced increase in dorsal horn PKC γ expression and contribute to the relief of below-level mechanical allodynia. Earlier studies have shown that ABIs help to re-establish spinal cord inhibitory function by upregulating SCI-induced impairments in GABAergic inhibition, restoring dorsal horn GABA expression, GAD-65/67, and KCC2 levels (Dugan et al. 2020; Dugan et al. 2021; Li et al. 2020; Tashiro et al. 2018; Tashiro et al. 2015). Therefore, the present

ABI paradigms may exert their effects by restoring SCI-impaired spinal cord inhibition, thereby suppressing maladaptive neuronal activation, including PKC γ . This reduction in PKC γ immunoreactivity in the spinal cord below the injury level contributes to the relief of below-level SCI-NP.

The current study did not investigate these spinal cord inhibition mechanisms. This is an avenue that needs to be further explored in future research, including the exploration of spinal cord inhibitory interneurons and their functional changes in response to SCI and ABI.

4.5. Conclusion and Future Perspectives

In conclusion, with the present study, I was able to show that early ABI treatment effectively reduces SCI-induced below-level mechanical allodynia by modulating nociceptive fiber structural changes, decreasing aberrant neuronal activation patterns, and reducing PKC γ + neuron hyperactivity within the dorsal horn of the below-lesion spinal cord. The study also underscores that sex does not significantly influence the development of SCI-NP or the efficacy of ABI in modulating underlying mechanisms, suggesting that ABI is a broadly applicable therapeutic strategy for managing SCI-NP. Future research should focus on further elucidating the specific cellular and molecular mechanisms through which ABI exerts its effects. My study showed increased central sprouting of CGRP+ nociceptive fibers under a hyperactive state of SCI-NP. Therefore, it would be worthwhile to examine the activity of these primary afferent neurons in response to treatment, particularly in the context of reduced sprouted fibers following ABI. Investigating the roles of spinal cord inhibitory interneurons and their functional changes in response to SCI and ABI will be crucial to more comprehensively understand their influence and connection with PKC γ + excitatory interneurons in gating mechanical allodynia. Additionally, given the promising results of this study showing that increased sensory stimulation during ABI enhances its efficiency in alleviating SCI-NP, conducting timed experiments with a focus on how different sensory input modulate SCI-NP-associated mechanistic alterations would be valuable in future studies.

5. Summary

Neuropathic pain (NP) following spinal cord injury (SCI) is a significant clinical challenge that severely impacts patients' quality of life. My doctoral dissertation investigates the mechanisms underlying NP using an experimental SCI model and evaluates the therapeutic potential of treadmill activity-based intervention (ABI) paradigms in alleviating this condition. Considering that sex may serve as a biological variable in the development of SCI-induced NP (SCI-NP) and its mitigation through ABI treatment, both adult female and male C57BL/6J mice were included to compare their NP-associated behavioral manifestations, the dynamic progression of NP, and response to ABI. Additionally, using a cohort of female mice, I conducted an experiment on ABI modification (treadmill belt replacement) to explore the role of sensory input during ABI and its influence on treatment outcomes for SCI-NP. The comparison of ABI paradigms using unpatterned and patterned belts underscores the importance of sensory input modulation and provides a foundation for future research aimed at optimizing therapeutic interventions for SCI-NP. Utilizing a combination of pain-associated behavioral assays (including both reflex-based and affective-cognitive concepts) and immunohistological analyses, my work examines changes in calcitonin gene-related peptide (CGRP)-expressing nociceptive fiber structural changes, spinal cord neuronal activation patterns (revealed by c-Fos expression), the activity of the gamma isoform of protein kinase C (PKC γ)-positive excitatory interneurons, and neuroglial-related inflammatory responses within the dorsal horn of the lumbar spinal cord (below the injury level). The results indicate that moderate thoracic contusion of the T11 spinal cord leads to robust and persistent below-level SCI-NP in mice of both sexes. Below the injury level, CGRP⁺ nociceptors sprout into the deeper dorsal horn of laminae III-IV, neuronal activation induced by innocuous stimuli increases across laminae I-V (mostly in III-V), and PKC γ expression in dorsal horn excitatory neurons is enhanced following SCI. Reactivated GFAP⁺ astrocytes and Iba1⁺ microglia were not detected under SCI-NP conditions. ABI treatment significantly modulates these maladaptive changes and alleviates pain by inhibiting CGRP⁺ nociceptor aberrant sprouting, reducing enhanced neuronal activation patterns, and depressing PKC γ ⁺ neuron hyperactivity

to levels comparable with sham animals. These findings suggest that targeting these associated mechanisms is a promising therapeutic strategy for managing SCI-NP. Furthermore, the results suggest that sex does not act as a significant variable in SCI-NP development, nor does it influence these mechanisms or their modulation by ABI.

6. Zusammenfassung

Neuropathischer Schmerz (NP) nach einer Rückenmarksverletzung (SCI) ist eine bedeutende klinische Herausforderung, die die Lebensqualität der Patienten erheblich beeinträchtigt. Meine Doktorarbeit untersucht die Mechanismen, die NP zugrunde liegen, anhand eines experimentellen SCI-Modells und bewertet das therapeutische Potenzial von aktivitätsbasierten Interventionen (ABI) auf dem Laufband zur Schmerzreduktion. In Anbetracht dessen, dass das Geschlecht als biologische Variable bei der Entwicklung von SCI-induziertem NP (SCI-NP) und dessen Milderung durch ABI-Behandlung eine Rolle spielen könnte, wurden sowohl adulte weibliche als auch männliche C57BL/6J-Mäuse einbezogen, um ihre NP-assoziierten Verhaltensmanifestationen, die dynamische Entwicklung von NP und die Reaktion auf ABI zu vergleichen. Zusätzlich führte ich mit einer Kohorte weiblicher Mäuse ein Experiment zur Modifikation von ABI (Laufbandmodifikation) durch, um die Rolle der sensorischen Eingabe während ABI und deren Einfluss auf die Behandlungsergebnisse bei SCI-NP zu untersuchen. Der Vergleich von ABI auf einem ungemusterten Laufband mit ABI auf einem gemusterten Laufband unterstreicht die Bedeutung der Modulation sensorischer Eingaben und bietet eine Grundlage für zukünftige Forschungen zur Optimierung therapeutischer Interventionen bei SCI-NP. Unter Verwendung einer Kombination von schmerzassoziierten Verhaltensuntersuchungen (einschließlich reflexbasierter und affektiv-kognitiver Konzepte) und immunhistologischen Analysen untersucht meine Arbeit Veränderungen in den strukturellen Veränderungen der Calcitonin Gene-Related Peptide (CGRP)-exprimierenden nozizeptiven Fasern, den neuronalen Aktivierungsmustern des Rückenmarks (aufgezeigt durch c-Fos-Expression), der Aktivität von PKC γ -positiven exzitatorischen Interneuronen und den neuroglialen Entzündungsreaktionen im Hinterhorn des lumbalen Rückenmarks (kaudal der Verletzungsebene). Die Ergebnisse zeigen, dass eine moderate thorakale Kontusion des Rückenmarks auf Höhe Th11 zu ausgeprägtem und anhaltendem NP unterhalb der Läsion bei Mäusen beider Geschlechter führt. Unterhalb der Verletzungsstelle sprossen CGRP+ Nozizeptoren in die tiefer liegenden Laminae III-IV des Hinterhorns, die neuronale Aktivierung durch harmlose Reize nimmt in den Laminae I-V

(meist in III-V) zu, und die PKC γ -Expression in exzitatorischen Neuronen des Hinterhorns wird nach SCI verstärkt. Reaktivierte GFAP⁺ Astrozyten und Iba1⁺ Mikroglia konnten in Verbindung mit NP nicht nachgewiesen werden. ABI moduliert diese maladaptiven Veränderungen signifikant und reduziert NP, indem sie das aberrante Sprossen von CGRP⁺ Nozizeptoren hemmt, verstärkte neuronale Aktivierungsmuster reduziert und die Hyperaktivität von PKC γ ⁺ Neuronen auf ein mit Kontrolltieren vergleichbares Niveau senkt. Diese Ergebnisse deuten darauf hin, dass das Aufgreifen assoziierter Mechanismen eine vielversprechende therapeutische Strategie zur Behandlung von SCI-NP darstellt. Darüber hinaus legen die Ergebnisse nahe, dass das Geschlecht keine signifikante Variable bei der Entwicklung von SCI-NP darstellt und auch diese Mechanismen oder deren Modulation durch ABI nicht beeinflusst.

7. Reference List

- Abraira, V. E. and Ginty, D. D. (2013). **The sensory neurons of touch**. *Neuron* 79 (4), 618-639, doi: 10.1016/j.neuron.2013.07.051.
- Ahn, S. N., Guu, J. J., Tobin, A. J., Edgerton, V. R. and Tillakaratne, N. J. (2006). **Use of c-fos to identify activity-dependent spinal neurons after stepping in intact adult rats**. *Spinal Cord* 44 (9), 547-559, doi: 10.1038/sj.sc.3101862.
- Bardoni, R., Takazawa, T., Tong, C. K., Choudhury, P., Scherrer, G. and Macdermott, A. B. (2013). **Pre- and postsynaptic inhibitory control in the spinal cord dorsal horn**. *Ann N Y Acad Sci* 1279, 90-96, doi: 10.1111/nyas.12056.
- Basbaum, A. (2000). **The perception of pain, Principles of Neural Science, Edited by Kandel ER, Schwartz JH, Jessell TM** (New York, McGraw-Hill).
- Basso, D. M., Fisher, L. C., Anderson, A. J., Jakeman, L. B., McTigue, D. M. and Popovich, P. G. (2006). **Basso Mouse Scale for locomotion detects differences in recovery after spinal cord injury in five common mouse strains**. *J Neurotrauma* 23 (5), 635-659, doi: 10.1089/neu.2006.23.635.
- Behrman, A. L. and Harkema, S. J. (2000). **Locomotor training after human spinal cord injury: a series of case studies**. *Phys Ther* 80 (7), 688-700.
- Berrocal, Y. A., Pearse, D. D., Andrade, C. M., Hechtman, J. F., Puentes, R. and Eaton, M. J. (2007). **Increased spinal c-Fos expression with noxious and non-noxious peripheral stimulation after severe spinal contusion**. *Neurosci Lett* 413 (1), 58-62, doi: 10.1016/j.neulet.2006.11.030.
- Blaesse, P. and Schmidt, T. (2015). **K-Cl cotransporter KCC2--a moonlighting protein in excitatory and inhibitory synapse development and function**. *Pflugers Arch* 467 (4), 615-624, doi: 10.1007/s00424-014-1547-6.
- Boadas-Vaello, P., Castany, S., Homs, J., Alvarez-Perez, B., Deulofeu, M. and Verdu, E. (2016). **Neuroplasticity of ascending and descending pathways after somatosensory system injury: reviewing knowledge to identify neuropathic pain therapeutic targets**. *Spinal Cord* 54 (5), 330-340, doi: 10.1038/sc.2015.225.
- Bokel, A., Dierks, M. L., Gutenbrunner, C., Weidner, N., Geng, V., Kalke, Y. B., Liebscher, T., Abel, F. R. and Sturm, C. (2020). **Perceived environmental barriers for people with spinal cord injury in Germany and their influence on quality of life**. *J Rehabil Med* 52 (8), jrm00090, doi: 10.2340/16501977-2717.

- Bourane, S., Grossmann, K. S., Britz, O., Dalet, A., Del Barrio, M. G., Stam, F. J., Garcia-Campmany, L., Koch, S. and Goulding, M. (2015). **Identification of a spinal circuit for light touch and fine motor control.** *Cell* 160 (3), 503-515, doi: 10.1016/j.cell.2015.01.011.
- Braz, J., Solorzano, C., Wang, X. and Basbaum, A. I. (2014). **Transmitting pain and itch messages: a contemporary view of the spinal cord circuits that generate gate control.** *Neuron* 82 (3), 522-536, doi: 10.1016/j.neuron.2014.01.018.
- Brown, E. V., Malik, A. F., Moese, E. R., McElroy, A. F. and Lepore, A. C. (2022). **Differential Activation of Pain Circuitry Neuron Populations in a Mouse Model of Spinal Cord Injury-Induced Neuropathic Pain.** *J Neurosci* 42 (15), 3271-3289, doi: 10.1523/JNEUROSCI.1596-21.2022.
- Bryce, T. N., Biering-Sorensen, F., Finnerup, N. B., Cardenas, D. D., Defrin, R., Lundeberg, T., Norrbrink, C., Richards, J. S., Siddall, P., Stripling, T., Treede, R. D., Waxman, S. G., Widerstrom-Noga, E., Yezierski, R. P. and Dijkers, M. (2012). **International spinal cord injury pain classification: part I. Background and description. March 6-7, 2009.** *Spinal Cord* 50 (6), 413-417, doi: 10.1038/sc.2011.156.
- Burke, D., Fullen, B. M., Stokes, D. and Lennon, O. (2017). **Neuropathic pain prevalence following spinal cord injury: A systematic review and meta-analysis.** *Eur J Pain* 21 (1), 29-44, doi: 10.1002/ejp.905.
- Burke, D., Lennon, O. and Fullen, B. M. (2018). **Quality of life after spinal cord injury: The impact of pain.** *Eur J Pain* 22 (9), 1662-1672, doi: 10.1002/ejp.1248.
- Carlton, S. M., Du, J., Tan, H. Y., Nestic, O., Hargett, G. L., Bopp, A. C., Yamani, A., Lin, Q., Willis, W. D. and Hulsebosch, C. E. (2009). **Peripheral and central sensitization in remote spinal cord regions contribute to central neuropathic pain after spinal cord injury.** *Pain* 147 (1-3), 265-276, doi: 10.1016/j.pain.2009.09.030.
- Cavalli, E., Mammana, S., Nicoletti, F., Bramanti, P. and Mazzon, E. (2019). **The neuropathic pain: An overview of the current treatment and future therapeutic approaches.** *Int J Immunopathol Pharmacol* 33, 2058738419838383, doi: 10.1177/2058738419838383.
- Chen, G., Luo, X., Qadri, M. Y., Berta, T. and Ji, R. R. (2018). **Sex-Dependent Glial Signaling in Pathological Pain: Distinct Roles of Spinal Microglia and Astrocytes.** *Neurosci Bull* 34 (1), 98-108, doi: 10.1007/s12264-017-0145-y.
- Chen, J., Weidner, N. and Puttagunta, R. (2022). **The Impact of Activity-Based Interventions on Neuropathic Pain in Experimental Spinal Cord Injury.** *Cells* 11 (19), doi: 10.3390/cells11193087.
- Chen, L. and Huang, L. Y. (1992). **Protein kinase C reduces Mg²⁺ block of NMDA-receptor channels as a mechanism of modulation.** *Nature* 356 (6369), 521-523, doi: 10.1038/356521a0.

- Chen, M. and Zheng, B. (2014). **Axon plasticity in the mammalian central nervous system after injury.** *Trends Neurosci* 37 (10), 583-593, doi: 10.1016/j.tins.2014.08.008.
- Cheng, X., Yu, Z., Hu, W., Chen, J., Chen, W., Wang, L., Li, X., Zhang, W., Chen, J., Zou, X., Chen, W. and Wan, Y. (2022). **Voluntary exercise ameliorates neuropathic pain by suppressing calcitonin gene-related peptide and ionized calcium-binding adapter molecule 1 overexpression in the lumbar dorsal horns in response to injury to the cervical spinal cord.** *Exp Neurol* 354, 114105, doi: 10.1016/j.expneurol.2022.114105.
- Chhaya, S. J., Quiros-Molina, D., Tamashiro-Orrego, A. D., Houle, J. D. and Detloff, M. R. (2019). **Exercise-Induced Changes to the Macrophage Response in the Dorsal Root Ganglia Prevent Neuropathic Pain after Spinal Cord Injury.** *J Neurotrauma* 36 (6), 877-890, doi: 10.1089/neu.2018.5819.
- Cioffi, C. L. (2021). **Inhibition of Glycine Re-Uptake: A Potential Approach for Treating Pain by Augmenting Glycine-Mediated Spinal Neurotransmission and Blunting Central Nociceptive Signaling.** *Biomolecules* 11 (6), doi: 10.3390/biom11060864.
- Cragg, J. J., Noonan, V. K., Noreau, L., Borisoff, J. F. and Kramer, J. K. (2015). **Neuropathic pain, depression, and cardiovascular disease: a national multicenter study.** *Neuroepidemiology* 44 (3), 130-137, doi: 10.1159/000377726.
- Crown, E. D., Gwak, Y. S., Ye, Z., Johnson, K. M. and Hulsebosch, C. E. (2008). **Activation of p38 MAP kinase is involved in central neuropathic pain following spinal cord injury.** *Exp Neurol* 213 (2), 257-267, doi: 10.1016/j.expneurol.2008.05.025.
- Crucianelli, L. and Morrison, I. (2023). **Skin-Mediated Interoception: The Perception of Affective Touch and Cutaneous Pain.** In: *Somatosensory Research Methods*, ed. Holmes, N. P., Springer US, New York, NY, pp. 199-224.
- Detloff, M. R., Fisher, L. C., McGaughy, V., Longbrake, E. E., Popovich, P. G. and Basso, D. M. (2008). **Remote activation of microglia and pro-inflammatory cytokines predict the onset and severity of below-level neuropathic pain after spinal cord injury in rats.** *Exp Neurol* 212 (2), 337-347, doi: 10.1016/j.expneurol.2008.04.009.
- Detloff, M. R., Smith, E. J., Quiros Molina, D., Ganzer, P. D. and Houle, J. D. (2014). **Acute exercise prevents the development of neuropathic pain and the sprouting of non-peptidergic (GDNF- and artemin-responsive) c-fibers after spinal cord injury.** *Exp Neurol* 255, 38-48, doi: 10.1016/j.expneurol.2014.02.013.

- Dominguez, C. A., Strom, M., Gao, T., Zhang, L., Olsson, T., Wiesenfeld-Hallin, Z., Xu, X. J. and Piehl, F. (2012). **Genetic and sex influence on neuropathic pain-like behaviour after spinal cord injury in the rat.** *Eur J Pain* 16 (10), 1368-1377, doi: 10.1002/j.1532-2149.2012.00144.x.
- Drew, G. M., Siddall, P. J. and Duggan, A. W. (2004). **Mechanical allodynia following contusion injury of the rat spinal cord is associated with loss of GABAergic inhibition in the dorsal horn.** *Pain* 109 (3), 379-388, doi: 10.1016/j.pain.2004.02.007.
- Dugan, E. A., Jergova, S. and Sagen, J. (2020). **Mutually beneficial effects of intensive exercise and GABAergic neural progenitor cell transplants in reducing neuropathic pain and spinal pathology in rats with spinal cord injury.** *Exp Neurol* 327, 113208, doi: 10.1016/j.expneurol.2020.113208.
- Dugan, E. A., Schachner, B., Jergova, S. and Sagen, J. (2021). **Intensive Locomotor Training Provides Sustained Alleviation of Chronic Spinal Cord Injury-Associated Neuropathic Pain: A Two-Year Pre-Clinical Study.** *J Neurotrauma* 38 (6), 789-802, doi: 10.1089/neu.2020.7378.
- Eisenach, James C. (2001). **Textbook of Pain, 4th Edition.** *Anesthesiology* 94 (5), 942-942, doi: 10.1097/00000542-200105000-00052.
- Ergen, E. and Ulkar, B. (2007). **Proprioception and Coordination.** In: *Clinical Sports Medicine*, pp. 237-255.
- Field-Fote, E. C. and Roach, K. E. (2011). **Influence of a locomotor training approach on walking speed and distance in people with chronic spinal cord injury: a randomized clinical trial.** *Phys Ther* 91 (1), 48-60, doi: 10.2522/ptj.20090359.
- Finnerup, N. B., Haroutounian, S., Kamerman, P., Baron, R., Bennett, D. L. H., Bouhassira, D., Cruccu, G., Freeman, R., Hansson, P., Nurmikko, T., Raja, S. N., Rice, A. S. C., Serra, J., Smith, B. H., Treede, R. D. and Jensen, T. S. (2016). **Neuropathic pain: an updated grading system for research and clinical practice.** *Pain* 157 (8), 1599-1606, doi: 10.1097/j.pain.0000000000000492.
- Finnerup, N. B., Norrbrink, C., Trok, K., Piehl, F., Johannesen, I. L., Sorensen, J. C., Jensen, T. S. and Werhagen, L. (2014). **Phenotypes and predictors of pain following traumatic spinal cord injury: a prospective study.** *J Pain* 15 (1), 40-48, doi: 10.1016/j.jpain.2013.09.008.
- Fiumelli, H. and Woodin, M. A. (2007). **Role of activity-dependent regulation of neuronal chloride homeostasis in development.** *Curr Opin Neurobiol* 17 (1), 81-86, doi: 10.1016/j.conb.2007.01.002.
- Fleming, J. C., Norenberg, M. D., Ramsay, D. A., Dekaban, G. A., Marcillo, A. E., Saenz, A. D., Pasquale-Styles, M., Dietrich, W. D. and Weaver, L. C. (2006). **The cellular inflammatory response in human spinal cords after injury.** *Brain* 129 (Pt 12), 3249-3269, doi: 10.1093/brain/awl296.

- Franz, S., Eck, U., Schuld, C., Heutehaus, L., Wolf, M., Wilder-Smith, E., Schulte-Mattler, W., Weber, M. A., Rupp, R. and Weidner, N. (2023). **Lower Motoneuron Dysfunction Impacts Spontaneous Motor Recovery in Acute Cervical Spinal Cord Injury**. *J Neurotrauma* 40 (9-10), 862-875, doi: 10.1089/neu.2022.0181.
- French, A. S. and Torkkeli, P. H. (2009). **Mechanoreceptors**. In: *Encyclopedia of Neuroscience*, pp. 689-695.
- Gan, Z., Li, H., Naser, P. V., Han, Y., Tan, L. L., Oswald, M. J. and Kuner, R. (2021a). **Repetitive non-invasive prefrontal stimulation reverses neuropathic pain via neural remodelling in mice**. *Prog Neurobiol* 201, 102009, doi: 10.1016/j.pneurobio.2021.102009.
- Gan, Z., Li, H., Naser, P. V., Oswald, M. J. and Kuner, R. (2021b). **Suppression of neuropathic pain and comorbidities by recurrent cycles of repetitive transcranial direct current motor cortex stimulation in mice**. *Sci Rep* 11 (1), 9735, doi: 10.1038/s41598-021-89122-6.
- Gatto, G., Bourane, S., Ren, X., Di Costanzo, S., Fenton, P. K., Halder, P., Seal, R. P. and Goulding, M. D. (2021). **A Functional Topographic Map for Spinal Sensorimotor Reflexes**. *Neuron* 109 (1), 91-104 e105, doi: 10.1016/j.neuron.2020.10.003.
- Gaudet, A. D., Ayala, M. T., Schleicher, W. E., Smith, E. J., Bateman, E. M., Maier, S. F. and Watkins, L. R. (2017). **Exploring acute-to-chronic neuropathic pain in rats after contusion spinal cord injury**. *Exp Neurol* 295, 46-54, doi: 10.1016/j.expneurol.2017.05.011.
- Gensel, J. C., Donahue, R. R., Bailey, W. M. and Taylor, B. K. (2019). **Sexual Dimorphism of Pain Control: Analgesic Effects of Pioglitazone and Azithromycin in Chronic Spinal Cord Injury**. *J Neurotrauma* 36 (15), 2372-2376, doi: 10.1089/neu.2018.6207.
- Ghasemlou, N., Kerr, B. J. and David, S. (2005). **Tissue displacement and impact force are important contributors to outcome after spinal cord contusion injury**. *Exp Neurol* 196 (1), 9-17, doi: 10.1016/j.expneurol.2005.05.017.
- Ghazisaeidi, S., Muley, M. M. and Salter, M. W. (2023). **Neuropathic Pain: Mechanisms, Sex Differences, and Potential Therapies for a Global Problem**. *Annu Rev Pharmacol Toxicol* 63, 565-583, doi: 10.1146/annurev-pharmtox-051421-112259.
- Grace, P. M., Hutchinson, M. R., Maier, S. F. and Watkins, L. R. (2014). **Pathological pain and the neuroimmune interface**. *Nat Rev Immunol* 14 (4), 217-231, doi: 10.1038/nri3621.
- Griesbach, G. S., Hovda, D. A., Molteni, R., Wu, A. and Gomez-Pinilla, F. (2004). **Voluntary exercise following traumatic brain injury: brain-derived neurotrophic factor upregulation and recovery of function**. *Neuroscience* 125 (1), 129-139, doi: 10.1016/j.neuroscience.2004.01.030.

- Gwak, Y. S., Crown, E. D., Unabia, G. C. and Hulsebosch, C. E. (2008). **Propentofylline attenuates allodynia, glial activation and modulates GABAergic tone after spinal cord injury in the rat.** *Pain* 138 (2), 410-422, doi: 10.1016/j.pain.2008.01.021.
- Gwak, Y. S. and Hulsebosch, C. E. (2009). **Remote astrocytic and microglial activation modulates neuronal hyperexcitability and below-level neuropathic pain after spinal injury in rat.** *Neuroscience* 161 (3), 895-903, doi: 10.1016/j.neuroscience.2009.03.055.
- Gwak, Y. S. and Hulsebosch, C. E. (2011a). **GABA and central neuropathic pain following spinal cord injury.** *Neuropharmacology* 60 (5), 799-808, doi: 10.1016/j.neuropharm.2010.12.030.
- Gwak, Y. S. and Hulsebosch, C. E. (2011b). **Neuronal hyperexcitability: a substrate for central neuropathic pain after spinal cord injury.** *Curr Pain Headache Rep* 15 (3), 215-222, doi: 10.1007/s11916-011-0186-2.
- Gwak, Y. S., Hulsebosch, C. E. and Leem, J. W. (2017). **Neuronal-Glial Interactions Maintain Chronic Neuropathic Pain after Spinal Cord Injury.** *Neural Plast* 2017, 2480689, doi: 10.1155/2017/2480689.
- Gwak, Y. S., Kang, J., Leem, J. W. and Hulsebosch, C. E. (2007). **Spinal AMPA receptor inhibition attenuates mechanical allodynia and neuronal hyperexcitability following spinal cord injury in rats.** *J Neurosci Res* 85 (11), 2352-2359, doi: 10.1002/jnr.21379.
- Gwak, Y. S., Kang, J., Unabia, G. C. and Hulsebosch, C. E. (2012). **Spatial and temporal activation of spinal glial cells: role of gliopathy in central neuropathic pain following spinal cord injury in rats.** *Exp Neurol* 234 (2), 362-372, doi: 10.1016/j.expneurol.2011.10.010.
- Gwak, Y. S., Unabia, G. C. and Hulsebosch, C. E. (2009). **Activation of p-38alpha MAPK contributes to neuronal hyperexcitability in caudal regions remote from spinal cord injury.** *Exp Neurol* 220 (1), 154-161, doi: 10.1016/j.expneurol.2009.08.012.
- Hains, B. C., Klein, J. P., Saab, C. Y., Craner, M. J., Black, J. A. and Waxman, S. G. (2003). **Upregulation of sodium channel Nav1.3 and functional involvement in neuronal hyperexcitability associated with central neuropathic pain after spinal cord injury.** *J Neurosci* 23 (26), 8881-8892, doi: 10.1523/JNEUROSCI.23-26-08881.2003.
- Hains, B. C. and Waxman, S. G. (2006). **Activated microglia contribute to the maintenance of chronic pain after spinal cord injury.** *J Neurosci* 26 (16), 4308-4317, doi: 10.1523/JNEUROSCI.0003-06.2006.
- Hao, J. X., Kupers, R. C. and Xu, X. J. (2004). **Response characteristics of spinal cord dorsal horn neurons in chronic allodynic rats after spinal cord injury.** *J Neurophysiol* 92 (3), 1391-1399, doi: 10.1152/jn.00121.2004.

- Harkema, S., Gerasimenko, Y., Hodes, J., Burdick, J., Angeli, C., Chen, Y., Ferreira, C., Willhite, A., Rejc, E., Grossman, R. G. and Edgerton, V. R. (2011). **Effect of epidural stimulation of the lumbosacral spinal cord on voluntary movement, standing, and assisted stepping after motor complete paraplegia: a case study.** *Lancet* 377 (9781), 1938-1947, doi: 10.1016/S0140-6736(11)60547-3.
- Hubner, C. A., Stein, V., Hermans-Borgmeyer, I., Meyer, T., Ballanyi, K. and Jentsch, T. J. (2001). **Disruption of KCC2 reveals an essential role of K-Cl cotransport already in early synaptic inhibition.** *Neuron* 30 (2), 515-524, doi: 10.1016/s0896-6273(01)00297-5.
- Hubscher, C. H., Fell, J. D. and Gupta, D. S. (2010). **Sex and hormonal variations in the development of at-level allodynia in a rat chronic spinal cord injury model.** *Neurosci Lett* 477 (3), 153-156, doi: 10.1016/j.neulet.2010.04.053.
- Hughes, D. I., Scott, D. T., Todd, A. J. and Riddell, J. S. (2003). **Lack of evidence for sprouting of Abeta afferents into the superficial laminae of the spinal cord dorsal horn after nerve section.** *J Neurosci* 23 (29), 9491-9499, doi: 10.1523/JNEUROSCI.23-29-09491.2003.
- Hulsebosch, C. E. (2008). **Gliopathy ensures persistent inflammation and chronic pain after spinal cord injury.** *Exp Neurol* 214 (1), 6-9, doi: 10.1016/j.expneurol.2008.07.016.
- Hulsebosch, C. E., Hains, B. C., Crown, E. D. and Carlton, S. M. (2009). **Mechanisms of chronic central neuropathic pain after spinal cord injury.** *Brain Res Rev* 60 (1), 202-213, doi: 10.1016/j.brainresrev.2008.12.010.
- Hunt, S. P., Pini, A. and Evan, G. (1987). **Induction of c- protein in spinal cord neurones following sensory stimulation.** *Regulatory Peptides* 18 (5-6), doi: 10.1016/0167-0115(87)90224-2.
- Ibuki, T., Hama, A. T., Wang, X. T., Pappas, G. D. and Sagen, J. (1997). **Loss of GABA-immunoreactivity in the spinal dorsal horn of rats with peripheral nerve injury and promotion of recovery by adrenal medullary grafts.** *Neuroscience* 76 (3), 845-858, doi: 10.1016/s0306-4522(96)00341-7.
- Ichiyama, R. M., Broman, J., Roy, R. R., Zhong, H., Edgerton, V. R. and Havton, L. A. (2011). **Locomotor training maintains normal inhibitory influence on both alpha- and gamma-motoneurons after neonatal spinal cord transection.** *J Neurosci* 31 (1), 26-33, doi: 10.1523/JNEUROSCI.6433-09.2011.
- Jergova, S., Dugan, E. A. and Sagen, J. (2023). **Attenuation of SCI-Induced Hypersensitivity by Intensive Locomotor Training and Recombinant GABAergic Cells.** *Bioengineering (Basel)* 10 (1), doi: 10.3390/bioengineering10010084.
- Ji, R. R., Chamesian, A. and Zhang, Y. Q. (2016). **Pain regulation by non-neuronal cells and inflammation.** *Science* 354 (6312), 572-577, doi: 10.1126/science.aaf8924.

- Kaila, K., Price, T. J., Payne, J. A., Puskarjov, M. and Voipio, J. (2014). **Cation-chloride cotransporters in neuronal development, plasticity and disease.** *Nat Rev Neurosci* 15 (10), 637-654, doi: 10.1038/nrn3819.
- Kami, K., Taguchi Ms, S., Tajima, F. and Senba, E. (2016). **Improvements in impaired GABA and GAD65/67 production in the spinal dorsal horn contribute to exercise-induced hypoalgesia in a mouse model of neuropathic pain.** *Mol Pain* 12, doi: 10.1177/1744806916629059.
- Kerr, B. J. and David, S. (2007). **Pain behaviors after spinal cord contusion injury in two commonly used mouse strains.** *Exp Neurol* 206 (2), 240-247, doi: 10.1016/j.expneurol.2007.04.014.
- Kim, H. Y., Lee, H. J., Kim, T. L., Kim, E., Ham, D., Lee, J., Kim, T., Shin, J. W., Son, M., Sung, J. H. and Han, Z. A. (2020). **Prevalence and Characteristics of Neuropathic Pain in Patients With Spinal Cord Injury Referred to a Rehabilitation Center.** *Ann Rehabil Med* 44 (6), 438-449, doi: 10.5535/arm.20081.
- Kim, J. Y., Choi, G. S., Cho, Y. W., Cho, H., Hwang, S. J. and Ahn, S. H. (2013). **Attenuation of spinal cord injury-induced astroglial and microglial activation by repetitive transcranial magnetic stimulation in rats.** *J Korean Med Sci* 28 (2), 295-299, doi: 10.3346/jkms.2013.28.2.295.
- Knerlich-Lukoschus, F. and Held-Feindt, J. (2015). **Chemokine-ligands/receptors: multiplayers in traumatic spinal cord injury.** *Mediators Inflamm* 2015, 486758, doi: 10.1155/2015/486758.
- Kramer, J. L., Minhas, N. K., Jutzeler, C. R., Erskine, E. L., Liu, L. J. and Ramer, M. S. (2017). **Neuropathic pain following traumatic spinal cord injury: Models, measurement, and mechanisms.** *J Neurosci Res* 95 (6), 1295-1306, doi: 10.1002/jnr.23881.
- Kuner, R. and Flor, H. (2016). **Structural plasticity and reorganisation in chronic pain.** *Nat Rev Neurosci* 18 (1), 20-30, doi: 10.1038/nrn.2016.162.
- Kwon, M., Altin, M., Duenas, H. and Alev, L. (2014). **The role of descending inhibitory pathways on chronic pain modulation and clinical implications.** *Pain Pract* 14 (7), 656-667, doi: 10.1111/papr.12145.
- Lee, S. E., Greenough, E. K., Oancea, P., Scheinfeld, A. R., Douglas, A. M. and Gaudet, A. D. (2023). **Sex Differences in Pain: Spinal Cord Injury in Female and Male Mice Elicits Behaviors Related to Neuropathic Pain.** *J Neurotrauma* 40 (9-10), 833-844, doi: 10.1089/neu.2022.0482.
- Leem, J. W., Kim, H. K., Hulsebosch, C. E. and Gwak, Y. S. (2010). **Ionotropic glutamate receptors contribute to maintained neuronal hyperexcitability following spinal cord injury in rats.** *Exp Neurol* 224 (1), 321-324, doi: 10.1016/j.expneurol.2010.02.012.

- Lepore, A. C., O'Donnell, J., Bonner, J. F., Paul, C., Miller, M. E., Rauck, B., Kushner, R. A., Rothstein, J. D., Fischer, I. and Maragakis, N. J. (2011). **Spatial and temporal changes in promoter activity of the astrocyte glutamate transporter GLT1 following traumatic spinal cord injury.** *J Neurosci Res* 89 (7), 1001-1017, doi: 10.1002/jnr.22624.
- Li, X., Wang, Q., Ding, J., Wang, S., Dong, C. and Wu, Q. (2020). **Exercise training modulates glutamic acid decarboxylase-65/67 expression through TrkB signaling to ameliorate neuropathic pain in rats with spinal cord injury.** *Mol Pain* 16, 1744806920924511, doi: 10.1177/1744806920924511.
- Liddel, S. A., Marsh, S. E. and Stevens, B. (2020). **Microglia and Astrocytes in Disease: Dynamic Duo or Partners in Crime?** *Trends Immunol* 41 (9), 820-835, doi: 10.1016/j.it.2020.07.006.
- Linher-Melville, K., Shah, A. and Singh, G. (2020). **Sex differences in neuro(auto)immunity and chronic sciatic nerve pain.** *Biol Sex Differ* 11 (1), 62, doi: 10.1186/s13293-020-00339-y.
- Liu, S., Bonalume, V., Gao, Q., Chen, J. T., Rohr, K., Hu, J. and Carr, R. (2022). **Pre-Synaptic GABA(A) in NaV1.8(+) Primary Afferents Is Required for the Development of Punctate but Not Dynamic Mechanical Allodynia following CFA Inflammation.** *Cells* 11 (15), doi: 10.3390/cells11152390.
- Liu, Y., Wang, X., Li, W., Zhang, Q., Li, Y., Zhang, Z., Zhu, J., Chen, B., Williams, P. R., Zhang, Y., Yu, B., Gu, X. and He, Z. (2017). **A Sensitized IGF1 Treatment Restores Corticospinal Axon-Dependent Functions.** *Neuron* 95 (4), 817-833 e814, doi: 10.1016/j.neuron.2017.07.037.
- Lu, Y., Dong, H., Gao, Y., Gong, Y., Ren, Y., Gu, N., Zhou, S., Xia, N., Sun, Y. Y., Ji, R. R. and Xiong, L. (2013). **A feed-forward spinal cord glycinergic neural circuit gates mechanical allodynia.** *J Clin Invest* 123 (9), 4050-4062, doi: 10.1172/JCI70026.
- Lu, Y. and Perl, E. R. (2005). **Modular organization of excitatory circuits between neurons of the spinal superficial dorsal horn (laminae I and II).** *J Neurosci* 25 (15), 3900-3907, doi: 10.1523/JNEUROSCI.0102-05.2005.
- Malcangio, M. (2018). **GABA(B) receptors and pain.** *Neuropharmacology* 136 (Pt A), 102-105, doi: 10.1016/j.neuropharm.2017.05.012.
- Malmberg, A. B., Chen, C., Tonegawa, S. and Basbaum, A. I. (1997). **Preserved acute pain and reduced neuropathic pain in mice lacking PKCgamma.** *Science* 278 (5336), 279-283, doi: 10.1126/science.278.5336.279.
- Mapplebeck, J. C., Beggs, S. and Salter, M. W. (2017). **Molecules in pain and sex: a developing story.** *Mol Brain* 10 (1), 9, doi: 10.1186/s13041-017-0289-8.

- Mapplebeck, J. C. S., Dalgarno, R., Tu, Y., Moriarty, O., Beggs, S., Kwok, C. H. T., Halievski, K., Assi, S., Mogil, J. S., Trang, T. and Salter, M. W. (2018). **Microglial P2X4R-evoked pain hypersensitivity is sexually dimorphic in rats**. *Pain* 159 (9), 1752-1763, doi: 10.1097/j.pain.0000000000001265.
- Martin, W. J., Liu, H., Wang, H., Malmberg, A. B. and Basbaum, A. I. (1999). **Inflammation-induced up-regulation of protein kinase Cgamma immunoreactivity in rat spinal cord correlates with enhanced nociceptive processing**. *Neuroscience* 88 (4), 1267-1274, doi: 10.1016/s0306-4522(98)00314-5.
- Martin, W. J., Malmberg, A. B. and Basbaum, A. I. (2001). **PKCgamma contributes to a subset of the NMDA-dependent spinal circuits that underlie injury-induced persistent pain**. *J Neurosci* 21 (14), 5321-5327, doi: 10.1523/JNEUROSCI.21-14-05321.2001.
- McFarlane, K., Otto, T. E., Bailey, W. M., Veldhorst, A. K., Donahue, R. R., Taylor, B. K. and Gensel, J. C. (2020). **Effect of Sex on Motor Function, Lesion Size, and Neuropathic Pain after Contusion Spinal Cord Injury in Mice**. *J Neurotrauma* 37 (18), 1983-1990, doi: 10.1089/neu.2019.6931.
- Mermet-Joret, N., Chatila, N., Pereira, B., Monconduit, L., Dallel, R. and Antri, M. (2017). **Lamina specific postnatal development of PKCgamma interneurons within the rat medullary dorsal horn**. *Dev Neurobiol* 77 (1), 102-119, doi: 10.1002/dneu.22414.
- Mesquida-Veny, F., Martinez-Torres, S., Del Rio, J. A. and Hervera, A. (2022). **Genetic control of neuronal activity enhances axonal growth only on permissive substrates**. *Mol Med* 28 (1), 97, doi: 10.1186/s10020-022-00524-2.
- Miracourt, L. S., Dallel, R. and Voisin, D. L. (2007). **Glycine inhibitory dysfunction turns touch into pain through PKCgamma interneurons**. *PLoS One* 2 (11), e1116, doi: 10.1371/journal.pone.0001116.
- Miracourt, L. S., Peirs, C., Dallel, R. and Voisin, D. L. (2011). **Glycine inhibitory dysfunction turns touch into pain through astrocyte-derived D-serine**. *Pain* 152 (6), 1340-1348, doi: 10.1016/j.pain.2011.02.021.
- Nees, T. A., Tappe-Theodor, A., Sliwinski, C., Motsch, M., Rupp, R., Kuner, R., Weidner, N. and Blesch, A. (2016). **Early-onset treadmill training reduces mechanical allodynia and modulates calcitonin gene-related peptide fiber density in lamina III/IV in a mouse model of spinal cord contusion injury**. *Pain* 157 (3), 687-697, doi: 10.1097/j.pain.0000000000000422.
- Netter, F. H. (2023). **The Netter Collection of Medical Illustrations: Nervous System, Volume 7, Part II - Spinal Cord and Peripheral Motor and Sensory Systems**, 3rd Edition. edn

- Neumann, S., Braz, J. M., Skinner, K., Llewellyn-Smith, I. J. and Basbaum, A. I. (2008). **Innocuous, not noxious, input activates PKC γ interneurons of the spinal dorsal horn via myelinated afferent fibers.** *J Neurosci* 28 (32), 7936-7944, doi: 10.1523/JNEUROSCI.1259-08.2008.
- Peirs, C., Patil, S., Bouali-Benazzouz, R., Artola, A., Landry, M. and Dallel, R. (2014). **Protein kinase C gamma interneurons in the rat medullary dorsal horn: distribution and synaptic inputs to these neurons, and subcellular localization of the enzyme.** *J Comp Neurol* 522 (2), 393-413, doi: 10.1002/cne.23407.
- Peirs, C. and Seal, R. P. (2016). **Neural circuits for pain: Recent advances and current views.** *Science* 354 (6312), 578-584, doi: 10.1126/science.aaf8933.
- Peirs, C., Williams, S. P., Zhao, X., Walsh, C. E., Gedeon, J. Y., Cagle, N. E., Goldring, A. C., Hioki, H., Liu, Z., Marell, P. S. and Seal, R. P. (2015). **Dorsal Horn Circuits for Persistent Mechanical Pain.** *Neuron* 87 (4), 797-812, doi: 10.1016/j.neuron.2015.07.029.
- Petitjean, H., Pawlowski, S. A., Fraine, S. L., Sharif, B., Hamad, D., Fatima, T., Berg, J., Brown, C. M., Jan, L. Y., Ribeiro-da-Silva, A., Braz, J. M., Basbaum, A. I. and Sharif-Naeini, R. (2015). **Dorsal Horn Parvalbumin Neurons Are Gate-Keepers of Touch-Evoked Pain after Nerve Injury.** *Cell Rep* 13 (6), 1246-1257, doi: 10.1016/j.celrep.2015.09.080.
- Polgar, E., Fowler, J. H., McGill, M. M. and Todd, A. J. (1999). **The types of neuron which contain protein kinase C gamma in rat spinal cord.** *Brain Res* 833 (1), 71-80, doi: 10.1016/s0006-8993(99)01500-0.
- Prabhala, T., Hellman, A., Walling, I., Maietta, T., Qian, J., Burdette, C., Neubauer, P., Shao, M., Stapleton, A., Thibodeau, J. and Pilitsis, J. G. (2018). **External focused ultrasound treatment for neuropathic pain induced by common peroneal nerve injury.** *Neurosci Lett* 684, 145-151, doi: 10.1016/j.neulet.2018.07.037.
- Proske, U. (2015). **The role of muscle proprioceptors in human limb position sense: a hypothesis.** *J Anat* 227 (2), 178-183, doi: 10.1111/joa.12289.
- Raymond, L. A., Blackstone, C. D. and Huganir, R. L. (1993). **Phosphorylation of amino acid neurotransmitter receptors in synaptic plasticity.** *Trends Neurosci* 16 (4), 147-153, doi: 10.1016/0166-2236(93)90123-4.
- Renier, N., Adams, E. L., Kirst, C., Wu, Z., Azevedo, R., Kohl, J., Autry, A. E., Kadiri, L., Umadevi Venkataraju, K., Zhou, Y., Wang, V. X., Tang, C. Y., Olsen, O., Dulac, C., Osten, P. and Tessier-Lavigne, M. (2016). **Mapping of Brain Activity by Automated Volume Analysis of Immediate Early Genes.** *Cell* 165 (7), 1789-1802, doi: 10.1016/j.cell.2016.05.007.

- Rosen, S., Ham, B. and Mogil, J. S. (2017). **Sex differences in neuroimmunity and pain.** *J Neurosci Res* 95 (1-2), 500-508, doi: 10.1002/jnr.23831.
- Saika, F., Matsuzaki, S., Kishioka, S. and Kiguchi, N. (2021). **Chemogenetic Activation of CX3CR1-Expressing Spinal Microglia Using Gq-DREADD Elicits Mechanical Allodynia in Male Mice.** *Cells* 10 (4), doi: 10.3390/cells10040874.
- Saika, F., Matsuzaki, S., Kobayashi, D., Ideguchi, Y., Nakamura, T. Y., Kishioka, S. and Kiguchi, N. (2020). **Chemogenetic Regulation of CX3CR1-Expressing Microglia Using Gi-DREADD Exerts Sex-Dependent Anti-Allodynic Effects in Mouse Models of Neuropathic Pain.** *Front Pharmacol* 11, 925, doi: 10.3389/fphar.2020.00925.
- Sanchez-Ventura, J., Gimenez-Llort, L., Penas, C. and Udina, E. (2021). **Voluntary wheel running preserves lumbar perineuronal nets, enhances motor functions and prevents hyperreflexia after spinal cord injury.** *Exp Neurol* 336, 113533, doi: 10.1016/j.expneurol.2020.113533.
- Sandkuhler, J. (2009). **Models and mechanisms of hyperalgesia and allodynia.** *Physiol Rev* 89 (2), 707-758, doi: 10.1152/physrev.00025.2008.
- Sandrow-Feinberg, H. R. and Houle, J. D. (2015). **Exercise after spinal cord injury as an agent for neuroprotection, regeneration and rehabilitation.** *Brain Res* 1619, 12-21, doi: 10.1016/j.brainres.2015.03.052.
- Siddall, P. J. and Loeser, J. D. (2001). **Pain following spinal cord injury.** *Spinal Cord* 39 (2), 63-73, doi: 10.1038/sj.sc.3101116.
- Siddall, P. J., McClelland, J. M., Rutkowski, S. B. and Cousins, M. J. (2003). **A longitudinal study of the prevalence and characteristics of pain in the first 5 years following spinal cord injury.** *Pain* 103 (3), 249-257, doi: 10.1016/S0304-3959(02)00452-9.
- Siddall, P. J., Xu, C. L., Floyd, N. and Keay, K. A. (1999). **C-fos expression in the spinal cord of rats exhibiting allodynia following contusive spinal cord injury.** *Brain Res* 851 (1-2), 281-286, doi: 10.1016/s0006-8993(99)02173-3.
- Sliwinski, C., Heutehaus, L., Taberner, F. J., Weiss, L., Kampanis, V., Tolou-Dabbaghian, B., Cheng, X., Motsch, M., Heppenstall, P. A., Kuner, R., Franz, S., Lechner, S. G., Weidner, N. and Puttagunta, R. (2024). **Contribution of mechanoreceptors to spinal cord injury-induced mechanical allodynia.** *Pain* 165 (6), 1336-1347, doi: 10.1097/j.pain.0000000000003139.
- Sliwinski, C., Nees, T. A., Puttagunta, R., Weidner, N. and Blesch, A. (2018). **Sensorimotor Activity Partially Ameliorates Pain and Reduces Nociceptive Fiber Density in the Chronically Injured Spinal Cord.** *J Neurotrauma* 35 (18), 2222-2238, doi: 10.1089/neu.2017.5431.

- Sofroniew, M. V. (2015). **Astrocyte barriers to neurotoxic inflammation**. *Nat Rev Neurosci* 16 (5), 249-263, doi: 10.1038/nrn3898.
- Sorge, R. E., LaCroix-Fralish, M. L., Tuttle, A. H., Sotocinal, S. G., Austin, J. S., Ritchie, J., Chanda, M. L., Graham, A. C., Topham, L., Beggs, S., Salter, M. W. and Mogil, J. S. (2011). **Spinal cord Toll-like receptor 4 mediates inflammatory and neuropathic hypersensitivity in male but not female mice**. *J Neurosci* 31 (43), 15450-15454, doi: 10.1523/JNEUROSCI.3859-11.2011.
- Sorge, R. E., Mapplebeck, J. C., Rosen, S., Beggs, S., Taves, S., Alexander, J. K., Martin, L. J., Austin, J. S., Sotocinal, S. G., Chen, D., Yang, M., Shi, X. Q., Huang, H., Pilon, N. J., Bilan, P. J., Tu, Y., Klip, A., Ji, R. R., Zhang, J., Salter, M. W. and Mogil, J. S. (2015). **Different immune cells mediate mechanical pain hypersensitivity in male and female mice**. *Nat Neurosci* 18 (8), 1081-1083, doi: 10.1038/nn.4053.
- Stegemann, A., Liu, S., Retana Romero, O. A., Oswald, M. J., Han, Y., Beretta, C. A., Gan, Z., Tan, L. L., Wisden, W., Graff, J. and Kuner, R. (2023). **Prefrontal engrams of long-term fear memory perpetuate pain perception**. *Nat Neurosci* 26 (5), 820-829, doi: 10.1038/s41593-023-01291-x.
- Stewart, A. N., MacLean, S. M., Stromberg, A. J., Whelan, J. P., Bailey, W. M., Gensel, J. C. and Wilson, M. E. (2020). **Considerations for Studying Sex as a Biological Variable in Spinal Cord Injury**. *Front Neurol* 11, 802, doi: 10.3389/fneur.2020.00802.
- Sugiura, Y., Lee, C. L. and Perl, E. R. (1986). **Central projections of identified, unmyelinated (C) afferent fibers innervating mammalian skin**. *Science* 234 (4774), 358-361, doi: 10.1126/science.3764416.
- Sun, C., Deng, J., Ma, Y., Meng, F., Cui, X., Li, M., Li, J., Li, J., Yin, P., Kong, L., Zhang, L. and Tang, P. (2023). **The dual role of microglia in neuropathic pain after spinal cord injury: Detrimental and protective effects**. *Exp Neurol* 370, 114570, doi: 10.1016/j.expneurol.2023.114570.
- Takazawa, T., Choudhury, P., Tong, C. K., Conway, C. M., Scherrer, G., Flood, P. D., Mukai, J. and MacDermott, A. B. (2017). **Inhibition Mediated by Glycinergic and GABAergic Receptors on Excitatory Neurons in Mouse Superficial Dorsal Horn Is Location-Specific but Modified by Inflammation**. *J Neurosci* 37 (9), 2336-2348, doi: 10.1523/JNEUROSCI.2354-16.2017.
- Takazawa, T. and MacDermott, A. B. (2010). **Synaptic pathways and inhibitory gates in the spinal cord dorsal horn**. *Ann N Y Acad Sci* 1198, 153-158, doi: 10.1111/j.1749-6632.2010.05501.x.
- Tashiro, S., Nishimura, S., Shinozaki, M., Takano, M., Konomi, T., Tsuji, O., Nagoshi, N., Toyama, Y., Liu, M., Okano, H. and Nakamura, M. (2018). **The Amelioration of Pain-Related Behavior in Mice with Chronic Spinal Cord Injury Treated with Neural Stem/Progenitor Cell Transplantation**

- Combined with Treadmill Training.** *J Neurotrauma* 35 (21), 2561-2571, doi: 10.1089/neu.2017.5537.
- Tashiro, S., Shinozaki, M., Mukaino, M., Renault-Mihara, F., Toyama, Y., Liu, M., Nakamura, M. and Okano, H. (2015). **BDNF Induced by Treadmill Training Contributes to the Suppression of Spasticity and Allodynia After Spinal Cord Injury via Upregulation of KCC2.** *Neurorehabil Neural Repair* 29 (7), 677-689, doi: 10.1177/1545968314562110.
- Todd, A. J. (2010). **Neuronal circuitry for pain processing in the dorsal horn.** *Nat Rev Neurosci* 11 (12), 823-836, doi: 10.1038/nrn2947.
- Torsney, C. and MacDermott, A. B. (2006). **Disinhibition opens the gate to pathological pain signaling in superficial neurokinin 1 receptor-expressing neurons in rat spinal cord.** *J Neurosci* 26 (6), 1833-1843, doi: 10.1523/JNEUROSCI.4584-05.2006.
- van Hedel, H. J., Dietz, V. and European Multicenter Study on Human Spinal Cord Injury Study, G. (2009). **Walking during daily life can be validly and responsively assessed in subjects with a spinal cord injury.** *Neurorehabil Neural Repair* 23 (2), 117-124, doi: 10.1177/1545968308320640.
- Vranken, J. H. (2013). **The Specific Condition: Central Neuropathic Pain.** In: *Neuropathic Pain*, eds. Toth, C. and Moulin, D. E., Cambridge University Press, Cambridge, pp. 145-176.
- Walker, C. L., Fry, C. M. E., Wang, J., Du, X., Zuzzio, K., Liu, N. K., Walker, M. J. and Xu, X. M. (2019). **Functional and Histological Gender Comparison of Age-Matched Rats after Moderate Thoracic Contusive Spinal Cord Injury.** *J Neurotrauma* 36 (12), 1974-1984, doi: 10.1089/neu.2018.6233.
- Walters, E. T. (2012). **Nociceptors as chronic drivers of pain and hyperreflexia after spinal cord injury: an adaptive-maladaptive hyperfunctional state hypothesis.** *Front Physiol* 3, 309, doi: 10.3389/fphys.2012.00309.
- Werhagen, L., Budh, C. N., Hultling, C. and Molander, C. (2004). **Neuropathic pain after traumatic spinal cord injury--relations to gender, spinal level, completeness, and age at the time of injury.** *Spinal Cord* 42 (12), 665-673, doi: 10.1038/sj.sc.3101641.
- Westlund, K. N. (2007). **Postsynaptic Dorsal Column Projection, Anatomical Organization.** In: *Encyclopedia of Pain*, eds. Schmidt, R. F. and Willis, W. D., Springer Berlin Heidelberg, Berlin, Heidelberg, pp. 1956-1959.
- Widerstrom-Noga, E. (2017). **Neuropathic Pain and Spinal Cord Injury: Phenotypes and Pharmacological Management.** *Drugs* 77 (9), 967-984, doi: 10.1007/s40265-017-0747-8.

- Widerstrom-Noga, E. (2023). **Neuropathic Pain and Spinal Cord Injury: Management, Phenotypes, and Biomarkers**. *Drugs* 83 (11), 1001-1025, doi: 10.1007/s40265-023-01903-7.
- Wrigley, P. J., Press, S. R., Gustin, S. M., Macefield, V. G., Gandevia, S. C., Cousins, M. J., Middleton, J. W., Henderson, L. A. and Siddall, P. J. (2009). **Neuropathic pain and primary somatosensory cortex reorganization following spinal cord injury**. *Pain* 141 (1-2), 52-59, doi: 10.1016/j.pain.2008.10.007.
- Wu, D., Jin, Y., Shapiro, T. M., Hinduja, A., Baas, P. W. and Tom, V. J. (2020). **Chronic neuronal activation increases dynamic microtubules to enhance functional axon regeneration after dorsal root crush injury**. *Nat Commun* 11 (1), 6131, doi: 10.1038/s41467-020-19914-3.
- Zeilhofer, H. U., Wildner, H. and Yevenes, G. E. (2012). **Fast synaptic inhibition in spinal sensory processing and pain control**. *Physiol Rev* 92 (1), 193-235, doi: 10.1152/physrev.00043.2010.
- Zhao, Y. Q., Yin, J. B., Wu, H. H., Ding, T., Wang, Y., Liang, J. C., Guo, X. J., Tang, K., Chen, D. S. and Chen, G. Z. (2018). **Contribution of Spinal PKC γ Expression to Short- and Long-lasting Pain Behaviors in Formalin-induced Inflamed Mice**. *Pain Physician* 21 (5), E555-E564.
- Zheng, J., Lu, Y. and Perl, E. R. (2010). **Inhibitory neurones of the spinal substantia gelatinosa mediate interaction of signals from primary afferents**. *J Physiol* 588 (Pt 12), 2065-2075, doi: 10.1113/jphysiol.2010.188052.

8. Personal Contribution to Data Acquisition / Assessment and Personal Publications

Considering my independent contribution to my doctoral project, all results and data presented in this dissertation were exclusively acquired and processed by me, with the assistance of my colleague, Yifeng Zheng, who blinded the group identities. This body of work, along with my upcoming results, will form the basis of a research article for publication, for which I will be the independent first author.

Personal Publications:

Chen, J., Weidner, N., & Puttagunta, R. (2022). **The Impact of Activity-Based Interventions on Neuropathic Pain in Experimental Spinal Cord Injury**. *Cells*, 11(19), 3087.

Gong, C., Zheng, X., Guo, F., Wang, Y., Zhang, S., Chen, J., Sun, X., Shah, S. Z. A., Zheng, Y., Li, X., Yin, Y., Li, Q., Huang, X., Guo, T., Han, X., Zhang, S. C., Wang, W., & Chen, H. (2021). **Human spinal GABA neurons alleviate spasticity and improve locomotion in rats with spinal cord injury**. *Cell reports*, 34(12), 108889.

Li, M., Sun, X., Li, Q., Li, Y., Luo, C., Huang, H., Chen, J., Gong, C., Li, Y., Zheng, Y., Zhang, S., Huang, X., & Chen, H. (2020). **Fucoidan exerts antidepressant-like effects in mice via regulating the stability of surface AMPARs**. *Biochemical and biophysical research communications*, 521(2), 318–325.

Tao, Y., Cao, J., Li, M., Hoffmann, B., Xu, K., Chen, J., Lu, X., Guo, F., Li, X., Phillips, M. J., Gamm, D. M., Chen, H., & Zhang, S. C. (2020). **PAX6D instructs neural retinal specification from human embryonic stem cell-derived neuroectoderm**. *EMBO reports*, 21(9), e50000.

Li, M. X., Li, Q., Sun, X. J., Luo, C., Li, Y., Wang, Y. N., Chen, J., Gong, C. Z., Li, Y. J., Shi, L. P., Zheng, Y. F., Li, R. C., Huang, X. L., Xiong, Q. J., & Chen, H. (2019). **Increased Homer1-mGluR5 mediates chronic stress-induced depressive-like behaviors and glutamatergic dysregulation via activation of PERK-eIF2 α** . *Progress in neuro-psychopharmacology & biological psychiatry*, 95, 109682.

Appendix / Appendices

(Supplementary Figures)

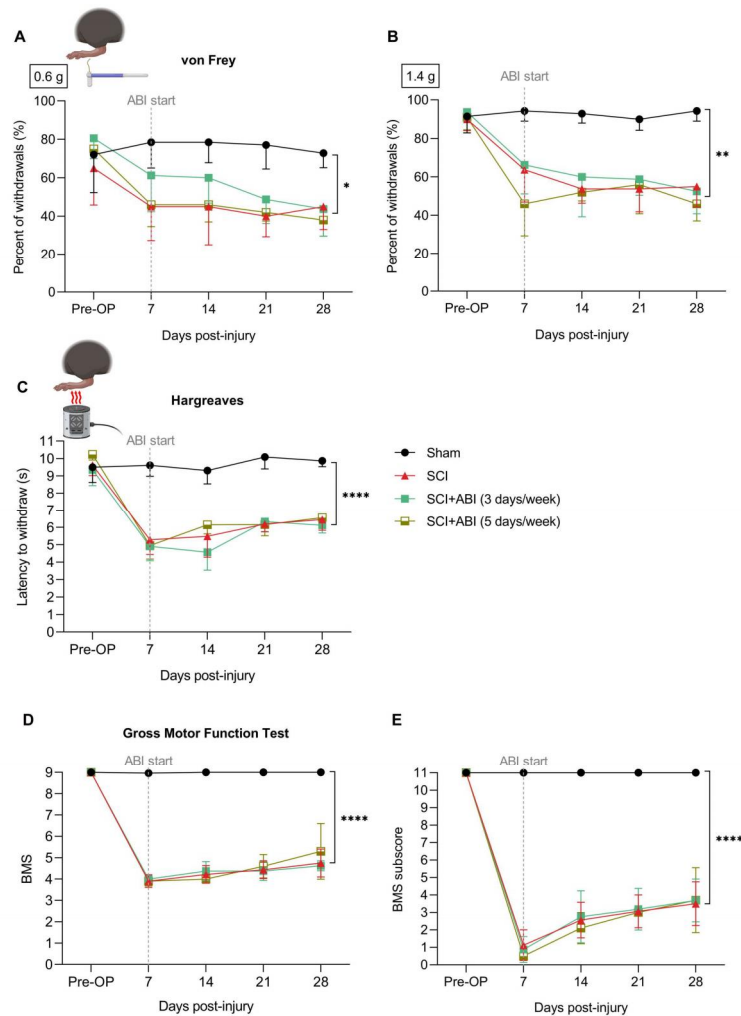


Figure S1: Both high-frequency and lower-frequency ABI paradigms fail to improve partial hindlimb sensorimotor deficits in SCI mice.

Both high- and lower-frequency ABI paradigms show no beneficial effects on improving SCI-induced mechanical hypoalgesia (tested by 0.6 (A) and 1.4 g (B) von Frey hair filaments), thermal hyperalgesia (assessed with the Hargreaves method, C), or hindlimb gross motor deficits (evaluated using BMS (D) and subscores (E)) (female, sham: n = 7; SCI: n = 8; SCI+ABI (3 days/week): n = 8; SCI+ABI (5 days/week): n = 5). Mean ± SD. Two-way repeated measures ANOVA, group differences, * $p < 0.05$, ** $p < 0.01$, **** $p < 0.0001$.

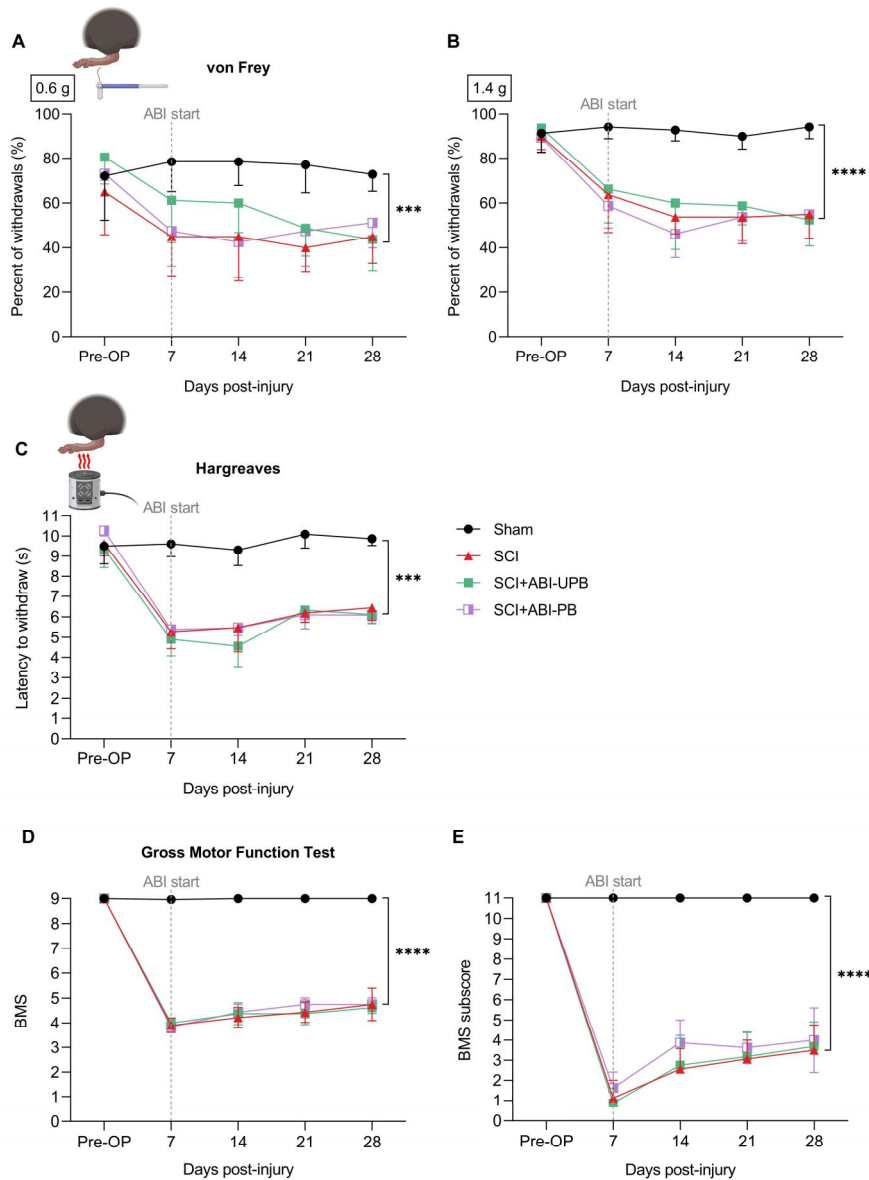


Figure S2: Both unpatterned and patterned ABI paradigms fail to improve partial hindlimb sensorimotor deficits in SCI mice.

Both patterned and unpatterned ABI paradigms show no beneficial effects on improving SCI-induced mechanical hypoalgesia (tested by 0.6 (A) and 1.4 g (B) von Frey hair filaments), thermal hyperalgesia (assessed with the Hargreaves method, C), or hindlimb gross motor deficits (evaluated using BMS (D) and subscores (E)) (female, sham: n = 7; SCI: n = 8; SCI+ABI-UPB: n = 8; SCI+ABI-PB: n = 8). Mean ± SD.

Two-way repeated measures ANOVA group differences, *** $p < 0.001$, **** $p < 0.0001$.

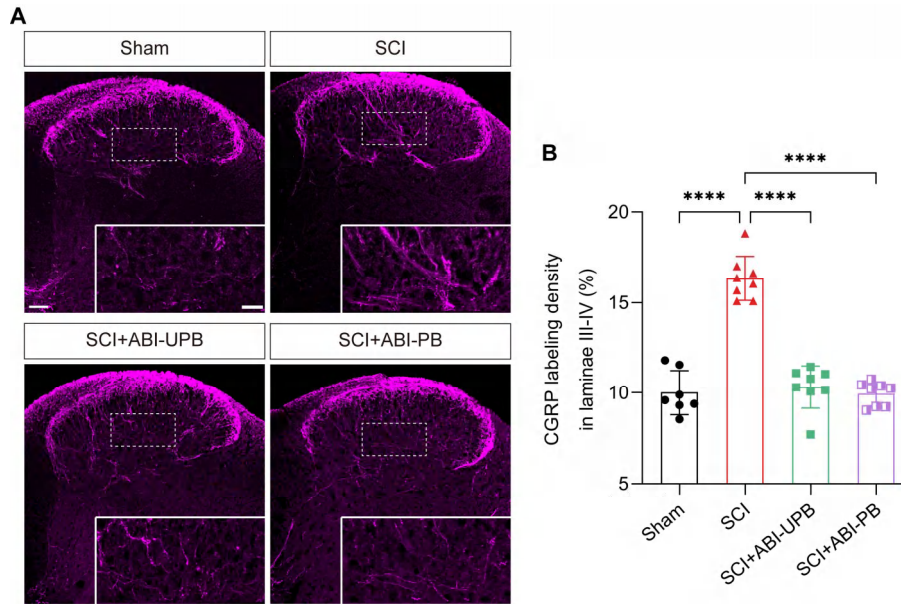


Figure S3: Both unpatterned and patterned ABI paradigms successfully inhibit SCI-induced sprouting of CGRP-expressing nociceptors into the deeper dorsal horn within the below-level spinal cord.

Immunofluorescence staining of lumbar spinal cord sections shows CGRP-positive expression (A, scale bars in main images: 50 μm , in magnified images: 20 μm). Quantification of the percentage of CGRP-labeled area in laminae III-IV of the spinal cord dorsal horn (B). SCI mice exhibit significant increase in sprouting of CGRP+ nociceptors within laminae III-IV compared to sham controls. Both ABI paradigms effectively reduce this aberrant sprouting to levels comparable to those of sham mice (female, sham: $n = 7$; SCI: $n = 8$; SCI+ABI-UPB: $n = 8$; SCI+ABI-PB: $n = 8$). Mean \pm SD. Ordinary one-way ANOVA ($p < 0.0001$), post hoc Tukey test: **** $p < 0.0001$.

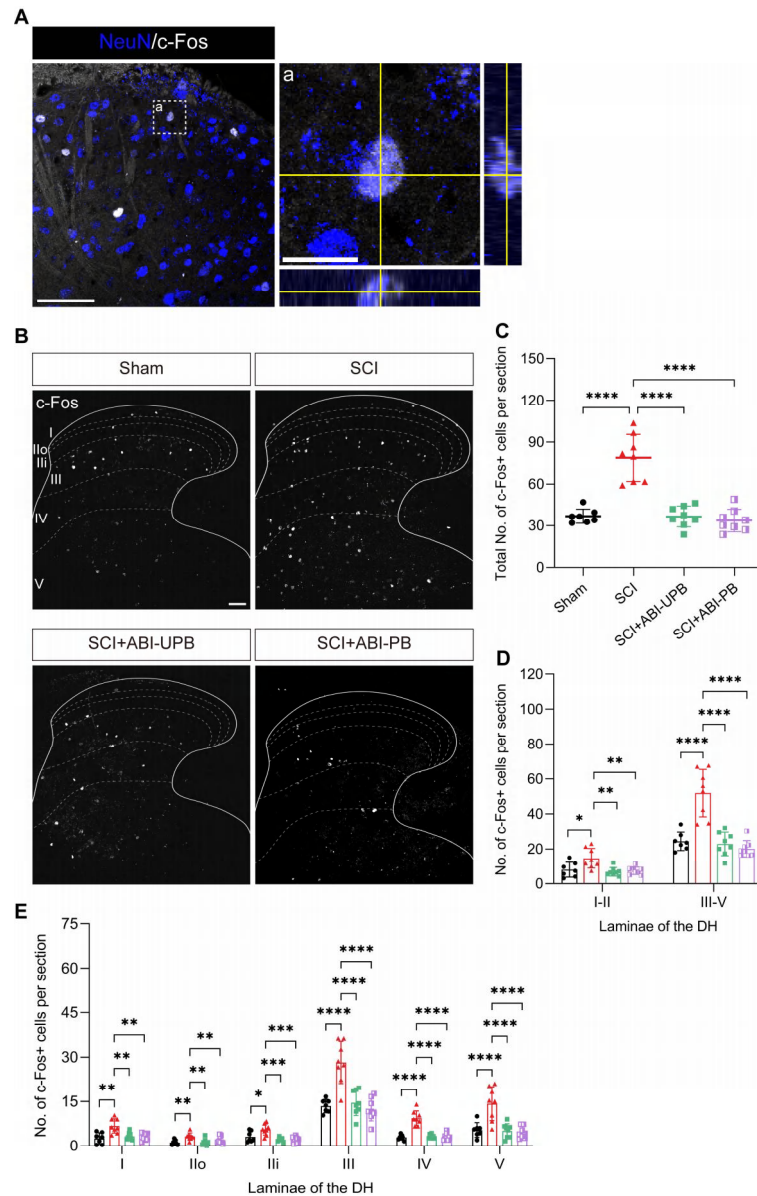


Figure S4: Both unpatterned and patterned ABI paradigms significantly depress the SCI-induced enhancement in touch-evoked c-Fos activation within the below-level spinal cord.

Immunofluorescence staining of lumbar spinal cord sections shows overlap between c-Fos+ and NeuN+ cells (A, scale bar in main image: 50 μ m, in magnified image (a): 10 μ m) and c-Fos expression based on laminar distribution (B, scale bars: 50 μ m). SCI mice show more c-Fos+ cells in the spinal cord dorsal horn after a non-noxious mechanical stimulus (B and C), mainly in deeper laminae III-V (D and E). Both ABI paradigms significantly reduce c-Fos+ cells across laminae I-V to sham levels (female, sham: n = 7; SCI: n = 8; SCI+ABI-UPB: n = 8; SCI+ABI-PB: n = 8). Mean \pm SD. Ordinary one-way ANOVA ($p < 0.0001$), post hoc Tukey test: * $p < 0.05$, ** $p < 0.01$, *** $p < 0.001$, **** $p < 0.0001$.

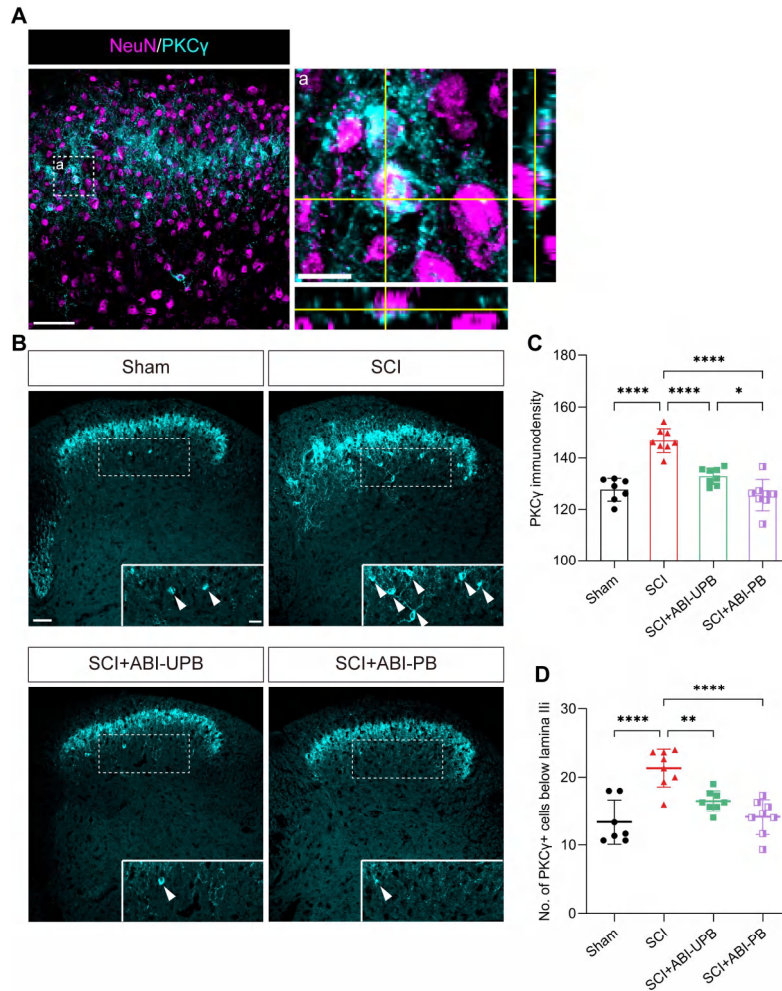


Figure S5: Both unpatterned and patterned ABI paradigms effectively reduce SCI-induced heightened reactivity of PKC γ -positive interneurons in the below-lesion spinal cord dorsal horn.

Immunofluorescence staining of lumbar spinal cord sections shows overlap between PKC γ + and NeuN+ cells (A, scale bar in main image: 50 μ m, in magnified image (a): 10 μ m) and PKC γ expression (B, scale bar in main image: 50 μ m, in magnified image: 20 μ m). SCI mice demonstrate enhanced PKC γ immunoreactivity in the spinal cord dorsal horn by exhibiting significantly higher immunodensity of PKC γ (B) and a greater number of PKC γ + cells below lamina III (C). Both ABI paradigms effectively depress the SCI-induced increase in PKC γ expression to the level of sham controls. Interestingly, the ABI paradigm on the patterned belt showed slightly higher efficiency in reducing PKC γ immunodensity in SCI mice when compared to ABI on an unpatterned belt (female, sham: n = 7; SCI: n = 8; SCI+ABI-UPB: n = 8; SCI+ABI-PB: n = 8). Mean \pm SD. Ordinary one-way ANOVA ($p < 0.0001$), post hoc Tukey test: * $p < 0.05$, ** $p < 0.01$, **** $p < 0.0001$.

Curriculum Vitae / Résumé

PERSONAL INFORMATION

Name Jing Chen
Date of Birth Feb. 2nd, 1995
Place of Birth Fujian
Nationality Chinese
Marital Status Single
E-mail belemchan48@gmail.com

EDUCATION

Apr. 2021 – Present **Ph.D. Candidate in Neurology** (Bei Dr. sc. hum. im Fach: Neurologie)
Laboratory of Experimental Neuroregeneration, Spinal Cord Injury Center, Heidelberg University Hospital

Sep. 2017 – Jun. 2020 **M.Med. in Rehabilitation Medicine and Physical Therapy**

- Thesis: Studies on the Key Factors in the Development of Excitatory Glutamatergic V3 Interneurons in Human Spinal Cord
- Supervisor: Prof. Dr. med. Hong Chen

Tongji-Wisconsin Stem Cell Application Technology Research Center, Tongji Hospital, Tongji Medical College, Huazhong University of Science and Technology

Sep. 2014 – Jan. 2015 **Exchange Study Programs in Occupational Therapy**
I-Shou University

Sep. 2013 – Jul. 2017 **B.Sc. in Rehabilitation Therapy-Occupational Therapy**
School of Rehabilitation Medicine, Fujian University of Traditional Chinese Medicine

PROFESSIONAL CAREER/EXPERIENCE

Clinical Experience:

Jul. 2016 – Jun. 2017 **Intern** in Yangzhi Affiliated Rehabilitation Hospital of Tongji University

Research Training:

Apr. 2021 – Present Conducted my doctoral project investigating **the impact of treadmill activity-based intervention (ABI) on neuropathic pain (NP) following experimental spinal cord injury (SCI):**

- I used both sexes of mice to explore sex as a biological variable in NP development and its alleviation by ABI. I also examined the mechanisms of SCI-NP and its amelioration by ABI, with plans to develop this work into a research article as the independent first author.

Sep. 2017 – Jun. 2020 Investigated **the therapeutic effects of stem cell therapy on SCI-induced dysfunctions, focused mainly on lower limb motor deficits and sensory impairment of NP:**

- Human embryonic stem cells (ESCs) were cultivated and differentiated into spinal cord p3 region neural precursor cells, which matured as Glutamatergic V3 Premotor Interneurons in vitro. These cells were transplanted into the thoracic spinal cord of rats in the subacute phase post-injury, enabling examining hindlimb motor function over three months and histological analysis showed cell survival and integration with the host tissue;
- Human ESCs were differentiated into GABAergic dl4 inhibitory interneuron progenitor cells and transplanted into rats with thoracic SCI. Improvements in lower limb NP and cell integration were observed over three months.

AWARDS AND HONORS

2017 – 2020	Received the First-Class Academic Scholarship every year
June 2017	Qunhao Scholarship for Outstanding Graduates
November 2016	First Place in the National Rehabilitation Therapy and Sports Rehabilitation Student Skills Competition
2013 – 2017	Received the First-Class Academic Scholarship every year

Acknowledgements

I would like to express my deepest gratitude to all the individuals who have supported and guided me throughout my doctoral journey in Heidelberg. I am profoundly thankful for the opportunity to collaborate with so many incredible scientists, clinicians, and individuals during my time at the Laboratory of Experimental Neuroregeneration, Spinal Cord Injury Center, Heidelberg University Hospital.

First and foremost, I extend my sincere thanks to my esteemed supervisor, Prof. Dr. med. Norbert Weidner, for entrusting me with the opportunity to start my doctoral journey here and for his invaluable guidance, unwavering support, and continuous encouragement. His profound knowledge and insightful feedback have been instrumental in shaping this dissertation.

I am deeply grateful to Dr. Radhika Puttagunta, the group leader of our laboratory, for her exceptional mentorship and for fostering a collaborative and innovative research environment. Her patient training and guidance have been invaluable to my growth as a scientist. Her unwavering support of my experiments motivated me to make consistent progress. She has generously shared her expertise in academic writing and oral presentations, providing numerous opportunities for me to present my scientific work at symposiums and departmental meetings. I learned a great deal from her comprehensive and professional perspective on scientific outcomes, which helped clarify my own thinking step by step. Without her professional feedback and support, this dissertation would not have been as successful or satisfying.

Special thanks go to our technical assistant, Melanie Motsch, whose expertise and assistance were crucial in overcoming numerous technical challenges during the experimental period. Melanie's help with setting up and adjusting the treadmill and her support in helping me acclimate to life in Germany were invaluable. I would like to acknowledge my colleagues who have been a constant source of support and inspiration. Dr. Naemi Sarah Kuehn helped me

become more familiar with the lab and the animals. Dr. Bahardokht Tolou Dabbaghian provided detailed guidance on animal surgery and behavioral testing and assisted me with performing the BMS for mice. Dr. med. Yifeng Zheng was an exceptional surgery assistant and played a key role in blinding the group identities for surgery, behavioral testing, and histological analysis. I am also thankful to Andrea Genthner, our dedicated animal caretaker, who took excellent care of the animals with her professional knowledge and expertise throughout the experimental duration. I would like to express my sincere appreciation to the late Mr. Wolfgang Roth for his invaluable contributions to our laboratory. He developed the small animal treadmill and assisted me in designing and improving the treadmill belt replacement, which was essential for the continuation of my experiments. His help laid the foundation for the successful completion of my experimental design, and I offer my heartfelt respect for his contributions.

I gratefully acknowledge the financial support provided by the China Scholarship Council, which made my doctoral study possible.

My heartfelt appreciation goes to my family. To my parents, who have always supported and loved me, giving me the strength and courage to pursue my dreams. Their unwavering belief in me has been a pillar of strength. To my dear brother, whose constant encouragement and trust have been a source of motivation and resilience.

Lastly, I would like to express my deepest love and gratitude to my partner and best friend, Yifeng Zheng. Your love, support, and companionship have been my anchor throughout this journey. Your belief in me has given me wings to soar higher.

Thank you all for being an integral part of my doctoral journey. My time in Heidelberg will always shine brightly in my memory and remain unforgettable forever.

Eidesstattliche Versicherung

1. Bei der eingereichten Dissertation zu dem Thema **Mechanisms and Therapeutic Potential of Treadmill Activity-Based Intervention in Alleviating Neuropathic Pain Following Spinal Cord Injury: Considering Sex Differences and Sensory Input Modulation** handelt es sich um meine eigenständig erbrachte Leistung.
2. Ich habe nur die angegebenen Quellen und Hilfsmittel benutzt und mich keiner unzulässigen Hilfe Dritter bedient. Insbesondere habe ich wörtlich oder sinngemäß aus anderen Werken übernommene Inhalte als solche kenntlich gemacht.
3. Die Arbeit oder Teile davon habe ich bislang nicht an einer Hochschule des In- oder Auslands als Bestandteil einer Prüfungs- oder Qualifikationsleistung vorgelegt.
4. Die Richtigkeit der vorstehenden Erklärungen bestätige ich.
5. Die Bedeutung der eidesstattlichen Versicherung und die strafrechtlichen Folgen einer unrichtigen oder unvollständigen eidesstattlichen Versicherung sind mir bekannt. Ich versichere an Eides statt, dass ich nach bestem Wissen die reine Wahrheit erkläre und nichts verschwiegen habe.

Ort und Datum

Unterschrift